Technical Report ITL-98-4
September 1998

US Army Corps of Engineers
Waterways Experiment Station

Computer-Aided Structural Engineering (CASE) Project

Investigation of At-Rest Soil Pressures due to Irregular Sloping Soil Surfaces and CSOILP User's Guide

by William P. Dawkins, Consultant
Michael E. Pace, WES

Prepared for Headquarters, U.S. Army Corps of Engineers

The contents of this report are not to be used for advertising, publication, or promotional purposes. Citation of trade names does not constitute an official endorsement or approval of the use of such commercial products.

The findings of this report are not to be construed as an official Department of the Army position, unless so designated by other authorized documents.

PRINTED ON RECYCLED PAPER

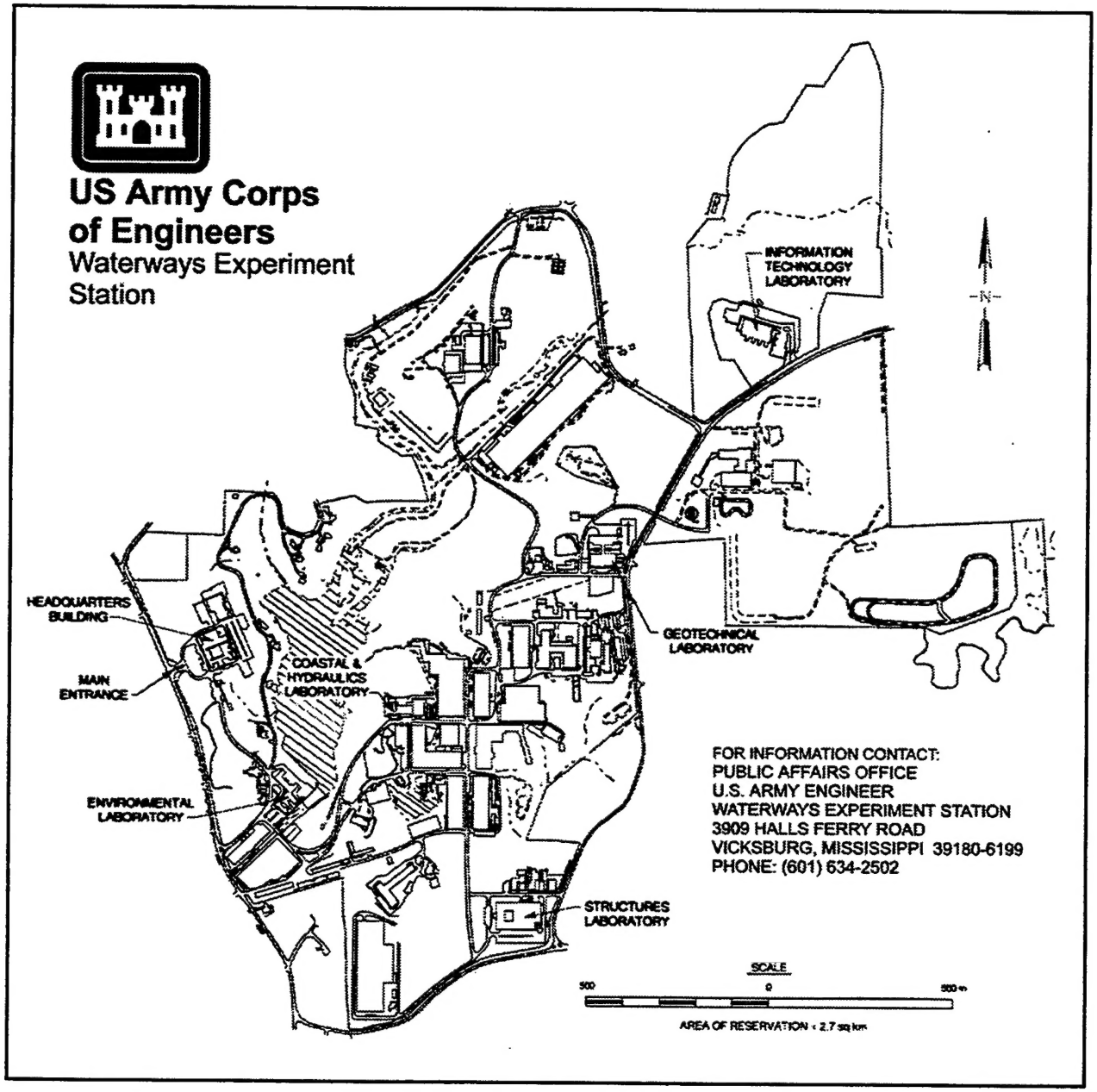

Waterways Experiment Station Cataloging-in-Publication Data

Dawkins, William P.

Investigation of at-rest soil pressures due to irregular sloping soil surfaces and CSOILP user's guide / by William P. Dawkins, Michael E. Pace ; prepared for U.S. Army Corps of Engineers.

126 p. : ill. ; 28 cm. -- (Technical report ; ITL-98-4)

Includes bibliographical references.

1. Earth pressure -- Testing. 2. Retaining walls -- Testing. 3. Slopes (Soil mechanics) -- Computer programs. 4. CSOILP (Computer programs) I. Pace, Michael E. II. United States. Army. Corps of Engineers. III. U.S. Army Engineer Waterways Experiment Station. IV. Information Technology Laboratory (U.S. Army Engineer Waterways Experiment Station) V. Computer-aided Structural Engineering Project. VI. Title. VII. Series: Technical report (U.S. Army Engineer Waterways Experiment Station) ; ITL-98-4.
TA7 W34 no.ITL-98-4

Contents

Preface

This report describes the development of a method to compute at-rest earth pressures by combining the results of a gravity turn-on analysis with theory of elasticity solutions. The user's manual for the program CSOILP, which performs these calculations, is also presented. The computer program and theoretical/ user's guide were written using funds provided to the U.S. Army Engineer Waterways Experiment Station (WES), Vicksburg, MS, by Headquarters, U.S. Army Corps of Engineers Civil Works Directorate, under Structural Engineering Research Program work unit 31589, Computer-Aided Structural Engineering (CASE).

The analytical finite element studies and comparisons were performed by Dr. William P. Dawkins, P.E., Houston, Texas. Dr. Dawkins also wrote the original CSOILP program. Later, Mr. Michael E. Pace, Computer-Aided Engineering Division (CAED), Information Technology Laboratory (ITL), WES, developed the Windows interface for the program and wrote the user's guide.

The work was managed, coordinated, and monitored by Dr. Reed Mosher, Chief, Structural Mechanics Division (SMD), Structures Laboratory (SL), WES; and Mr. Pace. Dr. Bryant Mather was Director, SL, Mr. H. Wayne Jones was Chief, CAED, and Dr. N. Radhakrishnan was Director, ITL.

At the time of publication of this report, Director of WES was Dr. Robert W. Whalin, and the Commander was COL Robin R. Cababa, EN.

1 Introduction

Background

At-rest soil pressures for horizontal soil surfaces are traditionally estimated by applying an at-rest pressure coefficient to the effective vertical pressure. No method for estimating at-rest pressures has gained general acceptance when the soil surface is not horizontal.

The use of elasticity solutions to account for the effects of surface surcharge loads on active and passive pressures for design of retaining walls is common[1,2]. It has been proposed that the at-rest pressures due to a sloping surface be estimated by treating the weight above a horizontal datum as a surcharge load. The contribution of the surcharge to the pressures below the datum would be evaluated using appropriate theory of elasticity solutions for surface loads on a semi-infinite elastic medium.

Scope

This report details a finite element study performed to explore the accuracy of the proposed method of determining at-rest pressures.

This report is organized into the following chapters. Chapter 2 details the finite element study performed on several configurations of a one-layered granular soil in a loose and a dense state. Chapter 3 details the finite element study performed on several two-layered soil configurations composed of a sand and a clay. A computer program called CSOILP has been written to automate the proposed process of computing at-rest earth pressures. The user's guide for CSOIL is presented in Chapter 4. Example problems for CSOILP are given in Chapter 5. Details of the finite element grids used in the studies are presented in Appendixes A and B.

[1] Joseph E. Bowles. (1977). *Foundation analysis and design.* 2nd ed., McGraw-Hill, New York.
[2] K. Terzaghi. (1943). *Theoretical soil mechanics.* John Wiley, New York.

2 One-Layered Granular Soil/Surface Systems

A limited number of surface configurations (Figure 1) for drained granular soil systems has been selected to investigate the appropriateness of elasticity equations for estimating at-rest pressures for these systems. These systems are assumed to be composed of a homogeneous, undrained granular material with properties shown in Table 1.

Table 1
Soil Properties

Soil Designation	Unit Weight lb/ft³ (kg/m³)	Angle of Internal Friction, deg	Initial Modulus Parameter K[1]	Modulus Exponent[1]	Initial Bulk Modulus Parameter K_B[1]	Bulk Modulus Exponent[1]	Unload Modulus Parameter[1]
L	120 (1,942)	35	500	0.4	250	0.2	600
H	130 (2,104)	40	1,500	0.4	750	0.2	600

[1] Hyperbolic stress-strain model parameter.
K = initial modulus parameter.
K_B = initial bulk modulus parameter.

Finite Element Analysis

Finite element analyses of the systems were performed with computer program SOILSTRUCT[1] using the parameters shown in Table 1 for the soils. The soil above elevation (el) 40 ft (Figure 1) was built up in five lifts for the systems shown in Figures 1a and 1c, and in seven lifts for the system shown in Figure 1b. Three iterations were performed for each lift.

The finite element models for the various systems are shown in Appendix A. The element dimensions and configuration below el 40 were maintained

[1] R.M. Ebeling, J. F. Peters, and G. W. Clough. (1991). "User's guide for the incremental construction, soil-structure interaction program SOILSTRUCT," Technical Report ITL-90-6, U.S. Army Engineer Waterways Experiment Station, Vicksburg, MS.

regardless of the surface shape. The element horizontal dimensions and configuration above el 40 were maintained for the systems shown in Figures 1a and 1b; however, the vertical dimensions were proportioned according to the slope of the surface. The left and right vertical boundaries and the bottom horizontal boundary were assumed to be frictionless. The horizontal stresses at the center of the first column of elements were taken as representative of the horizontal pressures on the left rigid boundary.

Initial stresses in all elements below el 40 were evaluated by gravity turn-on in SOILSTRUCT with an at-rest pressure coefficient equal to 0.5.

Theory of Elasticity Solutions

The theory of elasticity solutions used for comparison with the finite element solutions are based on an assumed radial stress distribution due to a distributed load applied to the surface of an elastic half space[1]. The three soil/surface systems described in the preceding section are represented for the elasticity solutions as shown in Figures 2, 3, and 4. These solutions have been used to represent surcharge loads on horizontal surfaces for various applications;[2] however, it is usually recommended that the horizontal stress obtained by the elasticity equations be doubled to represent the vertical plane as a plane of symmetry. This aspect will be discussed subsequently in this report.

Discussion of Results

Increasing surface slope

The horizontal pressures predicted by the finite element analyses on the left vertical surface of the system are shown in Figures 5 through 8 along with two variations of the pressures predicted by combining pressures predicted by the elasticity solutions and geostatic pressures for a horizontal surface at el 40. For both elasticity solutions the contribution of the surcharge (Figure 2) was **doubled**. The two curves labeled "elasticity" consider the uniform segment of the load to extend to a total of 48.8 m (160 ft) (the right boundary of the finite element model) and to infinity, respectively (i.e., for $\theta_2 = \pi/2$, in Figure 2). These two curves suggest that the proximity of the right-hand boundary of the model has a greater effect on the pressures at the left boundary for the stiffer soil (type H, Table 1) than for the softer soil (type L) but does not significantly influence the pressures for either soil. For all cases the elasticity solutions bound the finite element predictions as the depth increases and provide reasonable approximations elsewhere.

---

[1] S. Timoshenko and J. N. Goodier. (1951). *Theory of elasticity.* 2nd ed., McGraw-Hill, New York.

[2] Bowles, op. cit.

Decreasing surface slope

Comparisons of finite element and theory of elasticity solutions for the decreasing surface slopes are shown in Figures 9 through 12. The geostatic pressures for a horizontal surface at el 70 (Figures 9 and 10) and for el 80 (Figures 11 and 12) are included. The theory of elasticity solutions (Figure 3) are **not doubled** in these figures. The theory of elasticity solutions compare very favorably with the finite element solutions for the softer soil (soil L) for depths greater than 4.6 to 6.1 m (15 to 20 ft) below the datum. The theory of elasticity solution overestimates the horizontal pressure near the datum and provides no estimate of pressure above the datum. The solutions for finite element and theory of elasticity compare less favorably for the stiffer soil for both surface slopes. The finite element solutions indicate that the horizontal pressures on the rigid boundary actually decrease from the initial levels as the surface surcharge is increased for the stiffer soil. For both surface slopes and soil stiffnesses, the contribution of the theory of elasticity component to the total horizontal pressures decreases with depth. Below el 0 the primary source of horizontal pressure is the geostatic effect. The best approximation of the finite element results for decreasing slopes appears to be a linear increase of pressure with depth from zero at the maximum surface elevation to the geostatic pressure produced by a horizontal surface at the datum. These approximations are shown by the dotted lines in Figures 9 through 12.

Triangular surface

Comparisons of finite element and theory of elasticity solutions for the triangular surface are shown in Figures 13 and 14. The theory of elasticity solutions (Figure 4) are **not doubled** in these figures. The theory of elasticity provides excellent approximations of the pressures predicted by the finite element analyses for both soils.

Conclusions and Recommendations

Except for the decreasing surface slopes, the theory of elasticity approach provides excellent approximations for at-rest soil pressures. For decreasing surface slopes, the best approximation appears to be a simple linear increase in at-rest pressure with depth.

The following paragraphs recommend procedures for estimating at-rest pressures.

Increasing surface slopes

For surfaces that increase linearly with distance from the wall to a maximum uniform elevation, the at-rest pressure may be obtained by combining the geostatic pressure for a horizontal datum at the top of the wall with **twice** the horizontal pressures from the theory of elasticity solution (Figure 2) with the horizontal maximum surface assumed to extend to inifinity.

Decreasing surface slopes

For surfaces that decrease linearly with distance from the wall to a minimum uniform elevation (Figure 3), the at-rest pressure may be estimated by a linear increase of pressure with depth from zero at the maximum surface elevation to the geostatic pressure produced by horizontal surface at the datum for a depth below the datum equal to the horizontal distance to which the decreasing surface extends.

Triangular surfaces

For a surface that increases linearly with distance from the wall to a maximum elevation and then decreases linearly to a horizontal surface at the same elevation as the top of the wall, the at-rest pressure may be estimated by combining the geostatic pressure due to a horizontal datum with the pressure predicted by the theory of elasticity (Figure 4).

3 Two-Layered Soil/Surface Systems

Several irregular surface configurations (Figures 15 and 16) have been selected to investigate the appropriateness of elasticity equations for estimating at-rest pressures for these systems. These systems are assumed to be composed of various combinations of granular and cohesive soils with properties shown in Table 2.

Table 2
Soil Properties

Soil Notation	Sand		Clay
	L	H	
Unit weight, lb/ft^3 (kg/m^3)	120 (1,922.2)	130 (2,082.4)	120 (1,922.2)
Angle of internal friction, deg	35	40	0
Cohesion, lbf/ft^2 (kPa)	0	0	1,500 (71.8)
At-rest coefficient k_o	0.5	0.5	1.0
Initial modulus coefficient[1]	500	1,500	850
Modulus exponent[1]	0.4	0.4	N/A
Initial bulk modulus coefficient[1]	250	750	N/A
Bulk modulus exponent[1]	0.2	0.2	N/A
Failure ratio[1]	0.7	0.7	0.7
Poisson's ratio	N/A	N/A	0.49

[1] Hyperbolic stress-strain model parameters (Ebeling, Peters, and Clough, op. cit.)

Finite Element Analysis

Finite element analyses of the systems were performed with computer program SOILSTRUCT[1] using the parameters shown in Table 2 for the soils. The soil above el 40 was built up in several lifts, and three iterations were performed for each lift. Initial stresses in all elements below el 40 were evaluated by gravity turn-on in SOILSTRUCT with an at-rest pressure coefficient given in Table 2.

[1] Ebeling, Peters, and Clough, op.cit.

The finite element models for the various systems are shown in Appendix A. Details of the models are given in Table 3. The element dimensions and configuration below el 40 were maintained regardless of the shape of the surface. The element horizontal dimensions and configuration above el 40 were maintained; however, the vertical dimensions were proportioned according to the slope of the surface. The left and right vertical boundaries and the bottom horizontal boundary were assumed to be frictionless. The horizontal stresses at the center of the first column of elements were taken as representative of the horizontal pressures on the left rigid boundary.

Table 3
Details of Finite Element Models

Surface Designation	No. of Elements	No. of Nodes	No. of Surcharge Lifts
Ramp surface (S1)	1,125	1,163	15
Single triangle surface (S2)	890	933	9
Double triangle surface (S3)	922	960	9
Single triangle surface (S4)	1,001	1,054	14
Double triangle surface (S5)	1,033	1,081	14

Theory of Elasticity Solutions

The theory of elasticity solutions used for comparison with the finite element solutions are based on an assumed radial stress distribution due to a distributed load applied to the surface of an elastic half space[1]. The various surfaces were represented as combinations of the elasticity solutions as shown in Figure 17. These solutions have been used to represent surcharge loads on horizontal surfaces for various applications[2]; however, it is usually recommended that the horizontal stress obtained by the elasticity equations be doubled to represent the vertical plane as a plane of symmetry. This aspect will be discussed subsequently in this report. In all cases the solutions subsequently referred to as "elasticity" consist of the superposition of the stress obtained from the equations in Figure 17 on the geostatic horizontal earth pressures;

$$\sigma_{h,total} = p_v k_o + n\sigma_{h,elasticity} \tag{1}$$

where

p_v = effective vertical pressure below el 40 prior to application of the surcharge

k_o = at-rest coefficient given in Table 2

[1] Timoshenko and Goodier, op. cit.

[2] Bowles, op. cit.

n = 1 or 2, depending on the surface configuration

$\sigma_{h,elasticity}$ = effective horizontal stress computed using theory of elasticity

Discussion of Results

Ramp surfaces (S1)

The horizontal pressures on the left vertical surface of the system for initial surface slopes of 2, 3, and 4 vertical to 8 horizontal with various combinations of homogeneous and layered systems are shown in Figures 18 through 32. In all cases the elasticity component of the total stress (Equation 1) was **doubled**. It is apparent that the elasticity solution provides an excellent estimate of the horizontal pressure for all systems with homogeneous surcharge and base (Figures 18 through 23).

The elasticity solution underestimates the horizontal pressure for a homogeneous clay base as shown in Figures 24, 25, and 26, with the accuracy of the approximation decreasing as the surface slope increases. The erratic variation of the finite element solution for the 4V on 8H slope is due to high stress levels in the surcharge at the toe of the slope. Several elements in that location exhibited stress levels at or near a failure condition. This situation is due to spurious stress concentrations in the triangular elements in the finite element model.

For the layered sand-H over clay base, the elasticity solution accurately predicts the stresses in the lower clay layer (Figures 27, 28, and 29). However, as the surcharge load increases, the horizontal stresses in the upper sand-H layer appear to tend toward a passive condition to the extent that the discontinuity in geostatic stresses at the layer boundary becomes entirely obscured.

With a clay over sand-H layered base (Figures 30, 31, and 32), the elasticity solution accurately predicts the horizontal pressures for the lower 2V on 8H slope. As the surface slope increases, the finite element solution indicates a tendency toward a passive state in both layers with the discontinuity in geostatic stresses again being obscured.

Single triangle surfaces (S2)

The elasticity solution, with n = 1 in Equation 1, provides an excellent approximation of the horizontal stress for all combinations of homogeneous and layered systems (Figures 33 through 37).

Double triangle surfaces (S3)

The horizontal stresses in the homogeneous sand-L and sand-H systems (Figures 38 and 39) are accurately predicted by the elasticity solution with n = 1

in Equation 1. A factor $n = 2$ provides the better estimate of stresses in the homogeneous clay base (Figure 40). Elasticity solutions with $n = 1$ and $n = 2$ are shown for comparison with the finite element solution for layered bases in Figures 41 and 42. It is apparent that the stresses are best approximated with $n = 1$ for the sand-H layer and with $n = 2$ for the clay layer.

Single triangle surfaces (S4)

The elasticity solution, with n = 1, overestimates the horizontal pressure for all homogeneous sand-L and sand-H systems (Figures 43 through 48). The high stress near the surface of the base material (el 40) predicted by the elasticity solution is not indicated by the finite element solution. The finite element solution also indicates that the horizontal stresses at lower elevations are essentially unaffected by the surcharge.

Pressures from the elasticity solution compare favorably with those from the finite element analysis for lower elevations in the homogeneous clay base (Figures 49-51). Pressures in the base near el 40 are overestimated by the elasticity solution. The pressures above el 40 from the finite element analysis suggest that the material in the surcharge is tending toward an active state of stress.

The elasticity solution accurately predicts the horizontal pressures in the clay stratum in both layered base systems (Figures 52-57), and overestimates the pressures in the sand-H stratum in all systems.

Double triangle surfaces (S5)

The elasticity solution overestimates horizontal pressures for the homogeneous sand-L and sand-H systems (Figures 58 through 63) with error in the approximation increasing with surcharge intensity and material strength. Except for the combination of high initial surcharge slope (-4V on 8H) and higher material strength (sand-H) (Figure 63), the elasticity solution provides reasonable approximations of pressures at increasing depth. As with the previously discussed single triangle surface (S4), the high pressures indicated by the elasticity solution near el 40 are not reflected in the finite element results.

Pressures from both finite element and elasticity solutions agree well for the homogeneous clay base system (Figures 64-66) except near el 40 where the elasticity solution again predicts higher pressures than those from the finite element analysis.

The elasticity solution underestimates pressures in the sand-H stratum and overestimates those in the clay stratum for all layered systems (Figures 67-72). The solutions diverge with increases in surface slope and material strengths.

Conclusions and Recommendations

The reliability with which the theory of elasticity approach predicts the at-rest pressures in a system is dependent on the configuration of the surface and the materials below the selected datum. The following paragraphs suggest procedures that appear to yield the best approximations.

Ramp surfaces (S1)

The at-rest pressures for homogeneous sand systems are accurately predicted by Equation 1 with $n = 2$.

For a homogeneous clay base, Equation 1 with $n = 2$ underestimates the horizontal pressures in the base with the underestimation greatest near the top of the base and increasing with increasing surface slope at all depths. The following procedure alleviates the degree of underestimation near the top of the base and provides estimates within 20 percent at all depths:

a. Calculate the horizontal pressure from Equation 1 with $n = 1$ for several points in the base at a depth approximately equal to the maximum height of the overburden.

b. Extrapolate a straight line through the points obtained in *a* to the top of the base.

For layered bases with sand over clay, the elasticity solution is less reliable. For lightly loaded systems (low initial slopes), Equation 1 with a value of $n = 2$ accurately estimates the pressures in the clay layer but significantly underestimates the pressures in the upper sand stratum. A value of $n = 4$ to $n = 5$ in Equation 1 appears to be appropriate for the sand layer.

For layered bases with clay over sand, a multiple of $n = 2$ provides reasonable estimates of pressures in the lower sand stratum but significantly underestimates pressures in the clay layer near the top of the base. A procedure for estimating the pressures in the clay layer that reduces the errors near the top of the base is as follows:

a. Calculate the pressures predicted by Equation 1 with $n = 2$ for the lower sand layer and determine the slope of a straight line. This line is representative of the pressures in this region.

b. Calculate the pressures from Equation 1 with $n = 2$ for a point in the upper clay layer at the boundary between layers.

c. Represent the pressures in the clay layer by a straight line from the point obtained in *b* using the slope obtained in *a*.

Single triangle surfaces (S2)

Equation 1 with $n = 1$ provides an excellent indication of the distribution of pressures throughout all base configurations.

Double triangle surfaces (S3)

For the pressures in the base below the double triangle surface (and, presumably, for other undulating surfaces), Equation 1 with $n = 1$ accurately predicts the pressures throughout homogeneous sand bases.

For a homogeneous clay base, a factor of $n = 2$ provides the best estimate of pressures.

For layered bases, Equation 1 with values of $n = 1$ for sand layers and $n = 2$ for clay layers provides good estimates of pressures in the base.

Single triangle surfaces (S4)

The elasticity solution is less reliable for systems in which the surface slope is initially downward to a horizontal extension. For homogeneous sand bases the pressures appear to be approximated by the average of two distributions obtained by the following procedures:

a. Calculate the geostatic pressure at a depth in the base equal to the maximum height of the surcharge and connect this point with a straight line to zero at the top of the surcharge.

b. Calculate the pressure by Equation 1 with $n = 1$ at a point in the base at a depth equal to the height of the surcharge. Draw a straight line from this point to zero at the top of the surcharge.

The elasticity solution with $n = 1$ provides a good approximation of pressures in a homogeneous clay base for points below a depth in the base equal to the maximum height of the surcharge. However, it overestimates the pressures near the top of the base and provides no means of indicating the pressures in the surcharge. The following procedure appears to reasonably approximate the distribution of pressures throughout the system:

a. Calculate the pressures by Equation 1 with $n = 1$ for several points below a depth in the base equal to the maximum height of the surcharge.

b. Extrapolate a straight-line approximation to the points obtained in *a* to its intersection with the top of the base.

c. Draw a straight line from the terminus of the line in *b* at the top of the base to zero at the top of the surcharge.

For a layered base with a sand stratum above clay, Equation 1 with $n = 1$ provides a good estimate of the pressures in the clay layer but significantly overestimates pressures in the sand stratum and again provides no indication of pressures in the surcharge. The following procedure is suggested for this case:

a. Calculate the pressures from Equation 1 with $n = 1$ for the lower clay stratum.

b. Calculate the geostatic pressure in the sand layer at the boundary between layers. Draw a straight line from this point to zero pressure at the top of the surcharge.

For a layered base with a clay layer above sand, the following steps are suggested:

a. The pressures in the lower sand stratum appear to be relatively unaffected by the surcharge. Hence the initial geostatic pressures provide an adequate estimate.

b. Calculate the pressures from Equation 1 with $n = 1$ for several points in the clay layer near the boundary between layers. Extrapolate a straight-line approximation through these points to its intersection with the top of the base.

c. Calculate a horizontal pressure in the surcharge material at the top of the base from

$$p = \gamma_s h_s \tan^2(45 - \phi/2) \tag{2}$$

where

γ_s = unit weight of the surcharge material

h_s = maximum height of the surcharge

ϕ = angle of internal friction of the surcharge material

d. Draw a straight line from the point obtained in *c* to zero pressure at the top of the surcharge.

Double triangle surfaces (S5)

For undulating surfaces with initial downward slopes and homogeneous sand bases, the pressures throughout the system may be estimated by the same procedures as those for the single triangle surface (S4).

The pressures in a homogeneous clay base may be estimated by the same procedures as for a homogeneous clay base in a single triangle surface (S4). Pressures in the surcharge above the base may be approximated by the

procedures for a layered base with a sand stratum above clay in a single triangle surface (S4).

The procedures described for the single triangle surface (S4) may be used to estimate pressures for a layered system with sand overlying clay and for a layered system with a clay layer above sand.

4 CSOILP User's Guide

Purpose of CSOILP

CSOILP estimates the at-rest soil pressures against a vertical rigid wall by combining gravity turn-on and theory of elasticity stresses. CSOILP is written to operate under Microsoft Windows (3.1, 3.11, 95, NT). This chapter will discuss the operation of the program.

General Soil System

The general soil system accommodated by CSOILP is shown in Figure 73. The system is assumed to be uniform to the plane of the figure. A typical 0.3-m (1-ft) slice of the uniform system is used for analysis. All results are assumed to be "per 1 ft" of the system. (The input and output of CSOILP are in non-SI units.)

Soil surface

The soil surface is described by a sequence of distances from the wall and elevations for each point at which a change in surface slope occurs. The surface is assumed to be straight between successive points and to extend ad infinitum horizontally at the elevation of the last surface point. The elevation of the lowest surface point is referred to as the datum in subsequent paragraphs.

Soil profile

The soil profile is composed of up to 15 layers with straight horizontal boundaries between adjacent layers. Soil layer boundaries that do not intersect the soil surface are assumed to extend ad infinitum horizontally. The last layer input is assumed to extend ad infinitum downward.

Soil properties

Each soil layer is assumed to be homogeneous. The following properties are required for each layer:

a. Soil saturated unit weight γ_s, lbf/ft^2. The program determines the buoyant unit weight γ' for submerged soil according to

$$\gamma' = \gamma_s - \gamma_w \tag{3}$$

where γ_w is the unit weight of water.

b. Soil moist unit weight γ_m, lbf/ft^2. The most unit weight is used for all soil above the water surface.

c. Angle of internal friction ϕ , deg. The program uses the angle of internal friction for calculating an at-rest earth pressure coefficient k_o from Jaky's equation:

$$k_o = 1 - \sin \phi \tag{4}$$

Water

The location of the water surface within the soil profile affects the effective unit weight of the soil. No other effects of water are considered in CSOILP.

Soil Pressure Calculations

The following paragraphs describe the procedures used for calculating the various soil pressures reported by CSOILP.

Calculation points

Soil pressures are calculated at the following locations:

a. At the intersection of the soil surface with the rigid wall (i.e., at the elevation of the first surface point input).

b. At the elevation of the bottom of each soil layer. (Note: Although the last layer input is assumed to extend ad infinitum downward, soil pressure calculations are terminated at the bottom elevation provided for the last layer.)

c. At the elevation of the water surface if the water elevation is between the first surface point elevation and the bottom elevation of the last soil layer.

d. At the elevation of the datum.

e. At 1-ft intervals commencing at the elevation of the first surface point.

Effective vertical soil pressure

The effective vertical soil pressure p_v, lbf/ft^2, as used herein is defined as the cumulative effective weight of soil commencing at the elevation of the first surface point as if the soil surface were horizontal at that elevation:

$$p_v = \int_0^{z_1} \gamma_e dz \tag{5}$$

where z_1 is the depth below the first surface point and γ_e is the effective soil unit weight.

At-rest pressure estimate for horizontal surface

If the soil is horizontal, the at-rest pressure reported by CSOILP is given by

$$p_o = p_v \cdot k_o \tag{6}$$

where p_o is the at-rest pressure, lbf/ft^2.

At-rest pressure estimates for irregular surfaces

At-rest pressures are estimated by combining gravity turn-on at-rest soil pressures for a horizontal surface at the datum and theory of elasticity solutions for horizontal stresses where the soil above the datum is treated as an equivalent surcharge load.

Equivalent surcharge loads

Two systems with irregular soil surfaces are illustrated in Figures 74 and 75. The equivalent soil surcharge at any point is equal to the cumulative effective unit weight of the soil above the datum. For the system shown in Figure 74, the datum coincides with the first surface point and all other surface points including the assumed extension of the surface to infinity at the elevation for the last surface point lying above this elevation. Consequently, the equivalent soil surcharge extends uniformly to infinity at the value of the last surface point. For the system shown in Figure 75, the datum coincides with the elevation for the last surface point, and the equivalent soil surcharge beyond this point is zero.

Stresses due to equivalent surcharge loads

Horizontal stresses at the wall computed using the theory of elasticity σ_h due to an equivalent surcharge are obtained from the theory of elasticity according to

$$\sigma_h = \frac{2}{\pi}\int_0^{\frac{\pi}{2}} q_{(\theta)} \sin^2 \theta d\theta \qquad (7)$$

where $q_{(\theta)}$ is the equivalent surcharge at an angle θ.

Total at-rest pressure estimate

The total at-rest pressure at any point below the datum is obtained from

$$p_{o,\,total} = p_o + n\sigma_h \qquad (8)$$

where p_o is the pressure from Equation 6, σ_h is the stress from theory of elasticity, and elasticity stress coefficient n is a factor supplied by the user, which depends on the configuration of the surface and the type of the soil in the backfill. For more information on n see the recommendations for selecting n presented in Chapters 2 and 3.

Program Operation

Main program screen

The main screen for CSOILP, shown in the following sample screen, contains a tool bar, menu items, and a status bar.

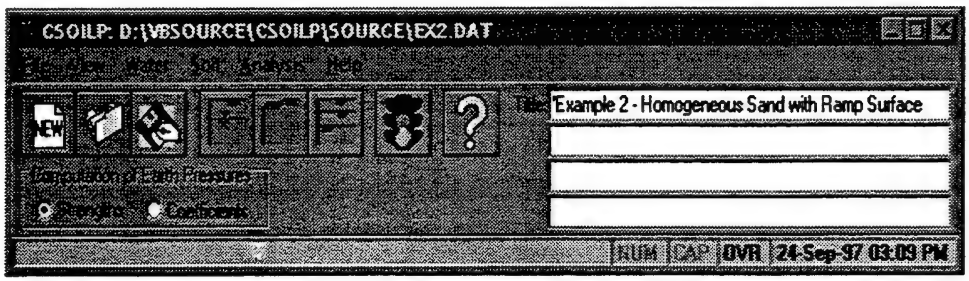

The functions of these components are described as follows:

a. The tool bar contains shortcuts to various program options and contains some control information that affects the input of data.

b. The menu items allow the input of data, saving of data, running of the analysis, and inspection of the output.

c. The status bar contains informational messages about current operations or items of data entry. The bar contains extended definitions of variables and applicable units.

The shortcut buttons duplicate the following menu items:

a. New

b. Open.

c. Save

d. Water information

e. Soil surface information

f. Soil properties and layers information

g. Run analysis

h. Help

The main menu contains the following menu and submenu items:

a. File: file operations

b. View: viewing of input and output

c. Water: input of water data

d. Soil: input of soil data

e. Analysis: run analysis

f. Help: viewing of help file

File menu. The file menu consists of the following items:

a. New: initializes the program for a new problem. Settings reset to defaults.

b. Open: opens a previously saved data file.

c. Save: saves the current input data to the currently opened file. Also saves the output to a desired file.

d. Save As: saves the current data to a file of the user's choosing.

e. Print: prints the input and output from the program.

f. Print setup: chooses the default printer and set the printer options.

g. Exit: exits from the program.

View menu. The view menu consists of the following items:

a. Input data: views the input data.

b. Analysis results: views the results of the analysis.

c. Plot of Input Geometry: views a plot of the input geometry to aid in checking data.

d. Plot of results: views a plot of the calculated earth pressures.

Soil menu. The soil menu consists of the following items:

a. Soil Surface Data

b. Soil properties and Layer Data

Water data

The dialog box for entry of the water data is shown in the following sample screen.

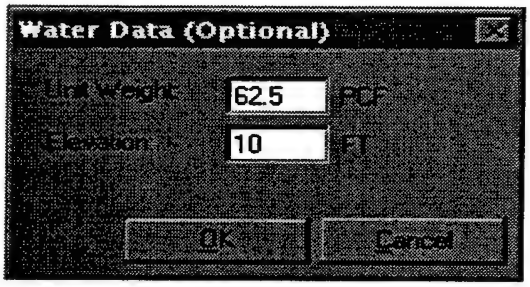

The water data consist of the following items:

a. Unit weight of water, lb/ft^3. The effective soil unit weight for submerged soil is calculated in the program by subtracting the weight of water from the saturated unit weight of the soil.

b. Elevation of the water table, ft. The water surface may be at any elevation. However, if the water surface is below the bottom elevation of the last soil layer, water will have no effect on soil pressures.

Soil surface data

The soil surface data entry screen is shown in the following sample screen.

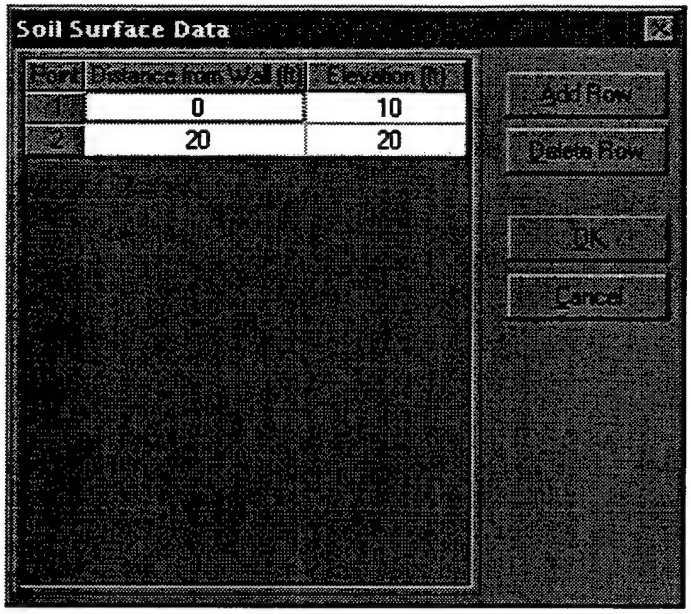

The soil surface data consist of the following:

a. Distance from the wall, ft

b. Elevation of the soil, ft

The program has the following characteristics:

a. The "Add Row" and "Delete Row" buttons may be used to add additional layers or to delete certain layers. To delete a layer, click on the row with the mouse and then click "Delete Row." Additional rows are always added to the end of the list.

b. To enter values in the grid, click on a cell or use the arrow keys to move to a cell and then type in a value.

c. At least one surface point is required. Up to 15 points are permitted.

d. If the distance of point 1 is greater than zero, a horizontal surface is assumed at the entered elevation of point 1 out to the distance entered for point 1.

e. If more than one surface is provided, distances and elevations must begin with the point nearest the wall and progress outward.

f. The surface is assumed to extend horizontally ad infinitum at the elevation of the last surface point provided.

g. The soil above the minimum of all surface point elevations (the datum) will be converted to an equivalent surcharge load for estimating at-rest pressures when an irregular soil surface is present.

Soil properties and layer data

The soil properties and layer dialog box is shown in the following sample screen.

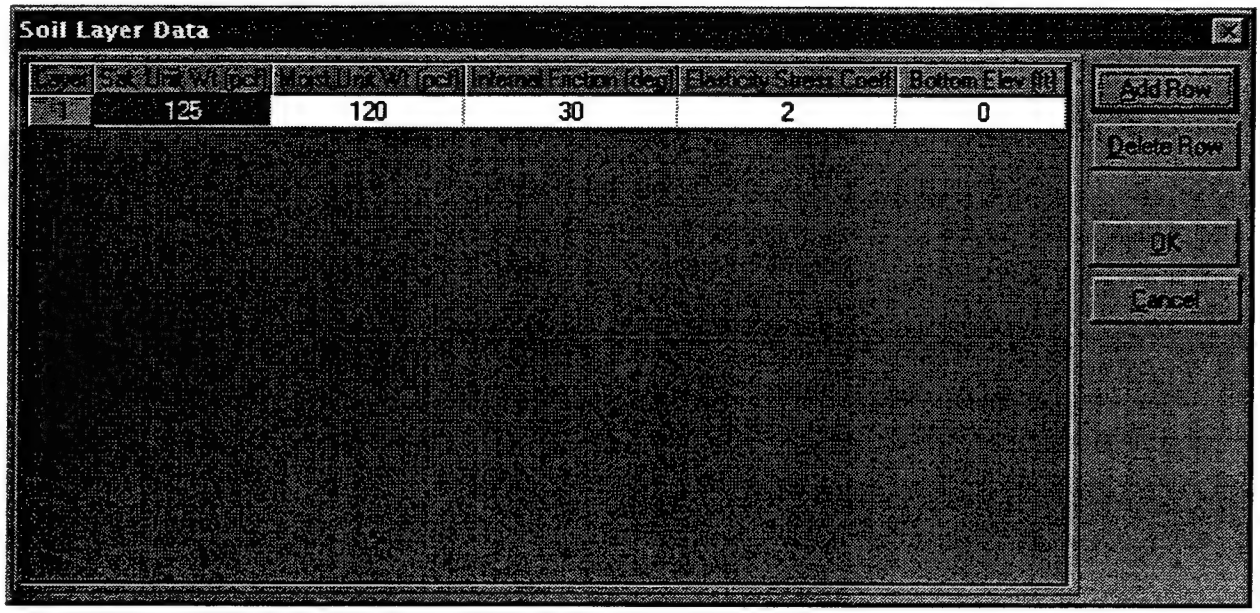

The following data items are included:

a. Saturated unit weight, lb/ft^3

b. Moist unit weight, lb/ft^3

c. Angle of internal friction, deg

d. At-rest pressure coefficient

e. Elasticity stress coefficient

f. Elevation of the bottom of the layer, ft

The program has the following characteristics:

a. The "Add Row" and "Delete Row" buttons may be used to add additional layers or to delete certain layers. To delete a layer, click on the row with the mouse and then click "Delete Row". Additional rows are always added to the end of the list.

b. To enter values in the grid, click on a cell or use the arrow keys to move to a cell and then type in a value.

c. Depending on whether "Strengths" or "Coefficients" was selected on the main screen, the soil layer data will require either the angle of internal friction or the at-rest pressure coefficient. The angle of internal friction is used to calculate the at-rest pressure coefficient.

d. At least one layer is required. Up to 15 layers are permitted.

e. Soil layer data must commence with the topmost layer and proceed sequentially downward.

f. The last soil layer is assumed to extend ad infinitum downward. The bottom elevation entered for the last layer is the depth to which soil pressures are calculated.

g. The layer bottom elevations must conform to the following guidelines:

(1) The bottom elevation of layer 1 must be less than the elevation of the first soil surface point.

(2) The bottom elevation of layer i must be less than layer $i = 1$.

h. The boundaries between adjacent layers are assumed to be horizontal.

i. If the top surface of layer 1 is irregular, then an elasticity stress coefficient will be required. Guidance for selection of the coefficient is discussed in the recommendations section of Chapters 2 and 3.

Plots of input geometry and results

The plots of the input geometry and results are shown in the following sample screens.

The plots have command buttons that let the user copy the picture as a Windows metafile to the clipboard. The user may then paste the graphic in a word processing program when preparing design reports. The user may also print the plot to the currently selected printer.

Output

The output from the program consists of a plot of the computed earth pressures and a tabular output of the computations. The tabular output consists of the gravity turn-on, theory of elasticity pressures, and the combined pressures at elevations down the wall.

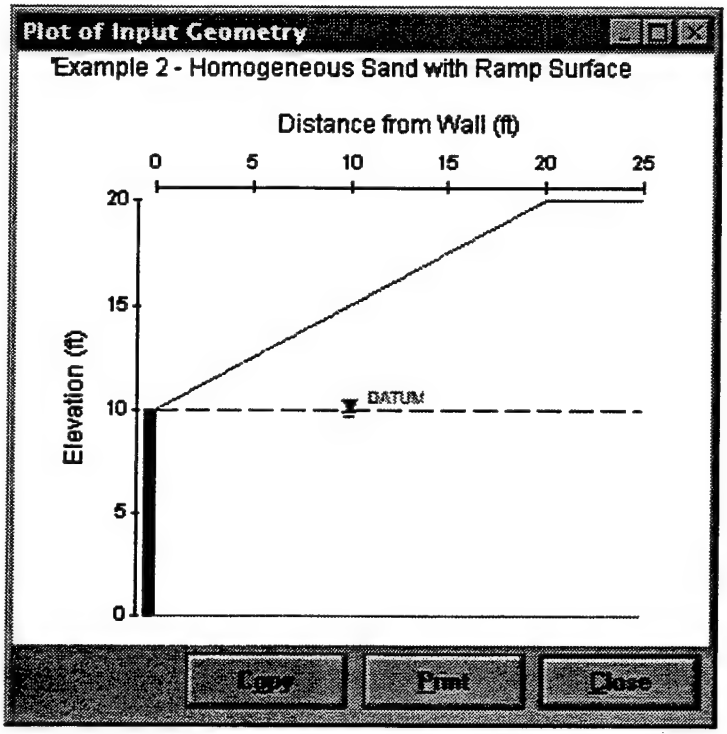
Plot of Input Geometry
Example 2 - Homogeneous Sand with Ramp Surface
Distance from Wall (ft)
0
5
10
15
20
25
Elevation (ft)
20
15
10
5
0
DATUM
Copy
Print
Close

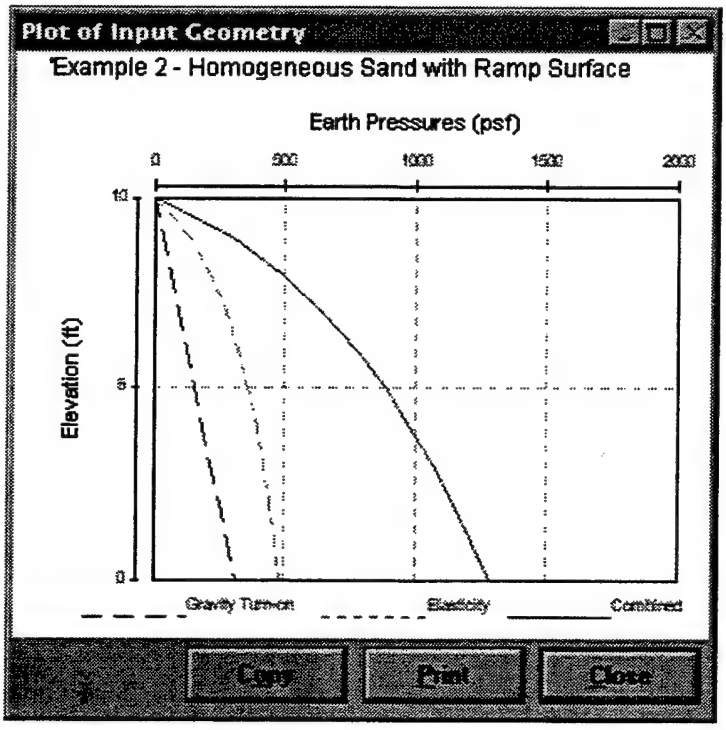
Plot of Input Geometry
Example 2 - Homogeneous Sand with Ramp Surface
Earth Pressures (psf)
0
500
1000
1500
2000
Elevation (ft)
10
5
0
Gravity Turn-on
Elasticity
Combined
Copy
Print
Close

Creating a Data File

The following discussion shows the format of the input data file. Units of feet and pounds are used by this program. To convert these units to SI units, use the following conversions: 1 ft = 0.3048 m; 1 lb = 0.454 kg; 1 lbf/ft^2 = 47.8 Pa; and 1 lb/ft^3 = 16.02 kg/m^3. Each command line is shown in bold print with an explanation of the variables shown immediately afterward. Variables in single quotes denote that the variable should be typed as shown or is a user-defined string. The format of the data file is as follows:

Heading (1 to 4 lines)

'heading'

'heading' = title line describing input. Must begin with a single apostrophe.

Soil Surface Data (1 or more lines)

'Surface' NSUR

Surface = command word
NSUR = number of surface points

DSUR(i) ELSUR(i)

DSUR(i) = horizontal distance from wall to *ith* surface point
ELSUR(i) = elevation of *ith* surface point

Soil Profile Data

'Soil' 'type' NLAYER

'Soil' = command word
'type' = 'Strengths' if friction angles are provided
'Coefficients' if at-rest coefficients are provided
NLAYER = number of soil layers (1 to 15)

GAMSAT GAMMST Property ELASCOF ELLAYB

GAMSAT = saturated unit weight of soil
GAMMST = moist unit weight of soil
Property = angle of internal friction if 'type' = 'Strengths'
at-rest pressure coefficient if 'type' = 'Coefficients'
ELASCOF = elasticity stress coefficient
ELLAYB = elevation of bottom of layer

Water Data

'Water' GAMWAT ELWAT

'Water'	= command word
GAMWAT	= unit weight of water
ELWAT	= elevation of water surface

Termination

'Finish'

'Finish'	= command word

5 CSOILP Examples

The example solutions described in the following paragraphs are intended only to illustrate the execution of CSOILP and are not to be construed as recommendations for its application to real systems.

Example 1

A soil system composed of a homogeneous sand with a horizontal surface is shown in Figure 76. The input data file for the system follows. Because of the horizontal surface, there is no theory of elasticity component of soil pressure and the total at-rest pressure is due only to the gravity turn-on component. Consequently the value of the elasticity coefficient is immaterial.

```
'Example 1 - Homogeneous Sand with Horizontal
Surface
SURFACE 1
 0          10
SOIL STRENGTHS   1
  125   120   30   0   0
WATER   62.4   10
FINISHED
```

The following are the echo print of the input data and the tabulated results of the analysis.

```
PROGRAM CSOILP - CALCULATION OF AT-REST PRESSURES BY
COMBINATION OF "GRAVITY-TURN-ON" AND THEORY OF
ELASTICITY COMPONENTS
DATE: 6-JULY-98                TIME: 12:35:25

                    **********
                    * INPUT DATA *
                    **********
```

I.—HEADING

'Example 1 - Homogeneous Sand with Horizontal Surface

II.—SURFACE POINTS

DIST. FROM WALL (FT)	ELEVATION (FT)
0.0	10.0

III.—SOIL LAYER DATA

<WEIGHT (PCF)> SAT.	MST.	INTERNAL FRICTION (DEG)	ELASTICITY COEFF.	BOTTOM ELEV. (FT)
125.0	120.0	30.0	0.00	0.0

IV.—WATER DATA

UNIT WEIGHT: 62.4 (PCF)
ELEVATION: 10.0 (FT)

PROGRAM CSOILP - CALCULATION OF AT-REST PRESSURES BY COMBINATION OF "GRAVITY-TURN-ON" AND THEORY OF ELASTICITY COMPONENTS

DATE: 6-JULY-98 TIME: 12:35:10

****
* RESULTS *
****

I.—HEADING

'Example 1 - Homogeneous Sand with Horizontal Surface

II.—EQUIVALENT SURCHARGE LOAD DUE TO IRREGULAR SURFACE ABOVE 10.0 (FT)
NONE

III.—PRESSURES ON WALL BELOW EL. 10.0 (FT)

ELEVATION (FT)	GRAVITY-TURN-ON PRESSURE (PSF)	ELASTICITY COMPONENT PRESSURE (PSF)	COMBINED GTO & ELASTICITY PRESSURE (PSF)
10.00	0.00	0.00	0.00
9.00	31.30	0.00	31.30
8.00	62.60	0.00	62.60
7.00	93.90	0.00	93.90
6.00	125.20	0.00	125.20

5.00	156.50	0.00	156.50
4.00	187.80	0.00	187.80
3.00	219.10	0.00	219.10
2.00	250.40	0.00	250.40
1.00	281.70	0.00	281.70
0.00+	313.00	0.00	313.00

Resultant Force for Combined Pressures = 1565.00 lbs
Resultant Location at elev. = 3.33 feet

The plot of the at-rest earth pressures is shown in Figure 77.

Example 2

A system with a "ramp" surface and the associated input data are shown in Figure 78. The soil above el 10 is treated as an equivalent surcharge on a horizontal datum at el 10. The total at-rest pressure is composed of the gravity turn-on pressure for a horizontal surface at el 10 and twice the theory of elasticity stresses due to the equivalent surcharge.

```
'Example 2 - Homogeneous Sand with Ramp Surface
SURFACE 2
0          10
20         20
SOIL STRENGTHS  1
125   120   30   2   0
WATER   62.5   10
FINISHED
```

The following are the echo print of the input data and results of the analysis.

```
PROGRAM CSOILP - CALCULATION OF AT-REST PRESSURES BY
COMBINATION OF "GRAVITY-TURN-ON" AND THEORY OF
ELASTICITY COMPONENTS
DATE: 6-JULY-98              TIME: 12:41:38

                    **********
                    * INPUT DATA *
                    **********

I.—HEADING

'Example 2 - Homogeneous Sand with Ramp Surface
```

II.—SURFACE POINTS

DIST. FROM WALL (FT)	ELEVATION (FT)
0.0	10.0
20.0	20.0

III.—SOIL LAYER DATA

<WEIGHT (PCF)> SAT.	MST.	INTERNAL FRICTION (DEG)	ELASTICITY COEFF.	BOTTOM ELEV. (FT)
125.0	120.0	30.0	2.00	0.0

IV.—WATER DATA

UNIT WEIGHT: 62.5 (PCF)
ELEVATION: 10.0 (FT)

PROGRAM CSOILP - CALCULATION OF AT-REST PRESSURES BY COMBINATION OF "GRAVITY-TURN-ON" AND THEORY OF ELASTICITY COMPONENTS
DATE: 6-JULY-98 TIME: 12:41:34

****
* RESULTS *
****

I.—HEADING

'Example 2 - Homogeneous Sand with Ramp Surface

II.—EQUIVALENT SURCHARGE LOAD DUE TO IRREGULAR SURFACE ABOVE 10.0 (FT)

DIST. FROM WALL (FT)	SURCHARGE LOAD (PSF)
0.00	0.00
20.00	1200.00

III.—PRESSURES ON WALL BELOW EL. 10.0 (FT)

ELEVATION (FT)	GRAVITY-TURN-ON PRESSURE (PSF)	ELASTICITY COMPONENT PRESSURE (PSF)	COMBINED GTO & ELASTICITY PRESSURE (PSF)
10.00	0.00	0.00	0.00
9.00	31.25	133.56	298.37
8.00	62.50	214.36	491.21
7.00	93.75	275.54	644.83

6.00	125.00	324.30	773.60
5.00	156.25	364.13	884.50
4.00	187.50	397.13	981.77
3.00	218.75	424.75	1068.25
2.00	250.00	448.02	1146.03
1.00	281.25	467.72	1216.69
0.00+	312.50	484.48	1281.46

Resultant Force for Combined Pressures = 8145.99 lbs
Resultant Location at elev. = 3.81 feet

The plot of the at-rest earth pressures is shown in Figure 79.

Example 3

A portion of a floodwall-levee system is shown in Figure 80. The soil system is composed of alternating sand layers. The soil above elevation 2 is treated as the equivalent surcharge on the horizontal datum as elevation 2.

```
'Example 3 - Levee Section, Granular Soil
'Irregular ground surface
'Interspersed strong and weak layers
SURFACE 3
 2        9
 26       3
 46       2
SOIL STRENGTHS  4
  102.5   102.5   23   1   4
  122.5   122.5   30   1  -1
  102.5   102.5   23   1  -4
  122.5   122.5   30   1  -10
WATER   62.5   14
FINISHED
```

The following are the echo print of the input data and the results of the analysis.

PROGRAM CSOILP - CALCULATION OF AT-REST PRESSURES BY COMBINATION OF "GRAVITY-TURN-ON" AND THEORY OF ELASTICITY COMPONENTS
DATE: 6-JULY-98 TIME: 12:53:12

****
* INPUT DATA *
****

I.—HEADING

'Example 3 - Levee Section, Granular Soil
'Irregular ground surface
'Interspersed strong and weak layers

II.—SURFACE POINTS

DIST. FROM WALL (FT)	ELEVATION (FT)
2.0	9.0
26.0	3.0
46.0	2.0

III.—SOIL LAYER DATA

<WEIGHT SAT.	(PCF)> MST.	INTERNAL FRICTION (DEG)	ELASTICITY COEFF.	BOTTOM ELEV. (FT)
102.5	102.5	23.0	1.00	4.0
122.5	122.5	30.0	1.00	-1.0
102.5	102.5	23.0	1.00	-4.0
122.5	122.5	30.0	1.00	-10.0

IV.—WATER DATA

UNIT WEIGHT: 62.5 (PCF)
ELEVATION: 14.0 (FT)

PROGRAM CSOILP - CALCULATION OF AT-REST PRESSURES BY COMBINATION OF "GRAVITY-TURN-ON" AND THEORY OF ELASTICITY COMPONENTS
DATE: 6-JULY-98 TIME: 12:53:09

****
* RESULTS *
****

I.—HEADING

'Example 3 - Levee Section, Granular Soil
'Irregular ground surface
'Interspersed strong and weak layers

II.—EQUIVALENT SURCHARGE LOAD DUE TO IRREGULAR SURFACE ABOVE 2.0 (FT)

DIST. FROM WALL (FT)	SURCHARGE LOAD (PSF)
0.00	320.00
2.00	320.00
22.00	120.00
26.00	60.00
46.00	0.00

III.—PRESSURES ON WALL BELOW EL. 2.0 (FT)

ELEVATION (FT)	GRAVITY-TURN-ON PRESSURE (PSF)	ELASTICITY COMPONENT PRESSURE (PSF)	COMBINED GTO & ELASTICITY PRESSURE (PSF)
2.00	0.00	0.00	0.00
1.00	30.00	142.53	172.53
0.00	60.00	127.13	187.13
-1.00+	90.00	114.06	204.06
-1.00-	109.67	114.06	223.73
-2.00	134.04	102.89	236.93
-3.00	158.41	93.21	251.62
-4.00+	182.78	84.73	267.51
-4.00-	150.00	84.73	234.73
-5.00	180.00	77.24	257.24
-6.00	210.00	70.58	280.58
-7.00	240.00	64.63	304.63
-8.00	270.00	59.30	329.30
-9.00	300.00	54.50	354.50
-10.00+	330.00	50.17	380.17

Resultant Force for Combined Pressures = 3029.53 lbs
Resultant Location at elev. = -4.96 feet

A plot of the at-rest soil pressures is shown in Figure 81.

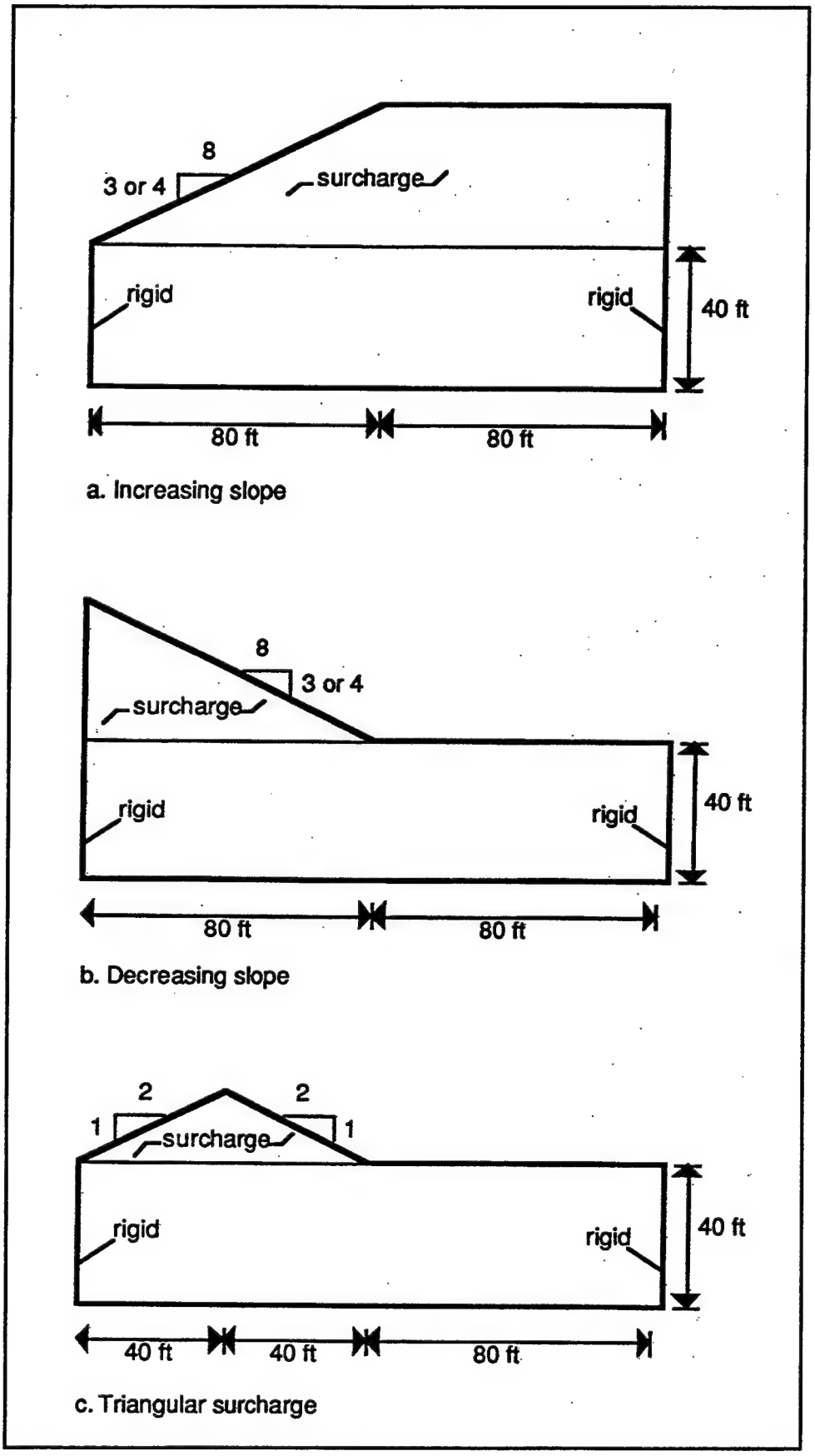

Figure 1. Soil systems (1 ft = 0.305 m)

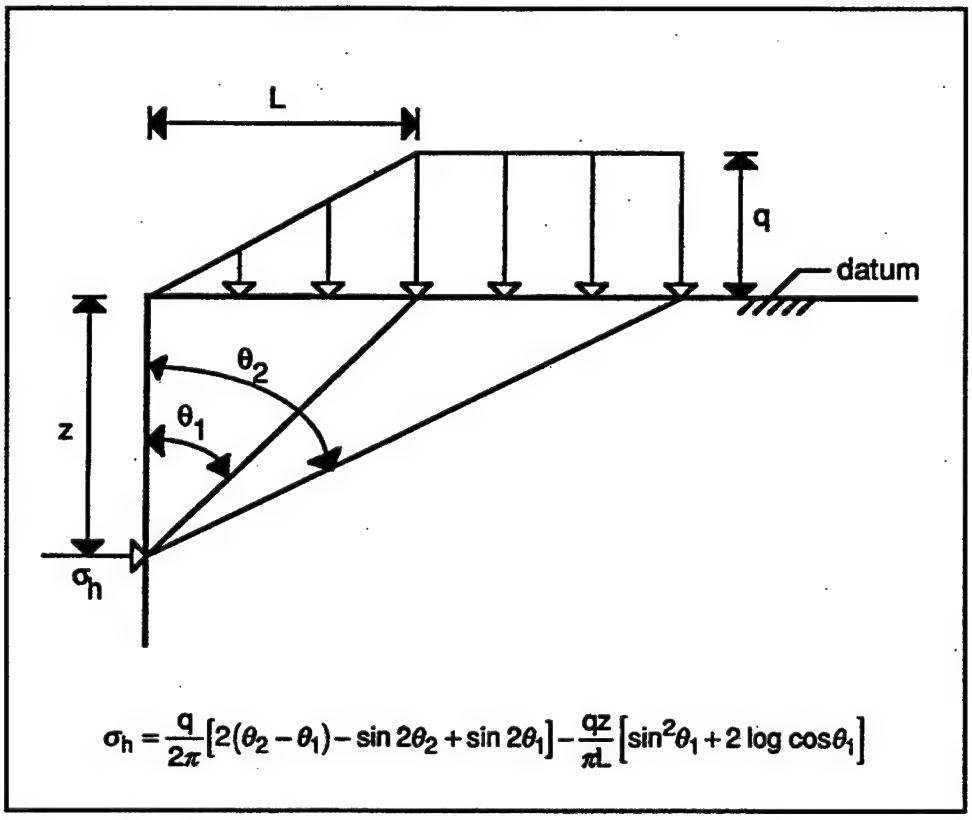

Figure 2. Theory of elasticity solution for increasing surface slope

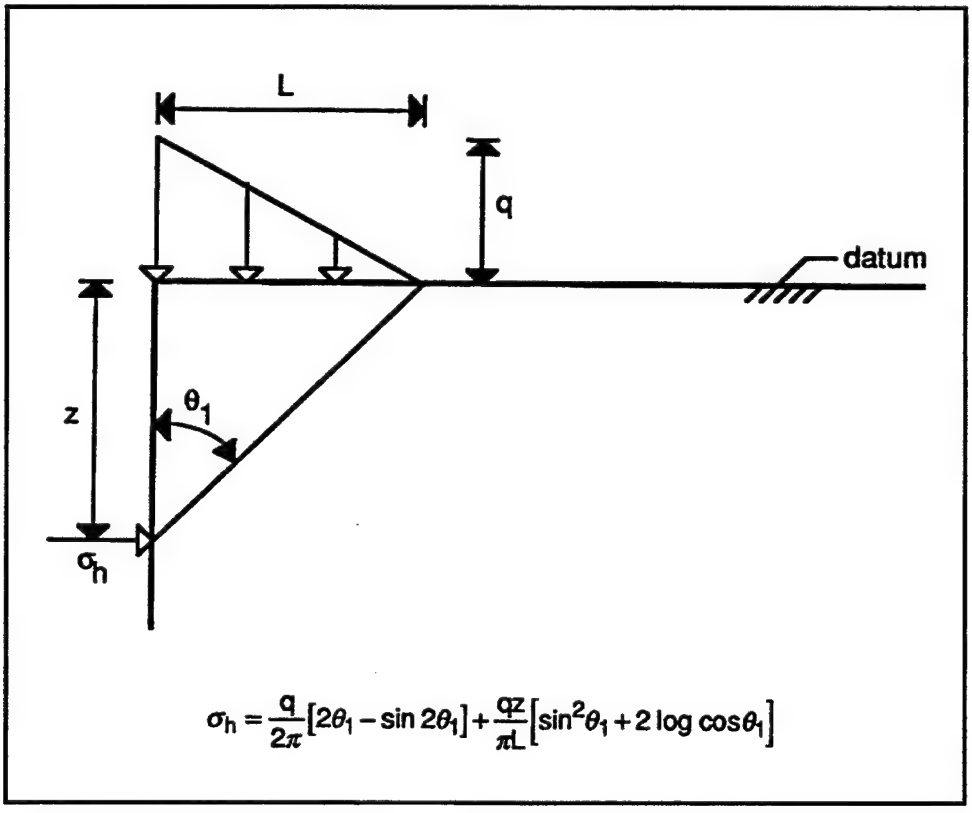

Figure 3. Theory of elasticity solution for decreasing surface slope

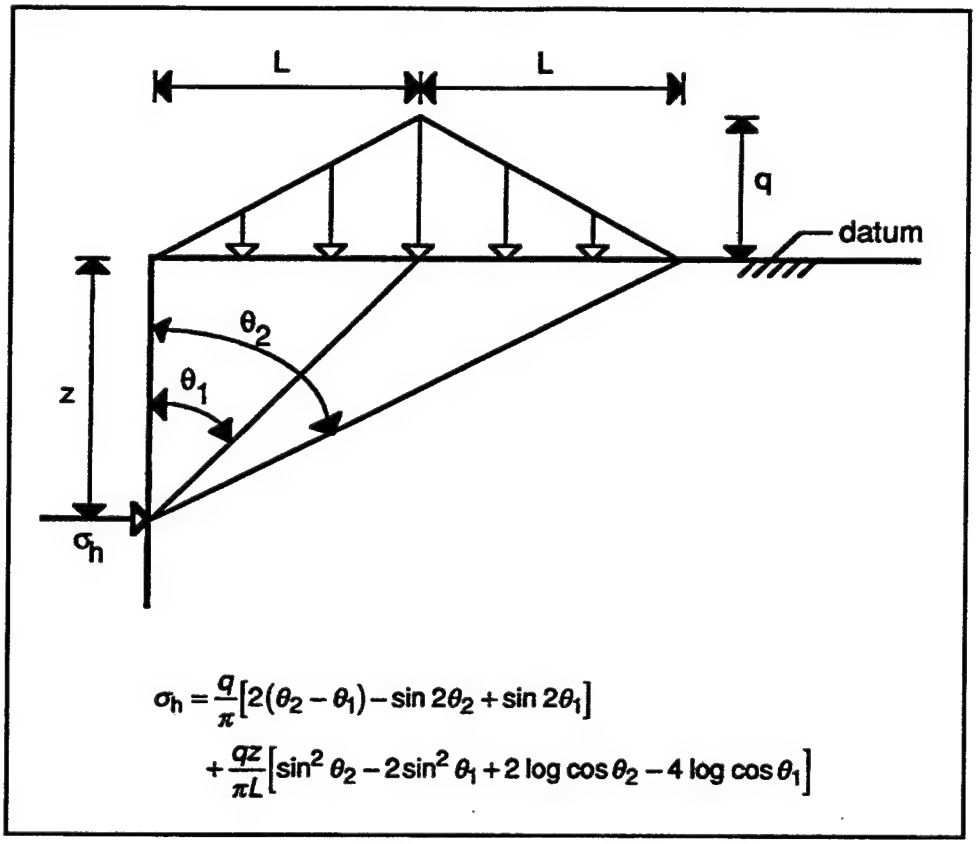

$$\sigma_h = \frac{q}{\pi}\left[2(\theta_2 - \theta_1) - \sin 2\theta_2 + \sin 2\theta_1\right]$$
$$+ \frac{qz}{\pi L}\left[\sin^2\theta_2 - 2\sin^2\theta_1 + 2\log\cos\theta_2 - 4\log\cos\theta_1\right]$$

Figure 4. Theory of elasticity solution for triangular surface

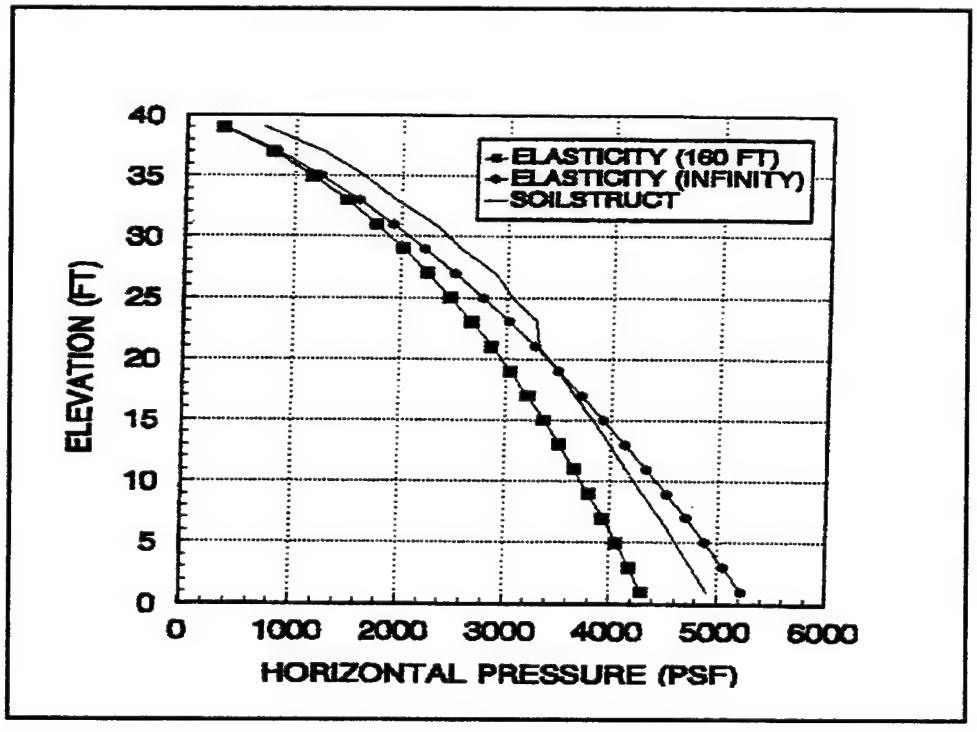

Figure 5. Soil pressures for increasing 3V on 8H surface slope ($K = 500$, $K_B = 250$), system for Figure 1a, soil type L (1 ft = 0.305 m; 1 lbf/ft^2 = 47.9 Pa)

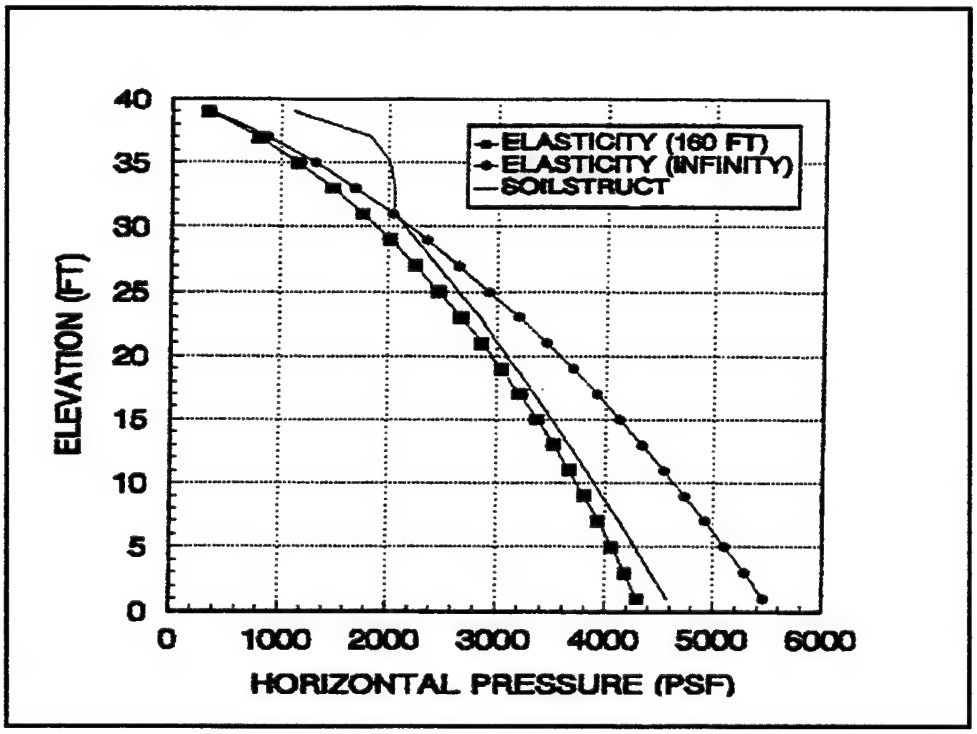

Figure 6. Soil pressures for increasing 3V on 8H surface slope ($K = 1{,}500$, $K_B = 750$), system for Figure 1a, soil type H (1 ft = 0.305 m; 1 lbf/ft^2 = 47.9 Pa)

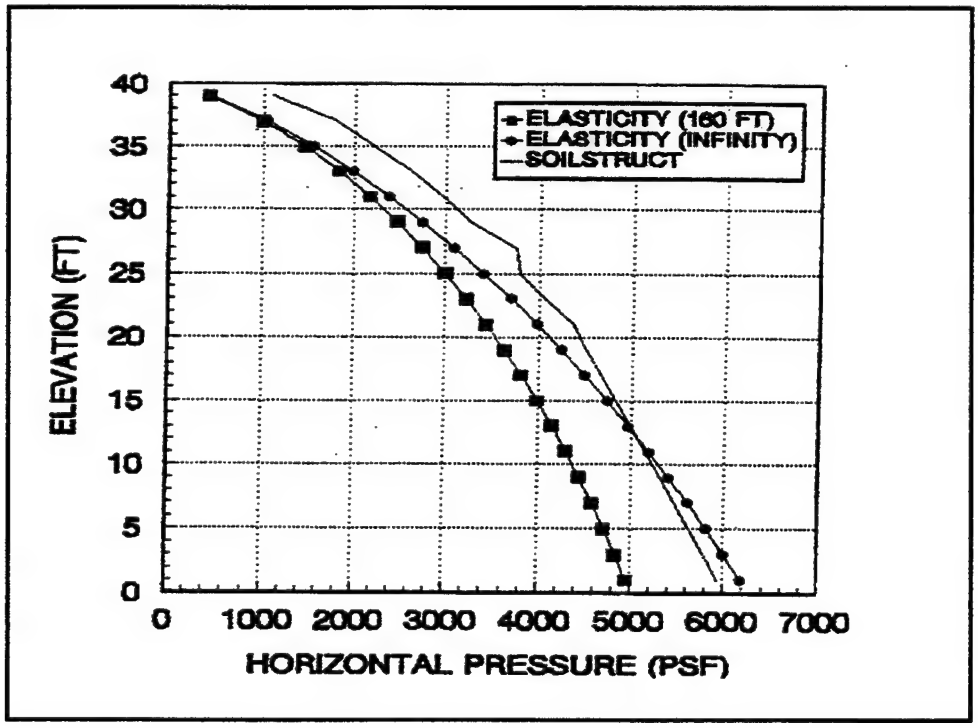

Figure 7. Soil pressures for increasing 4V on 8H surface slope ($K = 500$, $K_B = 250$), system for Figure 1a, soil type L (1 ft = 0.305 m; 1 lbf/ft^2 = 47.9 Pa)

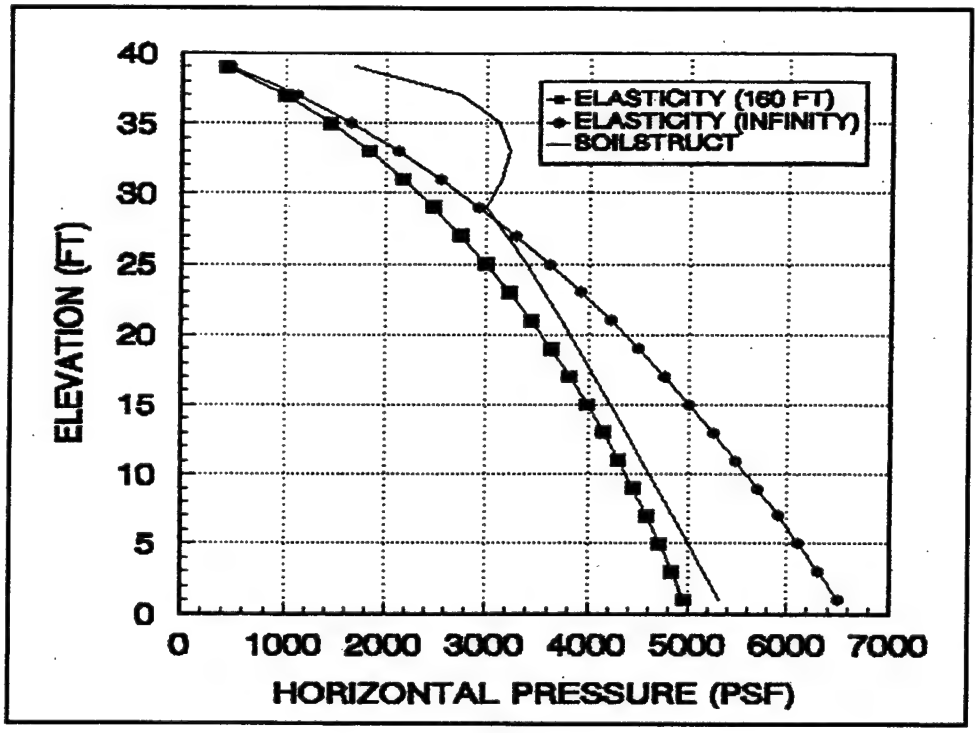

Figure 8. Soil pressures for increasing 4V on 8H surface slope ($K = 1{,}500$, $K_B = 750$), system for Figure 1a, soil type H (1 ft = 0.305 m; 1 lbf/ft^2 = 47.9 Pa)

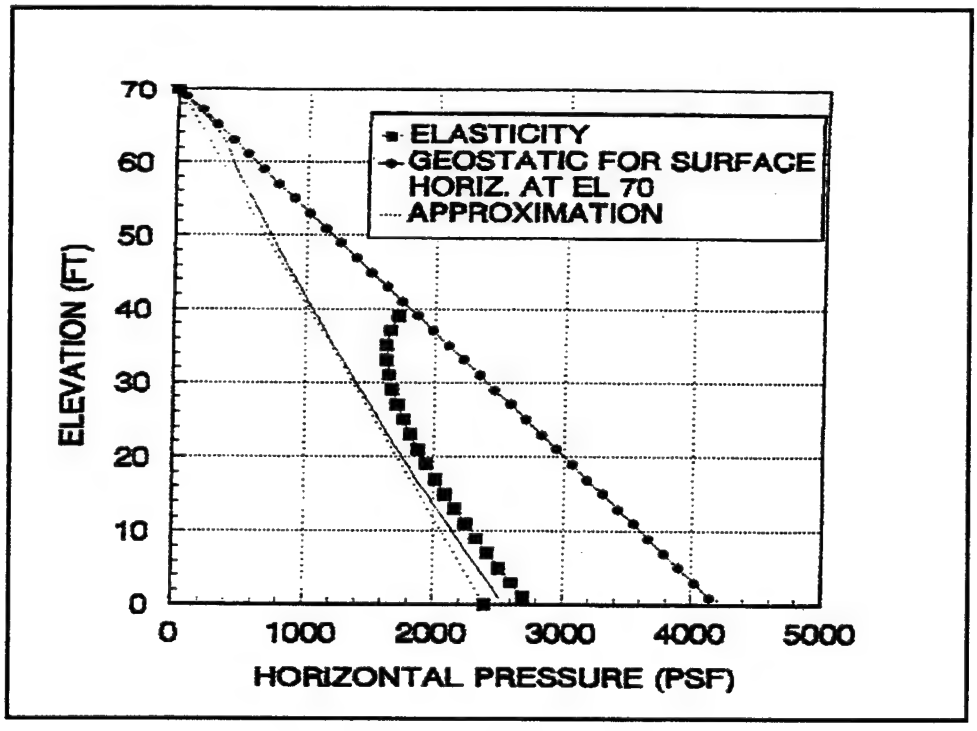

Figure 9. Soil pressures for decreasing 3V on 8H surface slope ($K = 500$, $K_B = 250$), system for Figure 1b, soil type L (1 ft = 0.305 m; 1 lbf/ft^2 = 47.9 Pa)

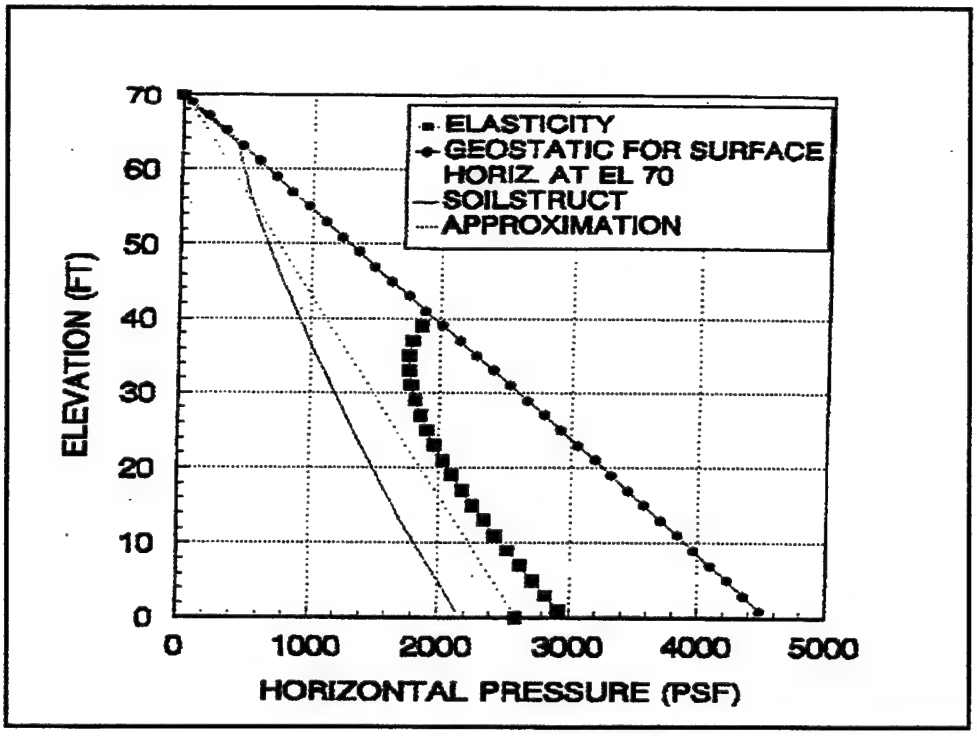

Figure 10. Soil pressures for decreasing 3V on 8H surface slope ($K = 1{,}500$, $K_B = 750$), system for Figure 1b, soil type H (1 ft = 0.305 m; 1 lbf/ft^2 = 47.9 Pa)

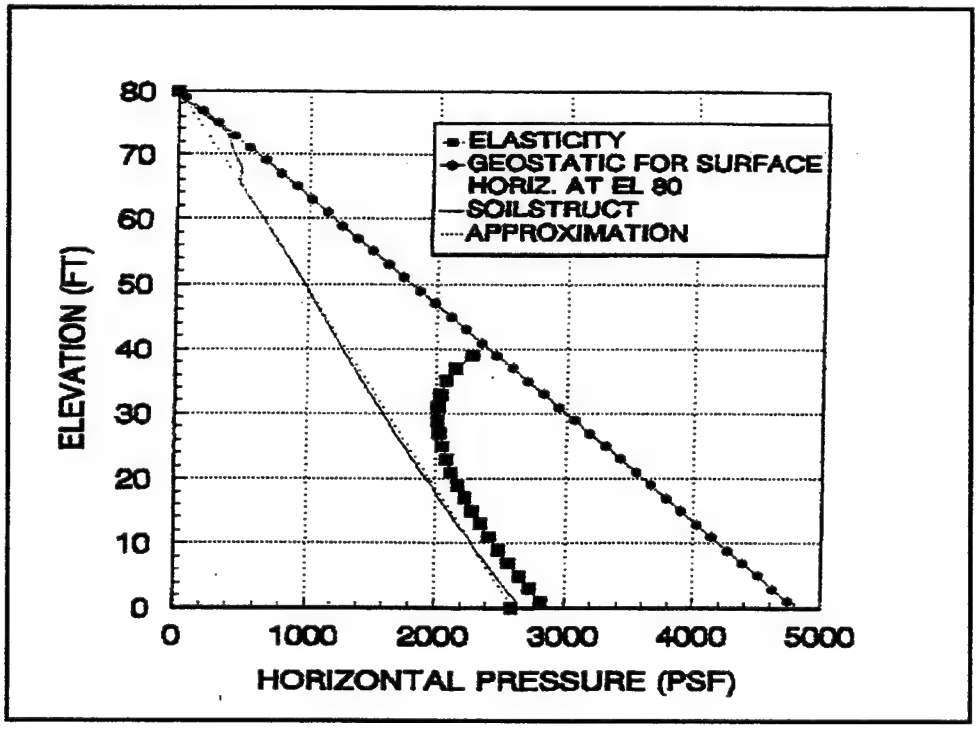

Figure 11. Soil pressures for decreasing 4V on 8H surface slope ($K = 500$, $K_B = 250$), system for Figure 1b, soil type L (1 ft = 0.305 m; 1 lbf/ft^2 = 47.9 Pa)

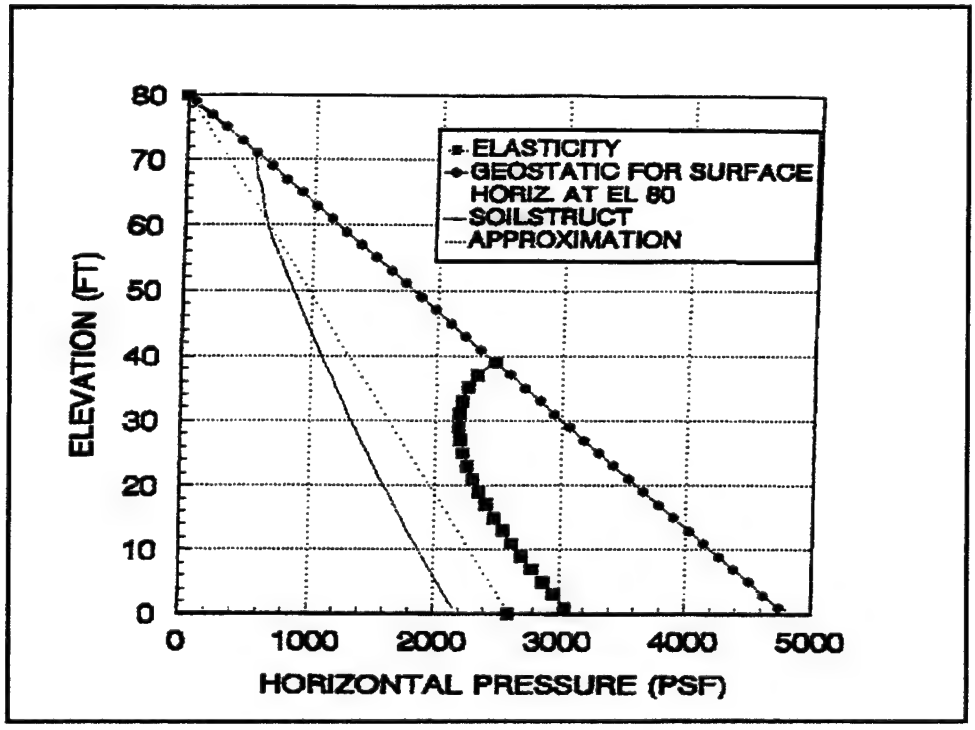

Figure 12. Soil pressures for decreasing 4V on 8H surface slope (K = 1,500, K_B = 750), system for Figure 1b, soil type H (1 ft = 0.305 m; 1 lbf/ft^2 = 47.9 Pa)

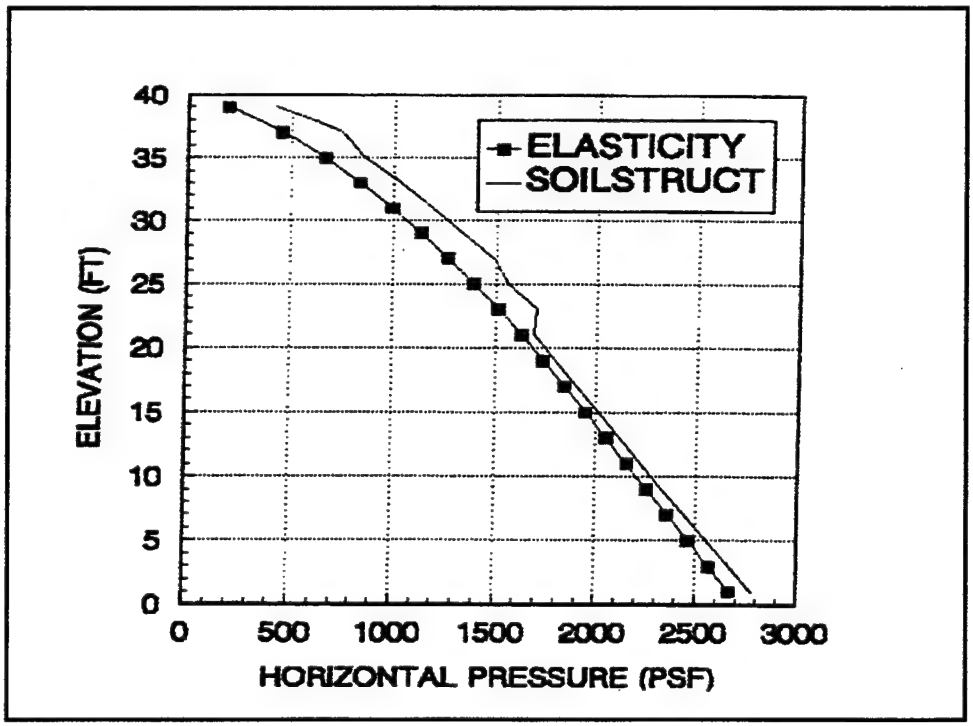

Figure 13. Soil pressures for triangular (1-2-1) surface to 24.4 m (80 ft) (K = 500, K_B = 250), system for Figure 1c, soil type L (1 ft = 0.305 m; 1 lbf/ft^2 = 47.9 Pa)

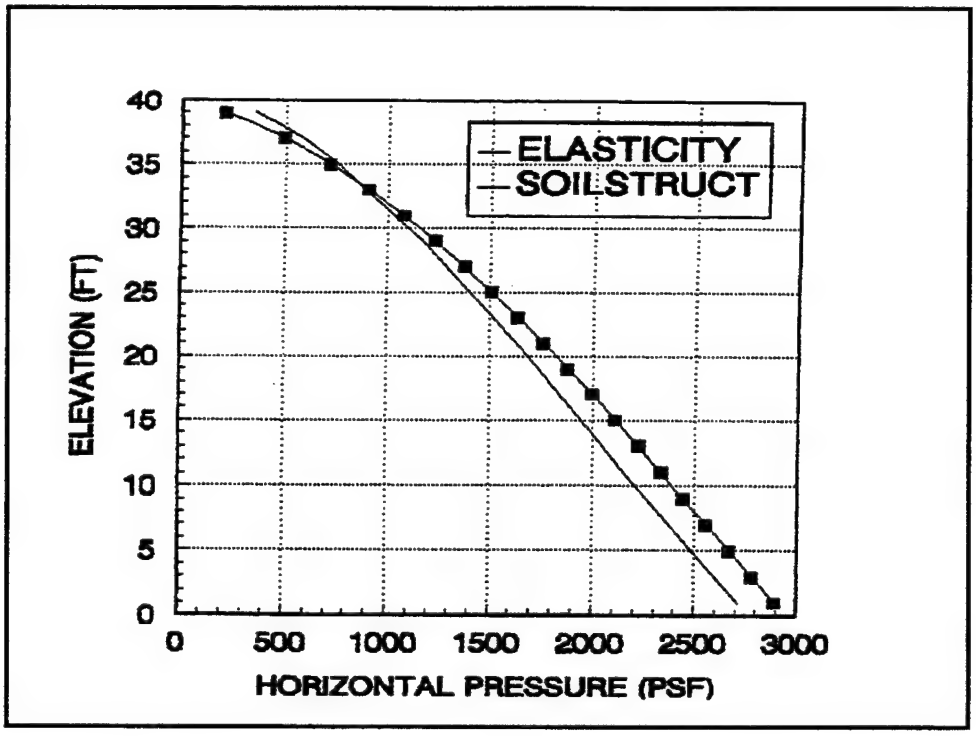

Figure 14. Soil pressures for triangular (1-2-1) surface to 24.4 m (80 ft) (K = 1,500, K_B = 750), system for Figure 1c, soil type H (1 ft = 0.305 m; 1 lbf/ft^2 = 47.9 Pa)

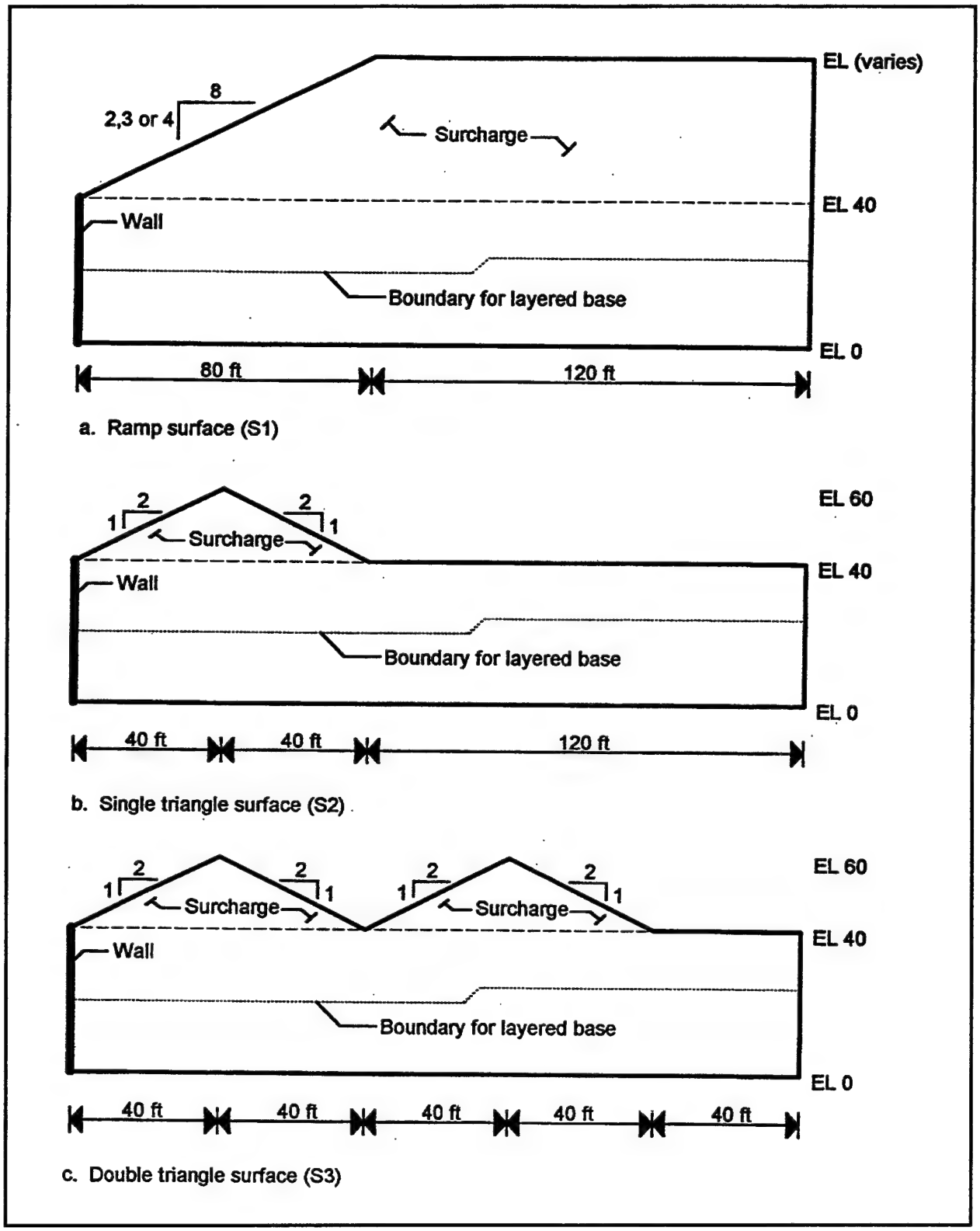

Figure 15. Surfaces sloping upward away from wall (1 ft = 0.305 m)

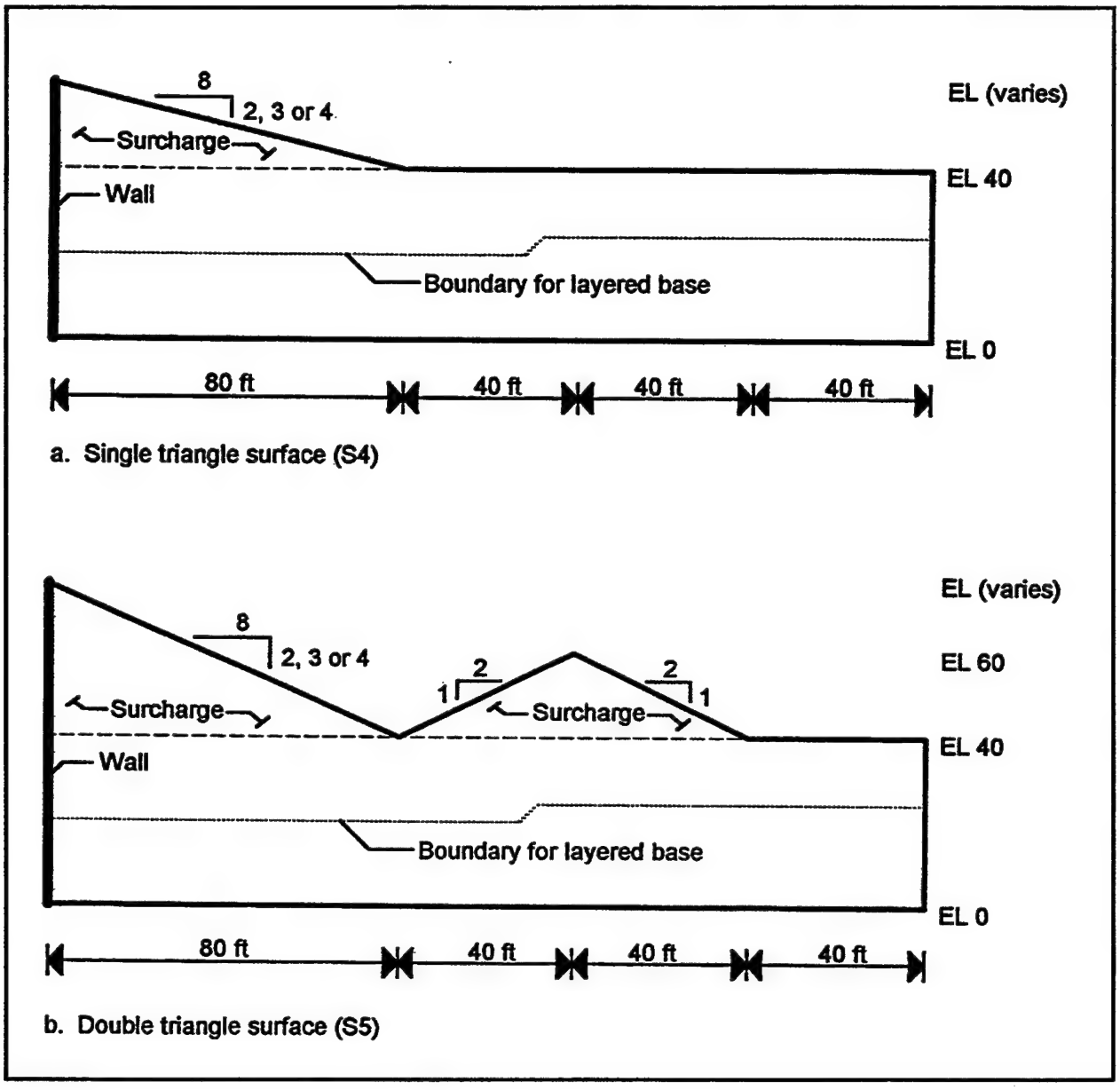

Figure 16. Surfaces sloping downward away from wall (1 ft = 0.304 m)

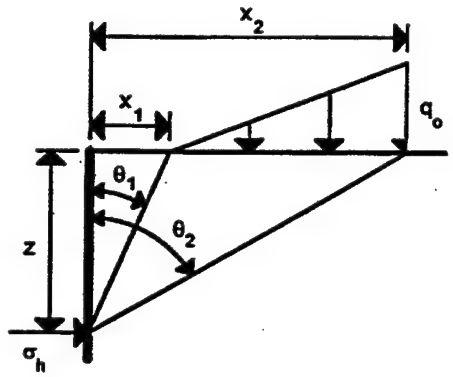

a. Upward sloping surcharge

$$\sigma_h = \frac{q_o z}{\pi(x_2 - x_1)}\left[\sin^2\theta_1 - \sin^2\theta_2 + 2\ln\cos\theta_1 - 2\ln\cos\theta_2\right] + \frac{qx_1}{2\pi(x_2 - x_1)}\left[2(\theta_1 - \theta_2) + \sin 2\theta_2 - \sin 2\theta_1\right]$$

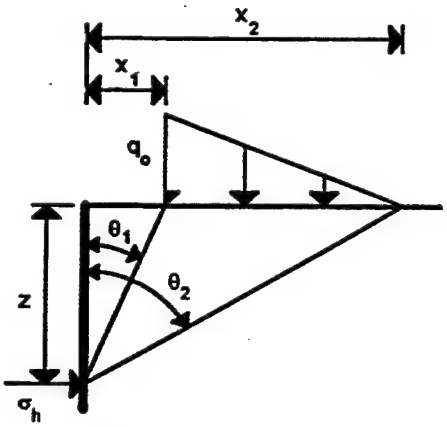

b. Downward sloping surcharge

$$\sigma_h = \frac{q_o z}{\pi(x_2 - x_1)}\left[\sin^2\theta_2 - \sin^2\theta_1 + 2\ln\cos\theta_2 - 2\ln\cos\theta_1\right] + \frac{qx_2}{2\pi(x_2 - x_1)}\left[2(\theta_2 - \theta_1) + \sin 2\theta_1 - \sin 2\theta_2\right]$$

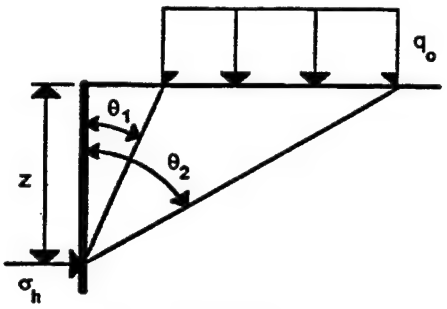

c. Uniform surcharge

$$\sigma_h = \frac{q_o}{2\pi}\left[2(\theta_2 - \theta_1) + \sin 2\theta_1 - \sin 2\theta_2\right]$$

Figure 17. Theory of elasticity solutions

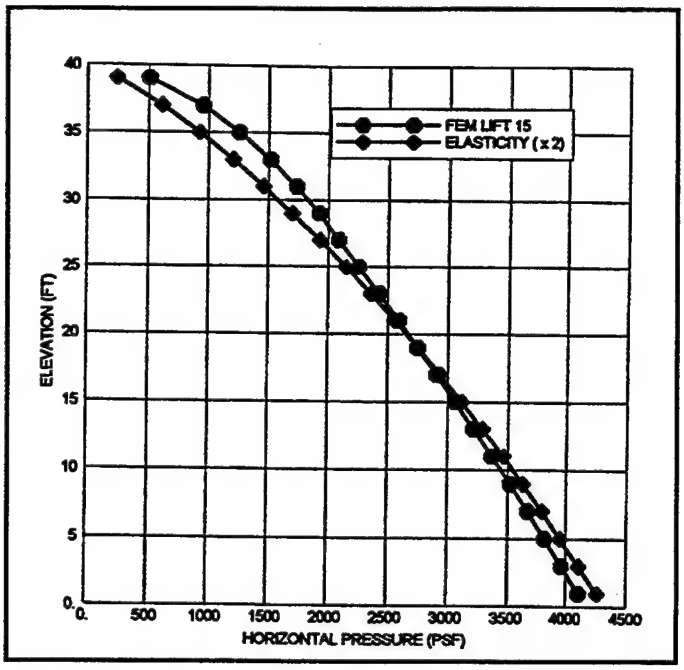

Figure 18. Ramp surface (S1), 2V on 8H slope, homogeneous sand-L surcharge and base (1 ft = 0.305 m; 1 lbf/ft^2 = 47.9 Pa)

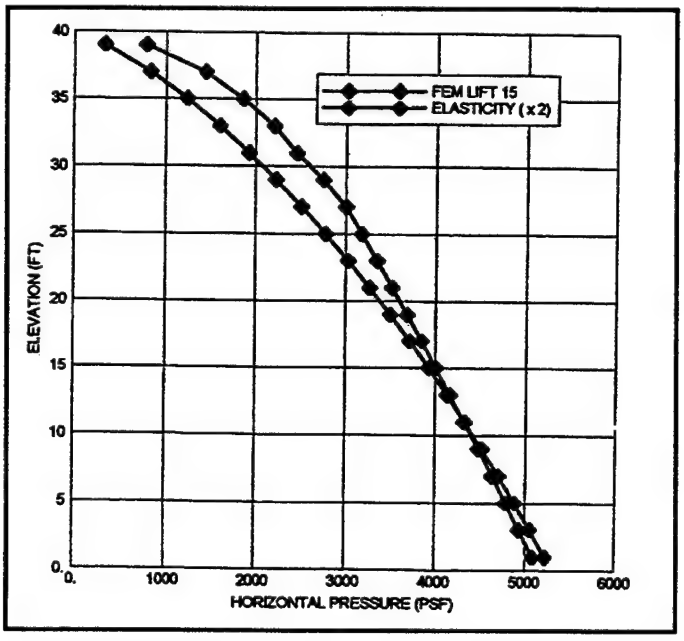

Figure 19. Ramp surface (S1), 3V on 8H slope, homogeneous sand-L surcharge and base (1 ft = 0.305 m; 1 lbf/ft^2 = 47.9 Pa)

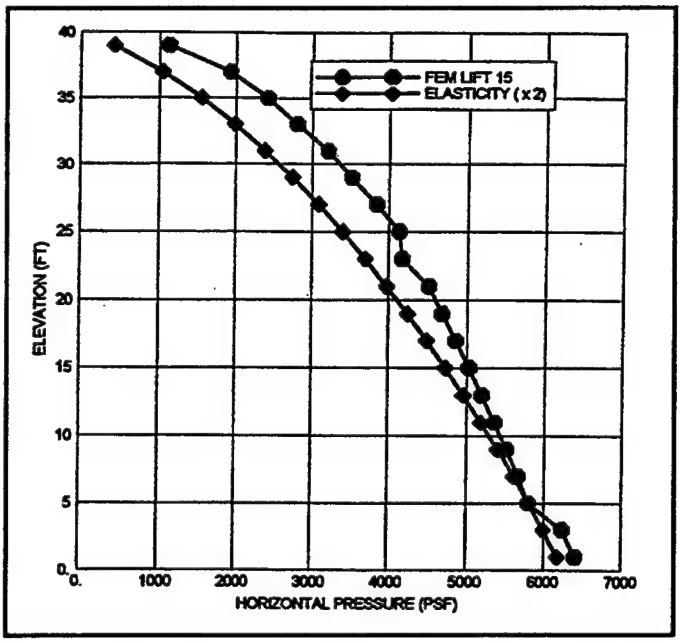

Figure 20. Ramp surface (S1), 4V on 8H slope, homogeneous sand-L surcharge and base (1 ft = 0.305 m; 1 lbf/ft^2 = 47.9 Pa)

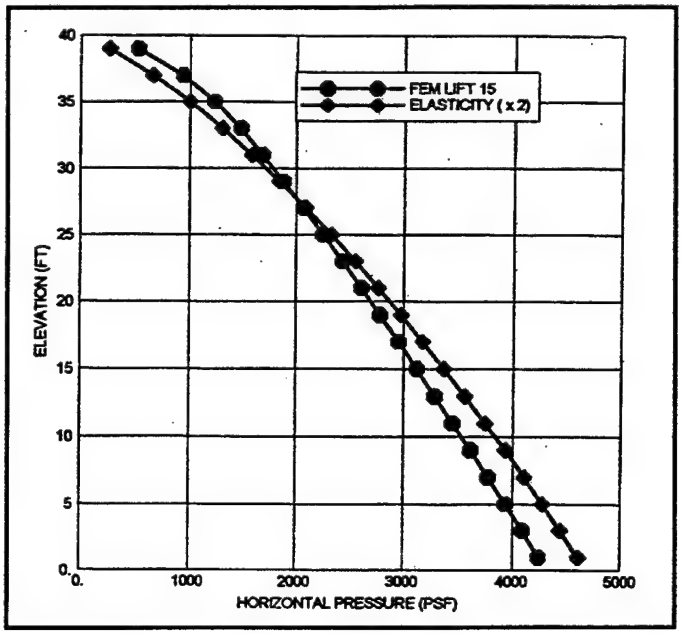

Figure 21. Ramp surface (S1), 2V on 8H slope, homogeneous sand-H surcharge and base (1 ft = 0.305 m; 1 lbf/ft^2 = 47.9 Pa)

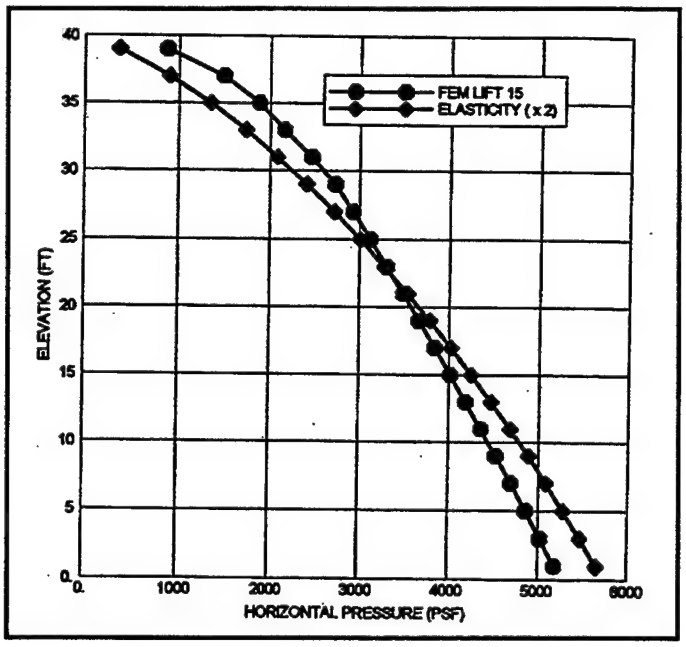

Figure 22. Ramp surface (S1), 3V on 8H slope, homogeneous sand-H surcharge and base (1 ft = 0.305 m; 1 lbf/ft^2 = 47.9 Pa)

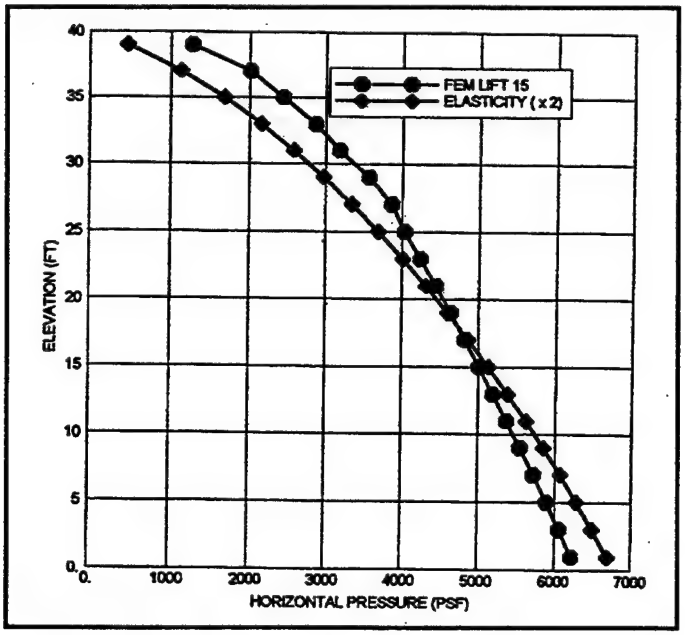

Figure 23. Ramp surface (S1), 4V on 8H slope, homogeneous sand-H surcharge and base (1 ft = 0.305 m; 1 lbf/ft^2 = 47.9 Pa)

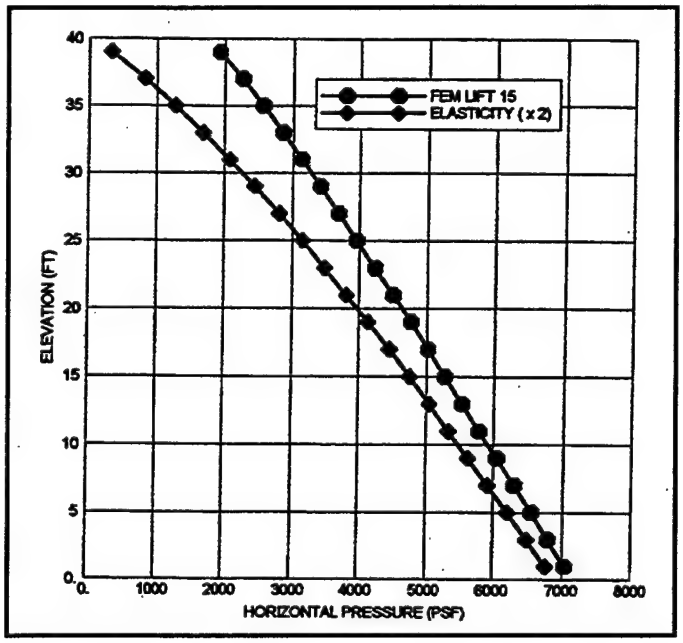

Figure 24. Ramp surface (S1), 2V on 8H slope, sand-H surcharge on homogeneous clay base (1 ft = 0.305 m; 1 lbf/ft^2 = 47.9 Pa)

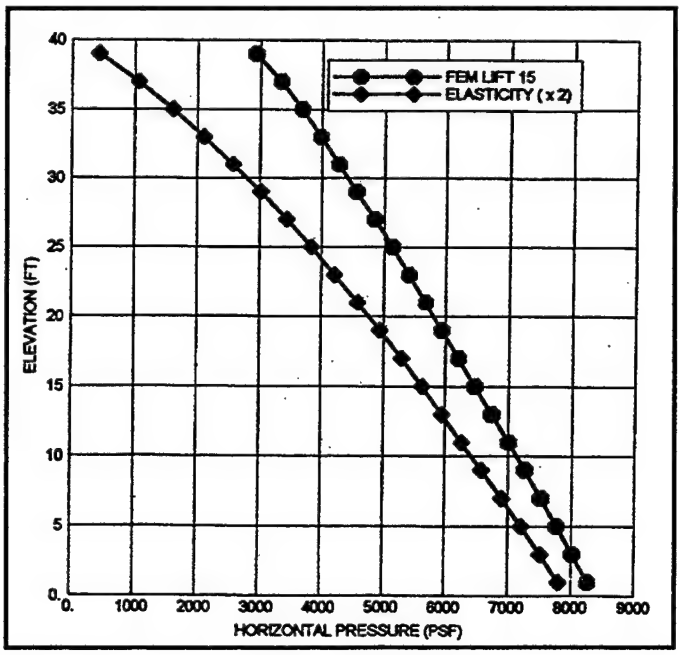

Figure 25. Ramp surface (S1), 3V on 8H slope, sand-H surcharge on homogeneous clay base (1 ft = 0.305 m; 1 lbf/ft^2 = 47.9 Pa)

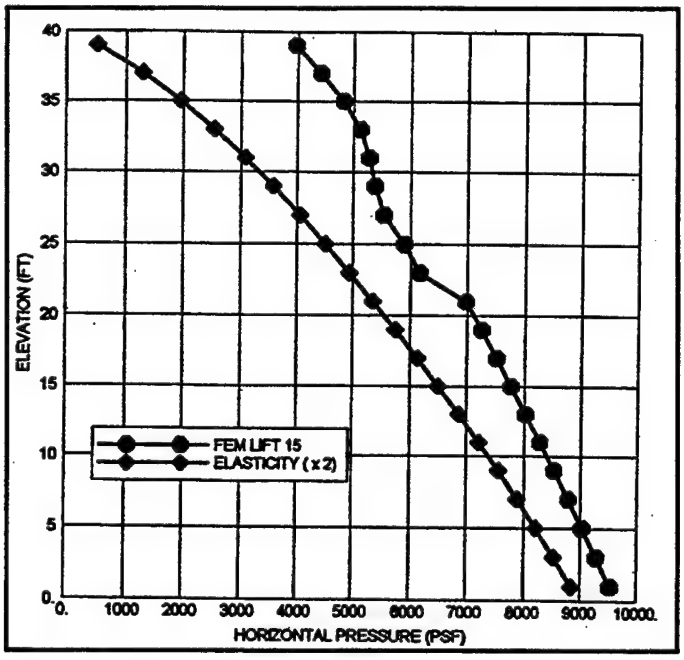

Figure 26. Ramp surface (S1), 4V on 8H slope, sand-H surcharge on homogeneous clay base (1 ft = 0.305 m; 1 lbf/ft^2 = 47.9 Pa)

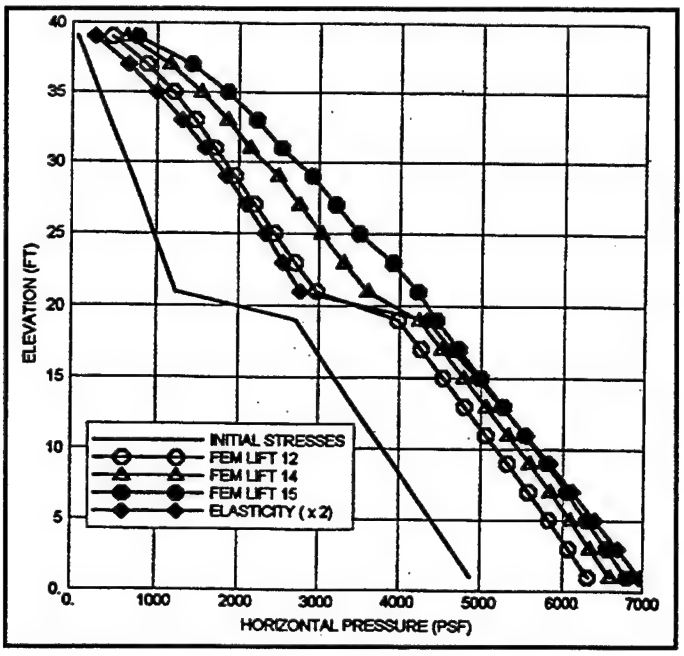

Figure 27. Ramp surface (S1), 2V on 8H slope, sand-H surcharge on layered sand-H over clay base (1 ft = 0.305 m; 1 lbf/ft^2 = 47.9 Pa)

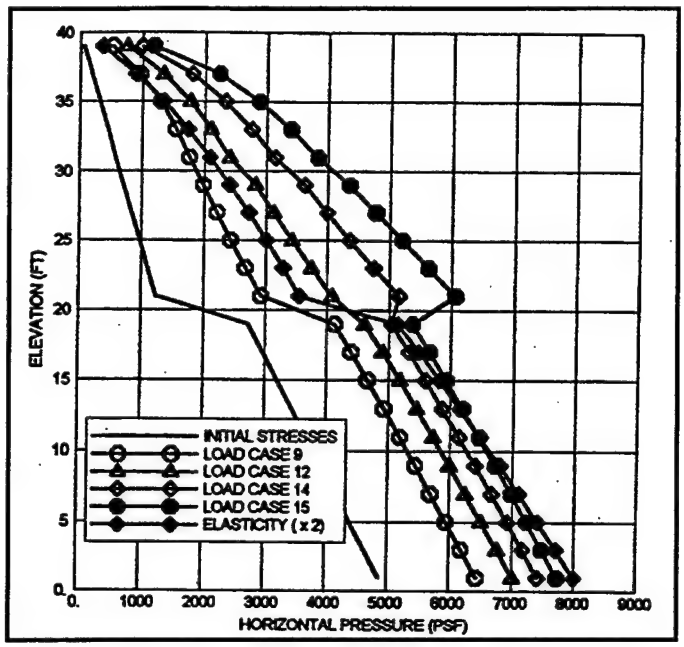

Figure 28. Ramp surface (S1), 3V on 8H slope, sand-H surcharge on layered sand-H over clay base (1 ft = 0.305 m; 1 lbf/ft^2 = 47.9 Pa)

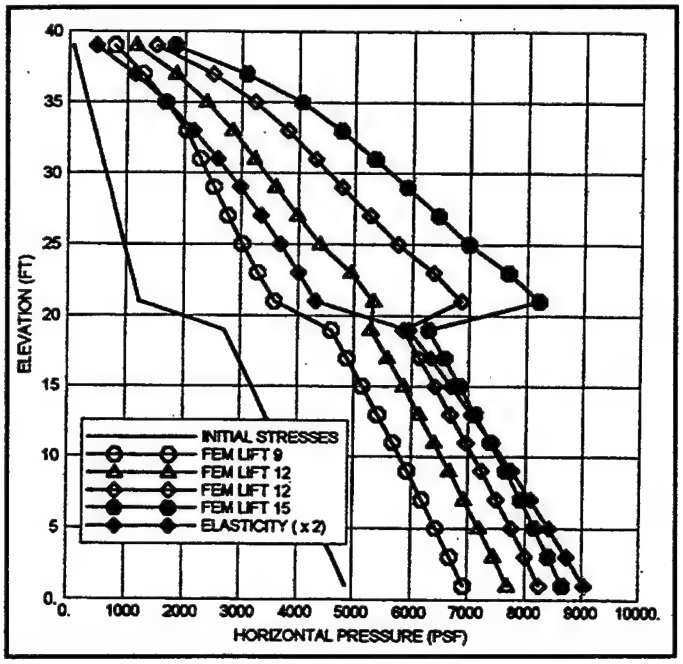

Figure 29. Ramp surface (S1), 4V on 8H slope, sand-H surcharge on layered sand-H over clay base (1 ft = 0.305 m; 1 lbf/ft^2 = 47.9 Pa)

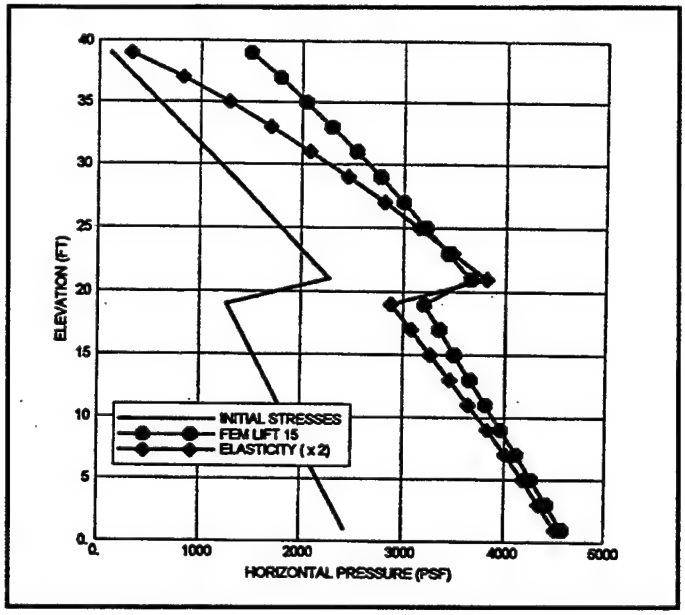

Figure 30. Ramp surface (S1), 2V on 8H slope, sand-H surcharge on layered clay over sand-H base (1 ft = 0.305 m; 1 lbf/ft^2 = 47.9 Pa)

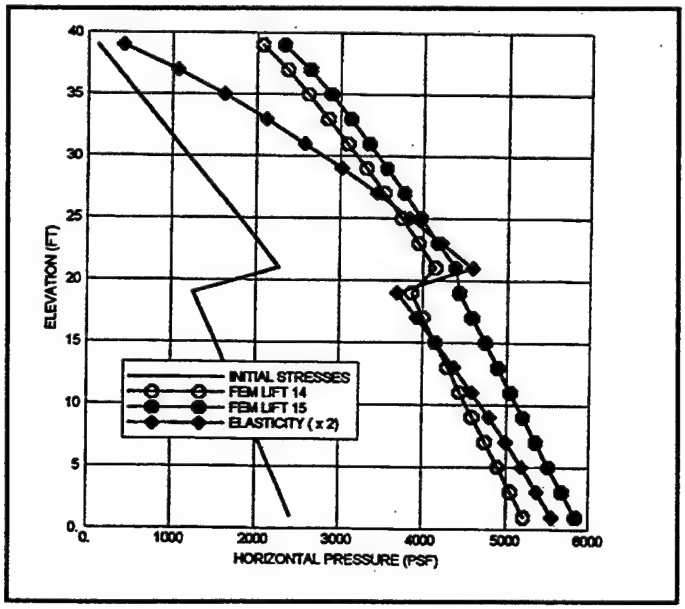

Figure 31. Ramp surface (S1), 3V on 8H slope, sand-H surcharge on layered clay over sand-H base (1 ft = 0.305 m; 1 lbf/ft^2 = 47.9 Pa)

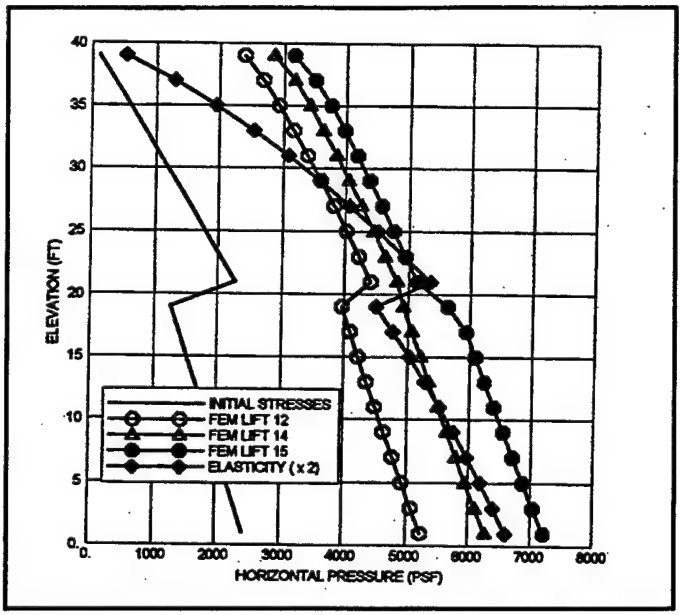

Figure 32. Ramp surface (S1), 4V on 8H slope, sand-H surcharge on layered clay over sand-H base (1 ft = 0.305 m; 1 lbf/ft^2 = 47.9 Pa)

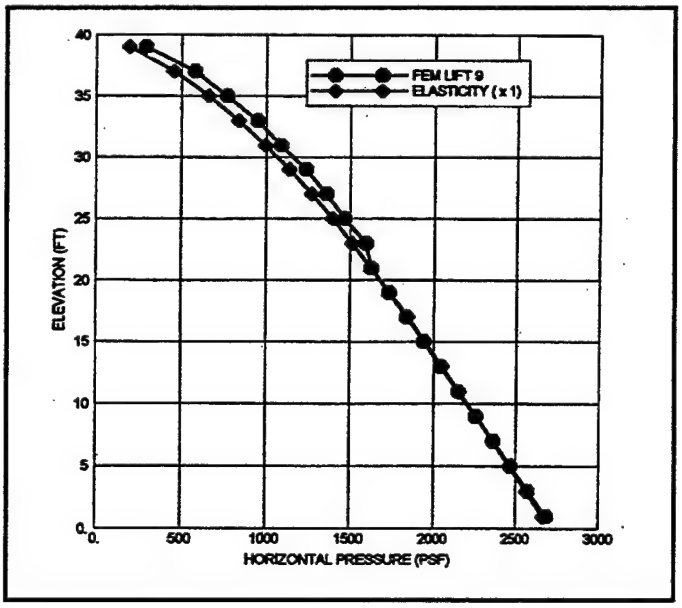

Figure 33. Single triangle surface (S2), homogeneous sand-L surcharge and base (1 ft = 0.305 m; 1 lbf/ft^2 = 47.9 Pa)

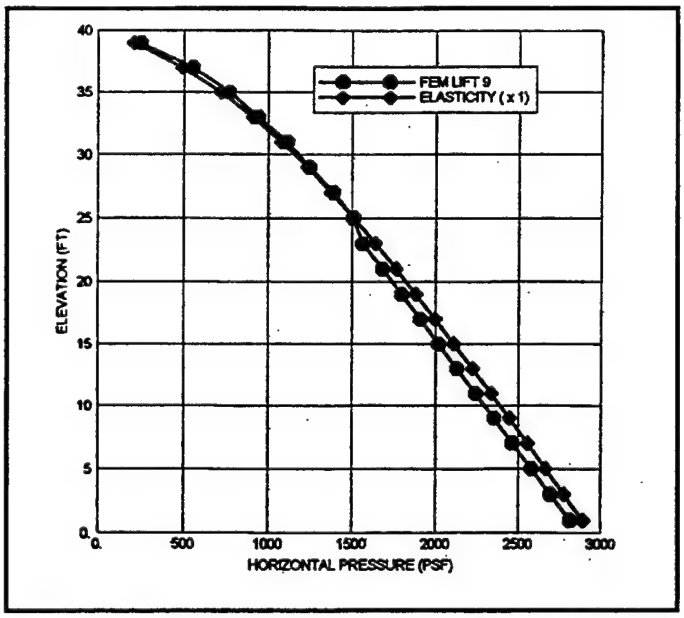

Figure 34. Single triangle surface (S2), homogeneous sand-H surcharge and base (1 ft = 0.305 m; 1 lbf/ft^2 = 47.9 Pa)

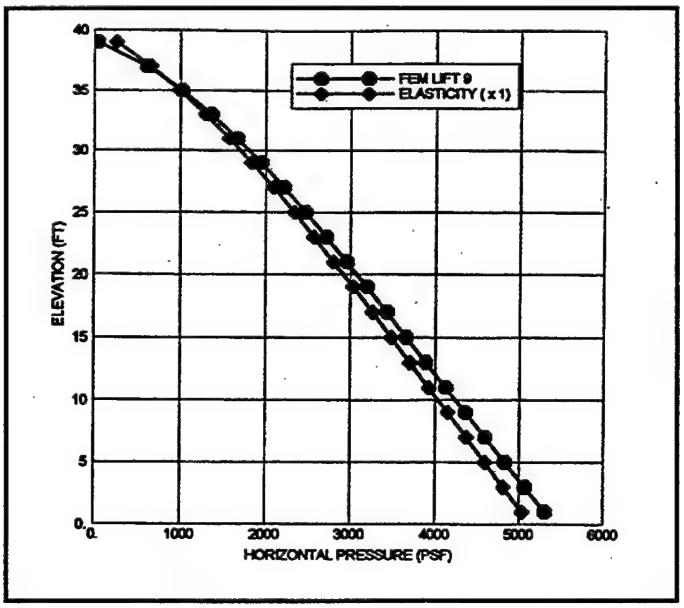

Figure 35. Single triangle surface (S2), sand-H surcharge on homogeneous clay base (1 ft = 0.305 m; 1 lbf/ft^2 = 47.9 Pa)

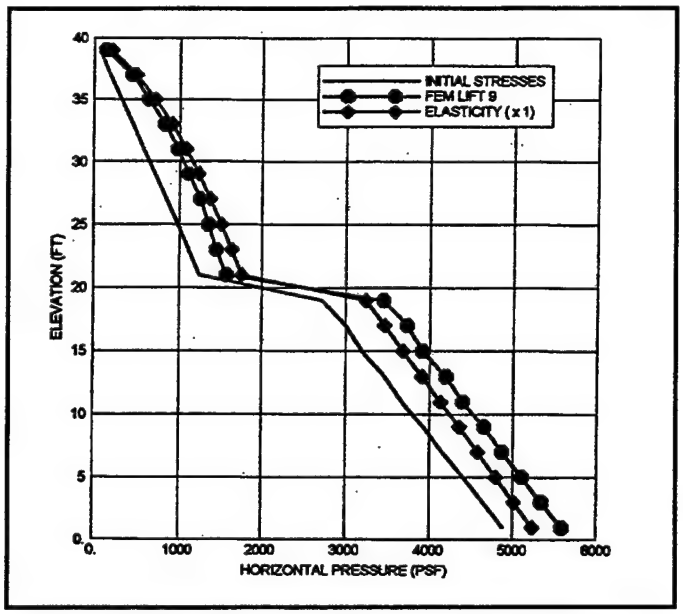

Figure 36. Single triangle surface (S2), sand-H surcharge on layered sand-H over clay base (1 ft = 0.305 m; 1 lbf/ft^2 = 47.9 Pa)

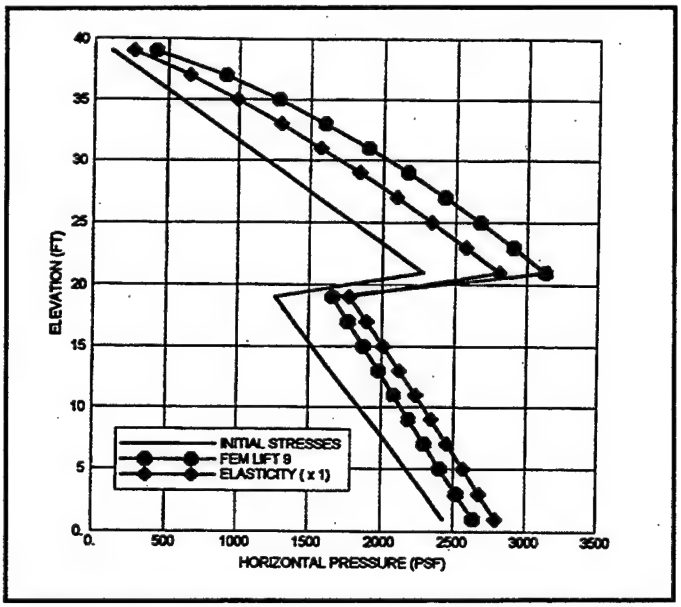

Figure 37. Single triangle surface (S2), sand-H surcharge on layered clay over sand-H base (1 ft = 0.305 m; 1 lbf/ft^2 = 47.9 Pa)

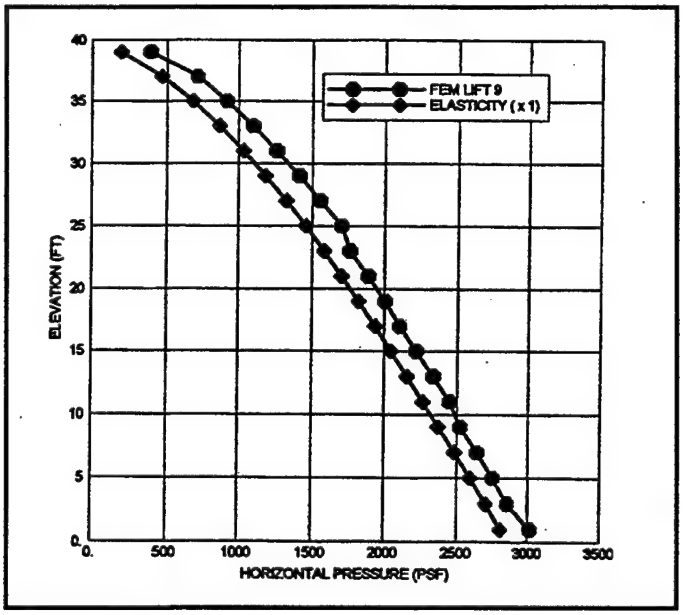

Figure 38. Double triangle surface (S3), homogeneous sand-L surcharge and base (1 ft = 0.305 m; 1 lbf/ft^2 = 47.9 Pa)

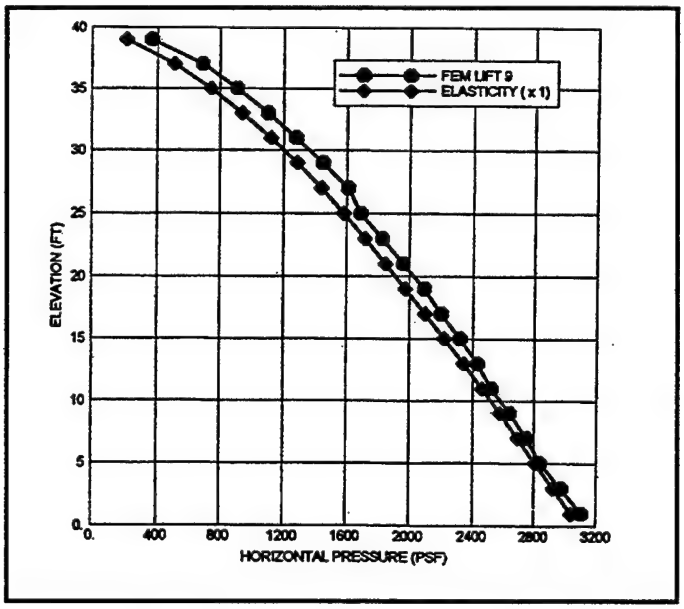

Figure 39. Double triangle surface (S3), homogeneous sand-H surcharge and base (1 ft = 0.305 m; 1 lbf/ft^2 = 47.9 Pa)

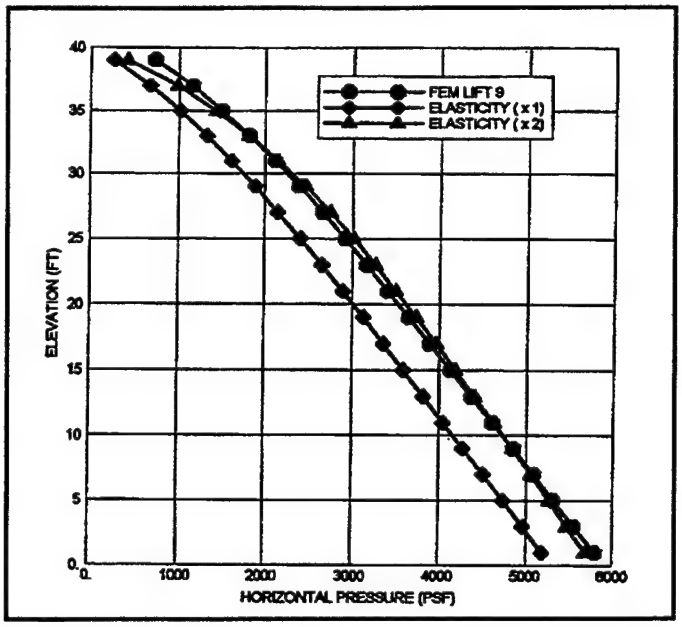

Figure 40. Double triangle surface (S3), sand-H surcharge on homogeneous clay base (1 ft = 0.305 m; 1 lbf/ft^2 = 47.9 Pa)

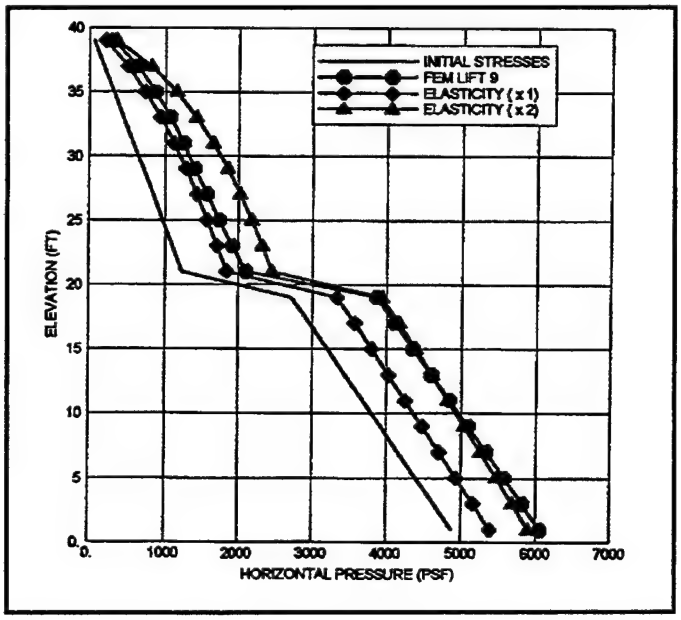

Figure 41. Double triangle surface (S3), sand-H surcharge on layered sand-H over clay base (1 ft = 0.305 m; 1 lbf/ft^2 = 47.9 Pa)

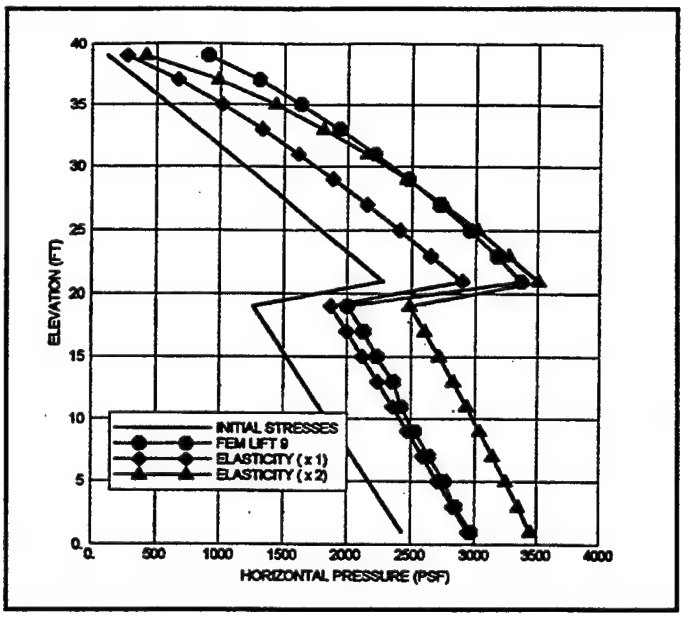

Figure 42. Single triangle surface (S3), sand-H surcharge on layered clay over sand-H base (1 ft = 0.305 m; 1 lbf/ft^2 = 47.9 Pa)

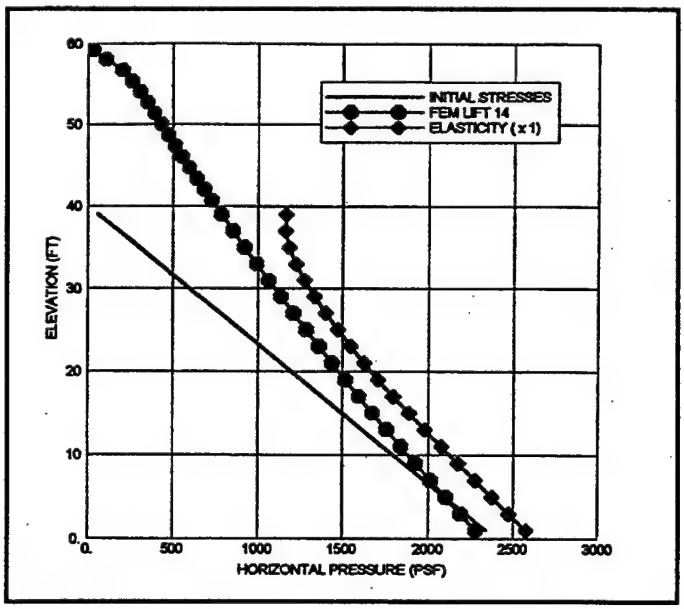

Figure 43. Single triangle surface (S4), -2V on 8H slope, homogeneous sand-L surcharge and base (1 ft = 0.305 m; 1 lbf/ft^2 = 47.9 Pa)

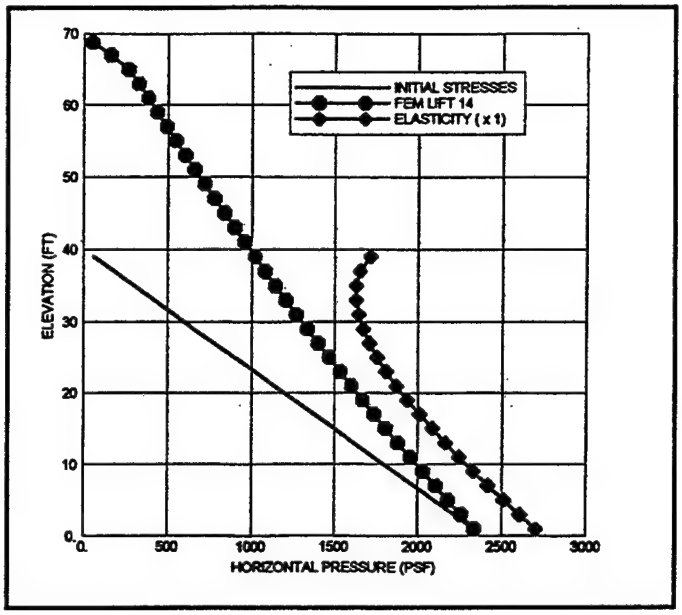

Figure 44. Single triangle surface (S4), -3V on 8H slope, homogeneous sand-L surcharge and base (1 ft = 0.305 m; 1 lbf/ft^2 = 47.9 Pa)

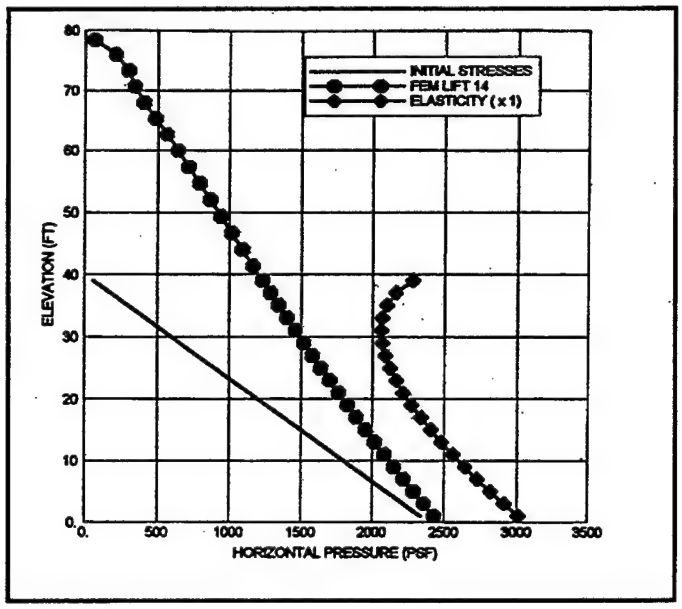

Figure 45. Single triangle surface (S4), -4V on 8H slope, homogeneous sand-L surcharge and base (1 ft = 0.305 m; 1 lbf/ft^2 = 47.9 Pa)

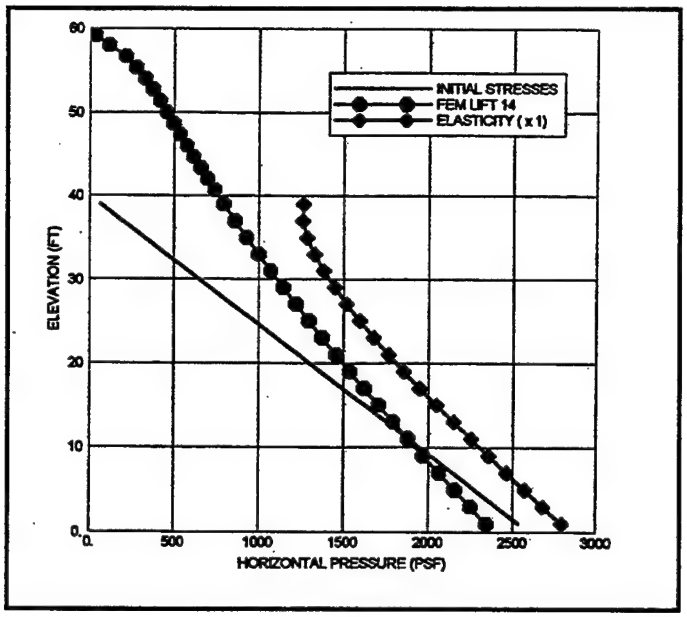

Figure 46. Single triangle surface (S4), -2V on 8H slope, homogeneous sand-H surcharge and base (1 ft = 0.305 m; 1 lbf/ft^2 = 47.9 Pa)

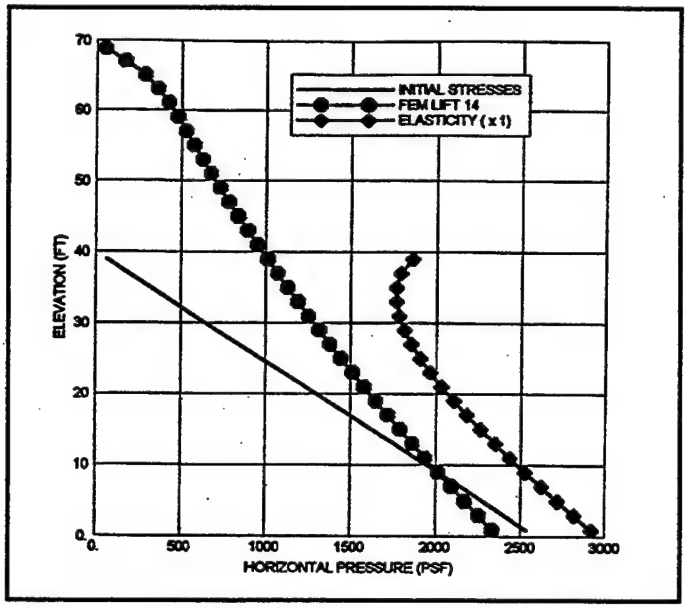

Figure 47. Single triangle slope (S4), -3V on 8H slope, homogeneous sand-H surcharge and base (1 ft = 0.305 m; 1 lbf/ft^2 = 47.9 Pa)

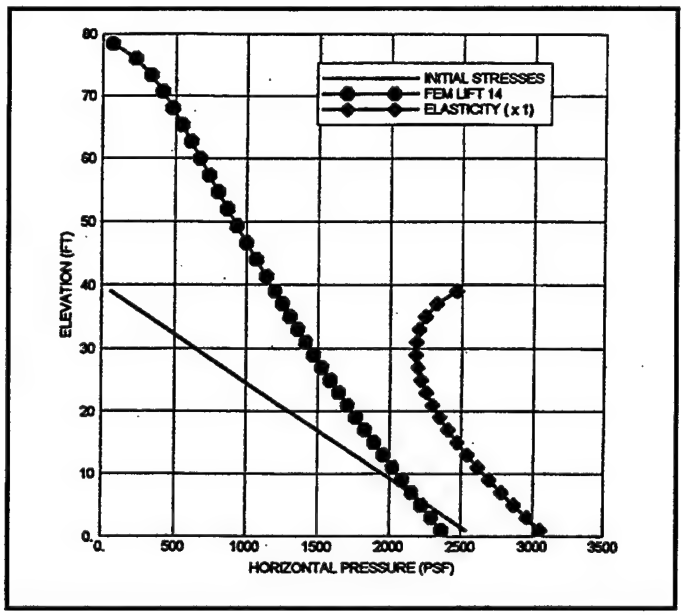

Figure 48. Single triangle surface (S4), -4V on 8H slope, homogeneous sand-H surcharge and base (1 ft = 0.305 m; 1 lbf/ft^2 = 47.9 Pa)

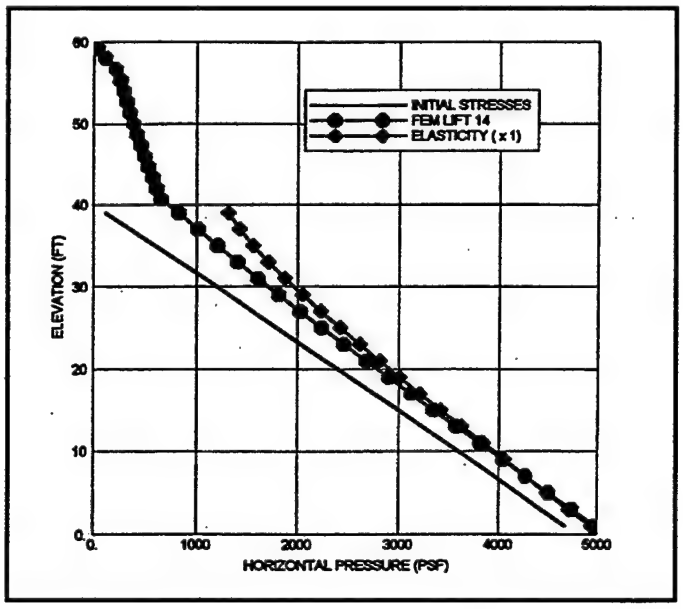

Figure 49. Single triangle surface (S4), -2V on 8H slope, sand-H surcharge on homogeneous clay base (1 ft = 0.305 m; 1 lbf/ft^2 = 47.9 Pa)

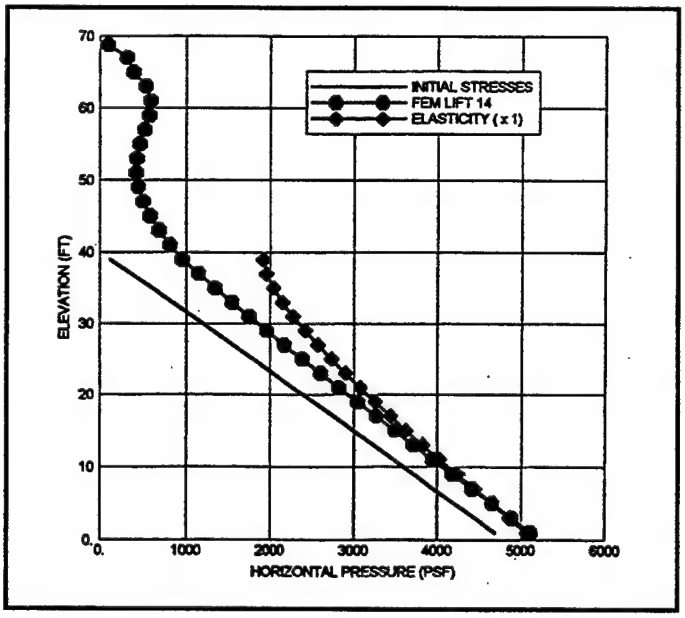

Figure 50. Single triangle surface (S4), -3V on 8H slope, sand-H surcharge on homogeneous clay base (1 ft = 0.305 m; 1 lbf/ft^2 = 47.9 Pa)

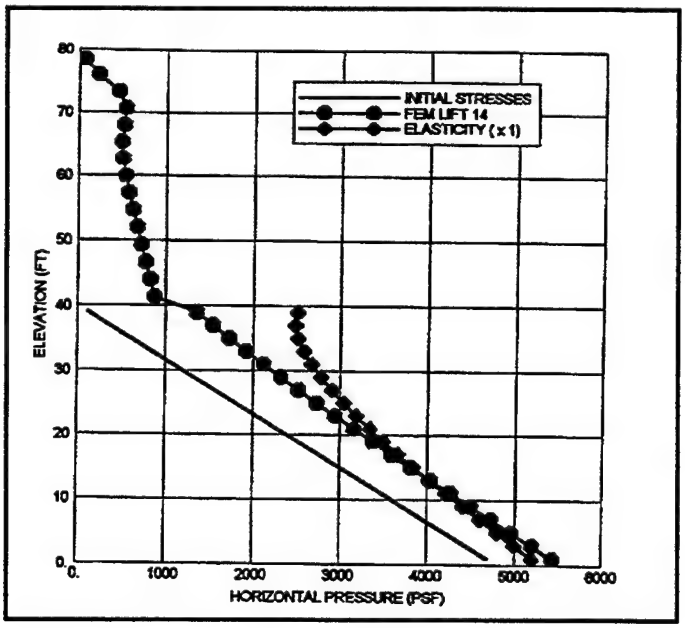

Figure 51. Single triangle surface (S4), -4V on 8H slope, sand-H surcharge on homogeneous clay base (1 ft = 0.305 m; 1 lbf/ft^2 = 47.9 Pa)

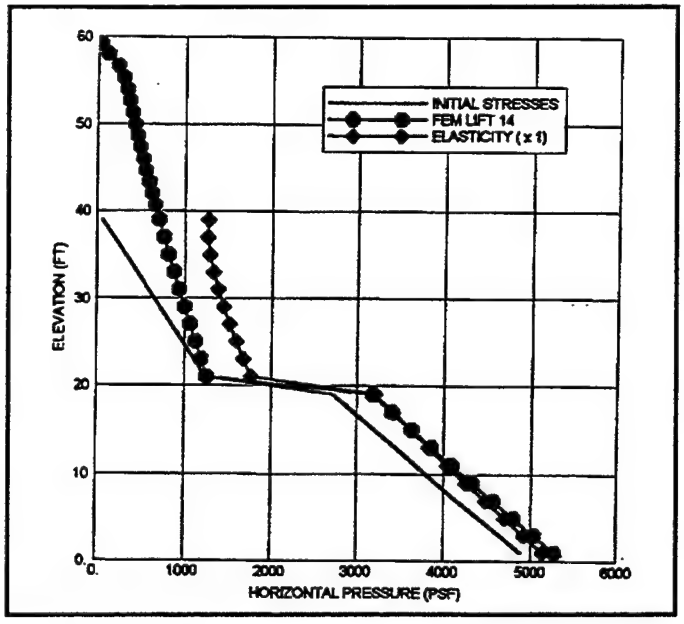

Figure 52. Single triangle surface (S4), -2V on 8H slope, sand-H surcharge on layered sand-H over clay base (1 ft = 0.305 m; 1 lbf/ft^2 = 47.9 Pa)

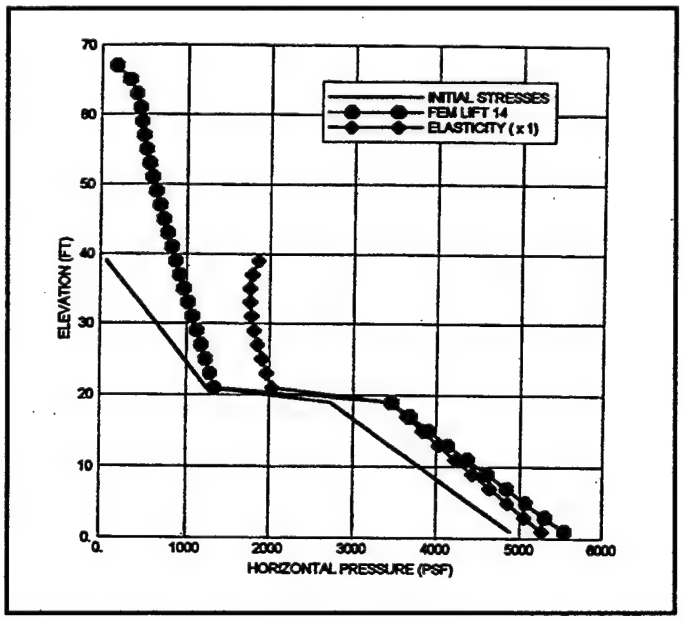

Figure 53. Single triangle surface (S4), -3V on 8H slope, sand-H surcharge on layered sand-H over clay base (1 ft = 0.305 m; 1 lbf/ft^2 = 47.9 Pa)

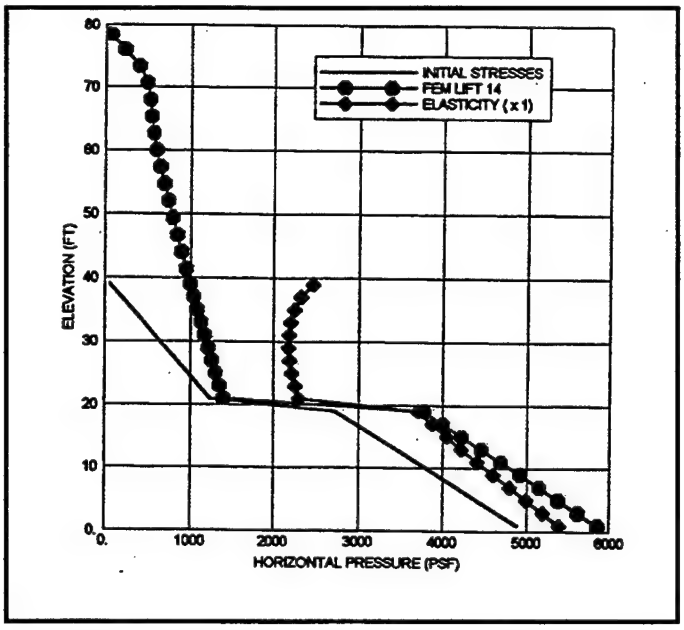

Figure 54. Single triangle surface (S4), -4V on 8H slope, sand-H surcharge on layered sand-H over clay base (1 ft = 0.305 m; 1 lbf/ft^2 = 47.9 Pa)

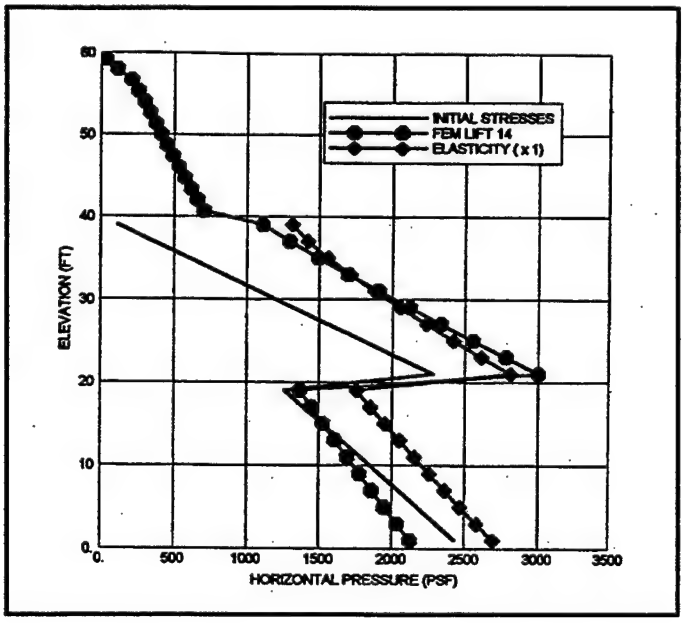

Figure 55. Single triangle surface (S4), -2V on 8H slope, sand-H surcharge on layered clay over sand-H base (1 ft = 0.305 m; 1 lbf/ft^2 = 47.9 Pa)

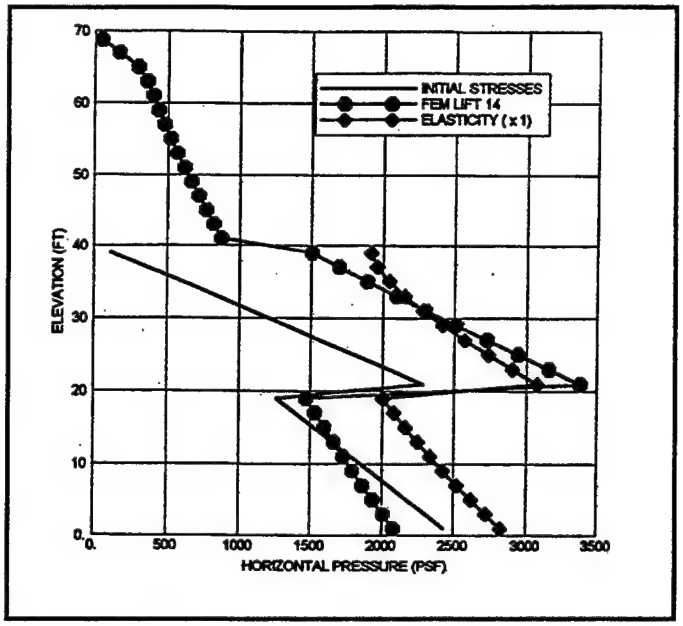

Figure 56. Single triangle surface (S4), -3V on 8H slope, sand-H surcharge on layered clay over sand-H base (1 ft = 0.305 m; 1 lbf/ft^2 = 47.9 Pa)

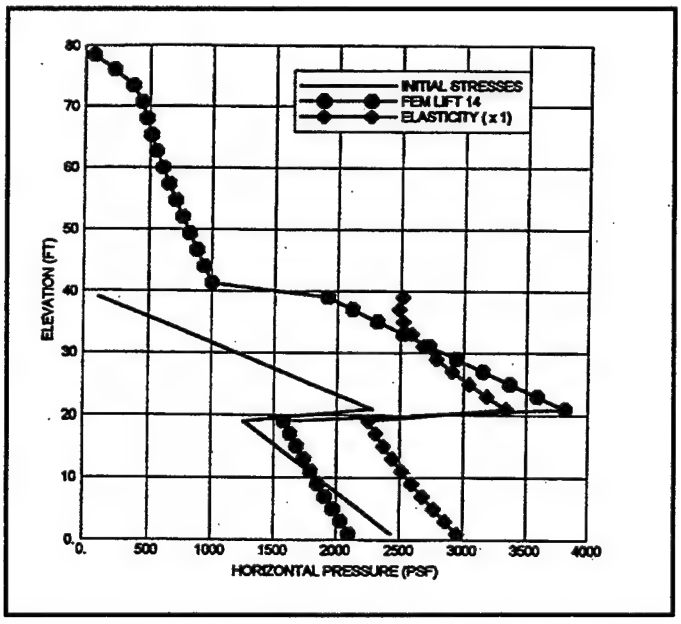

Figure 57. Single triangle surface (S4), -4V on 8H slope, sand-H surcharge on layered clay over sand-H base (1 ft = 0.305 m; 1 lbf/ft^2 = 47.9 Pa)

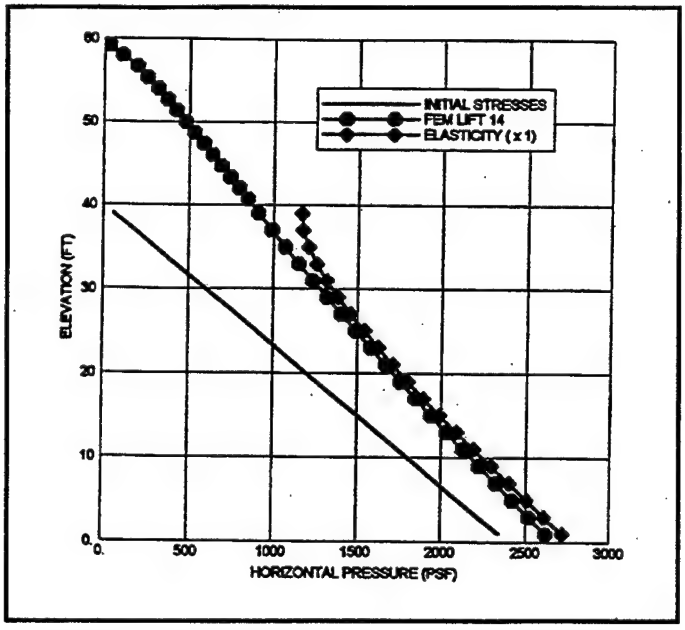

Figure 58. Double triangle surface (S5), -2V on 8H initial slope, homogeneous sand-L surcharge and base (1 ft = 0.305 m; 1 lbf/ft^2 = 47.9 Pa)

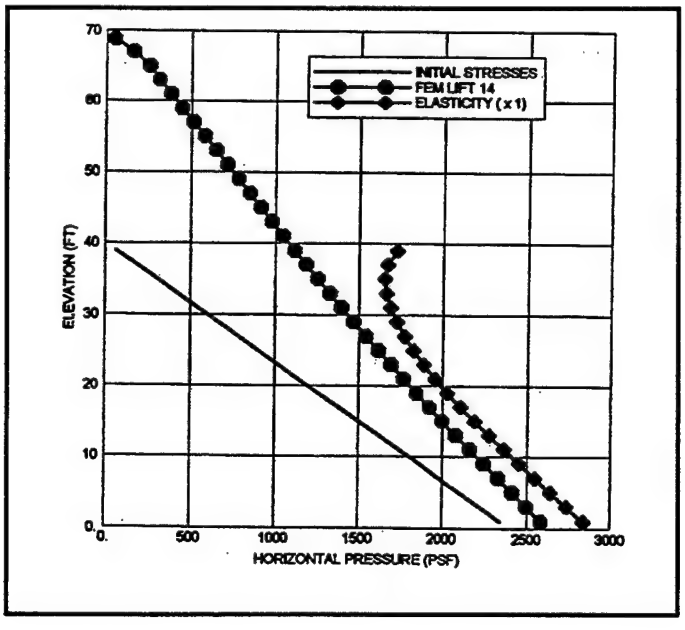

Figure 59. Double triangle surface (S5), -3V on 8H initial slope, homogeneous sand-L surcharge and base (1 ft = 0.305 m; 1 lbf/ft^2 = 47.9 Pa)

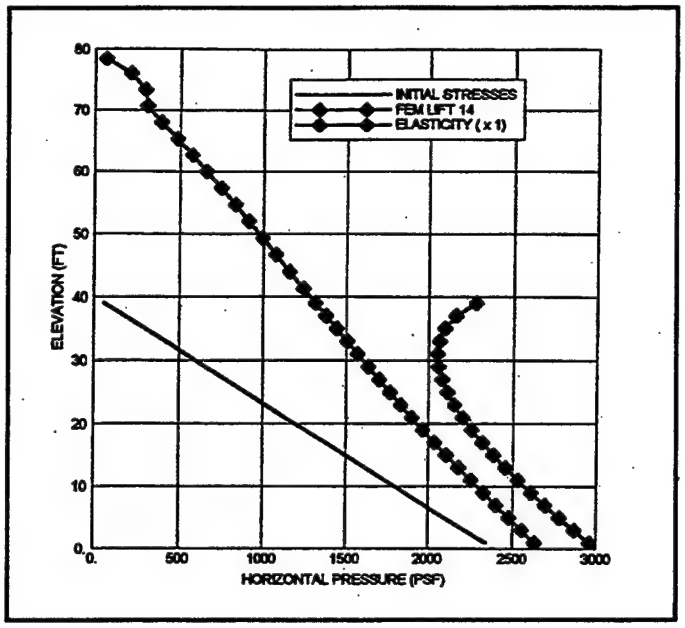

Figure 60. Double triangle surface (S5), -4V on 8H initial slope, homogeneous sand-L surcharge and base (1 ft = 0.305 m; 1 lbf/ft^2 = 47.9 Pa)

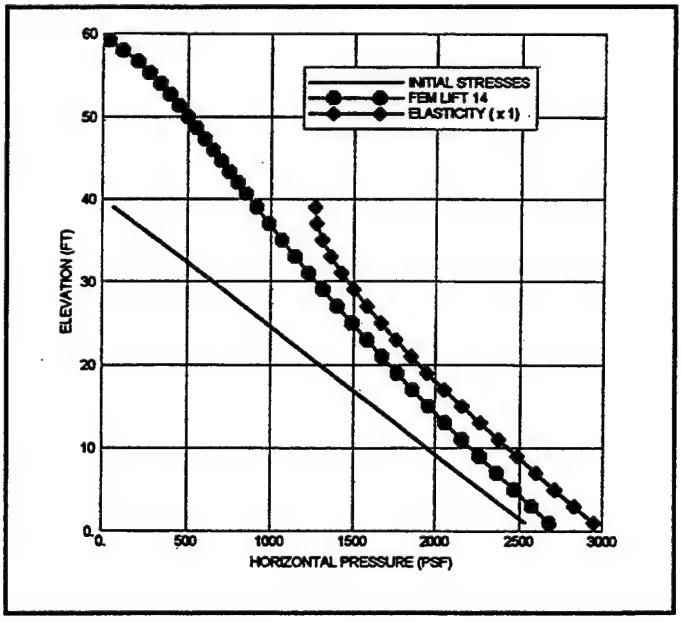

Figure 61. Double triangle surface (S5), -2V on 8H initial slope, homogeneous sand-H surcharge and base (1 ft = 0.305 m; 1 lbf/ft^2 = 47.9 Pa)

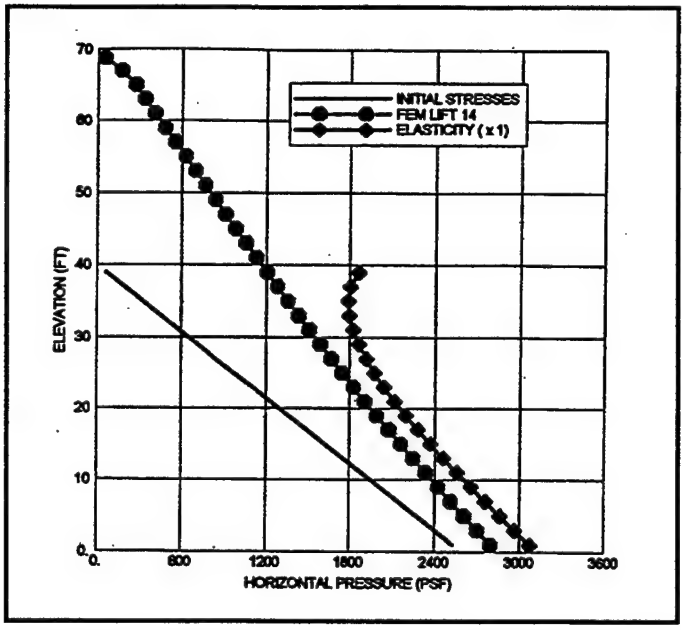

Figure 62. Double triangle surface (S5), -3V on 8H initial slope, homogeneous sand-H surcharge and base (1 ft = 0.305 m; 1 lbf/ft^2 = 47.9 Pa)

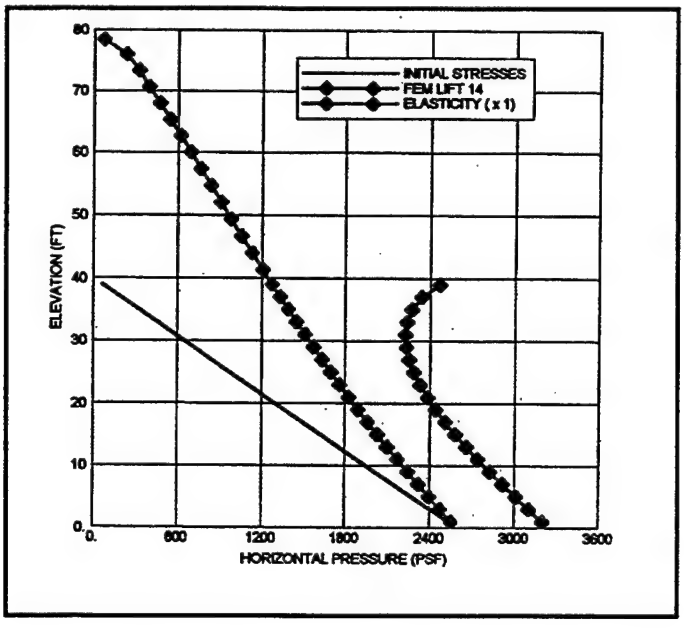

Figure 63. Double triangle surface (S5), -4V on 8H initial slope, homogeneous sand-H surcharge and base (1 ft = 0.305 m; 1 lbf/ft^2 = 47.9 Pa)

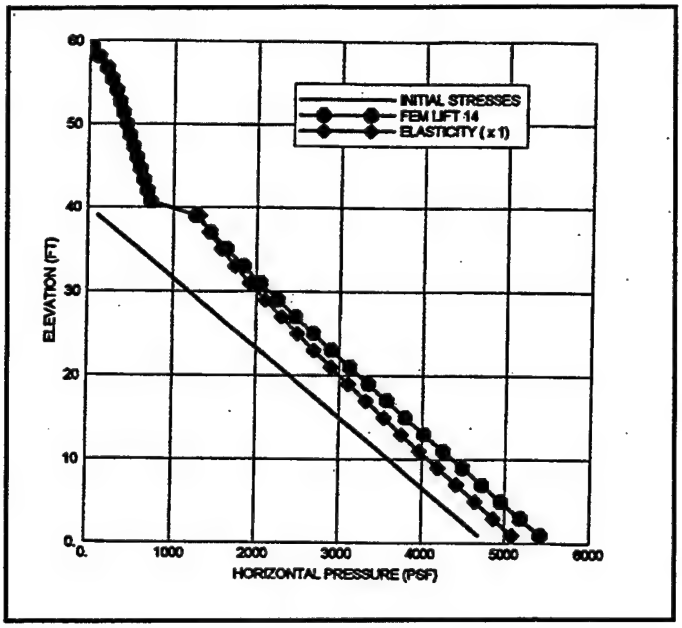

Figure 64. Double triangle surface (S5), -2V on 8H initial slope, sand-H surcharge on homogeneous clay base (1 ft = 0.305 m; 1 lbf/ft^2 = 47.9 Pa)

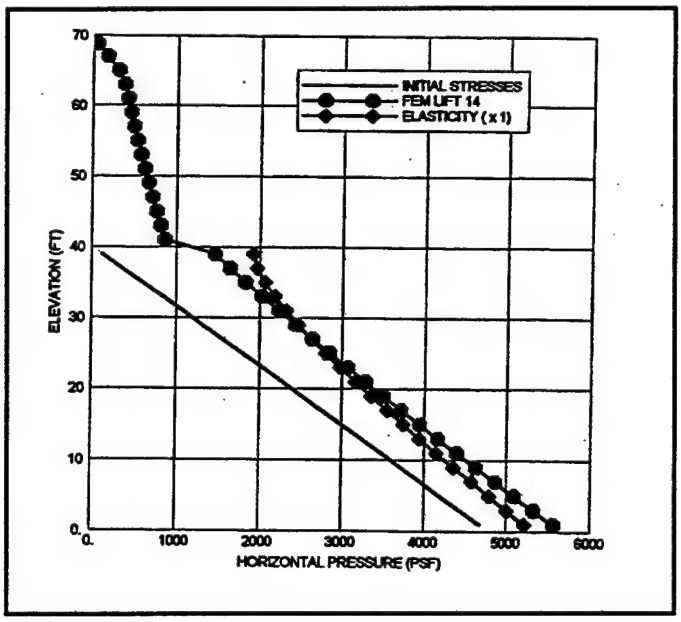

Figure 65. Double triangle surface (S5), -3V on 8H initial slope, sand-H surcharge on homogeneous clay base (1 ft = 0.305 m; 1 lbf/ft^2 = 47.9 Pa)

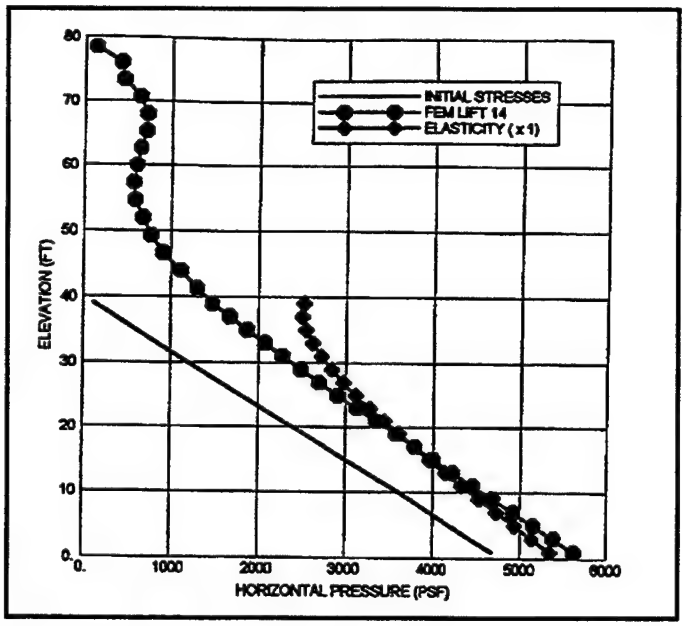

Figure 66. Double triangle surface (S5), -4V on 8H initial slope, sand-H surcharge on homogeneous clay base (1 ft = 0.305 m; 1 lbf/ft^2 = 47.9 Pa)

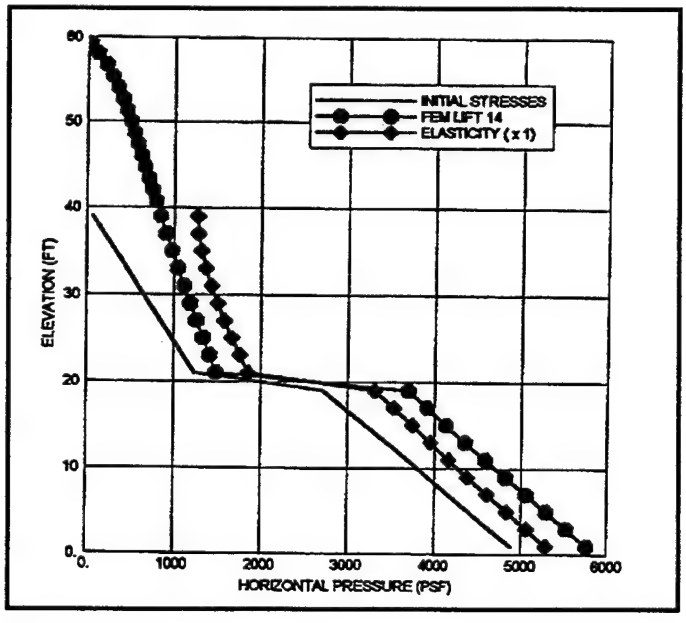

Figure 67. Double triangle surface (S5), -2V on 8H initial slope, sand-H surcharge on layered sand-H over clay base (1 ft = 0.305 m; 1 lbf/ft^2 = 47.9 Pa)

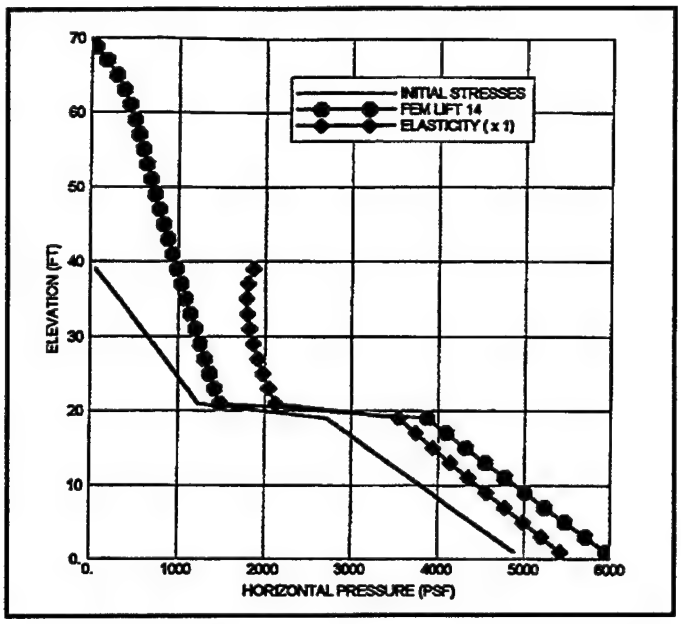

Figure 68. Double triangle surface (S5), -3V on 8H initial slope, sand-H surcharge on layered sand-H over clay base (1 ft = 0.305 m; 1 lbf/ft^2 = 47.9 Pa)

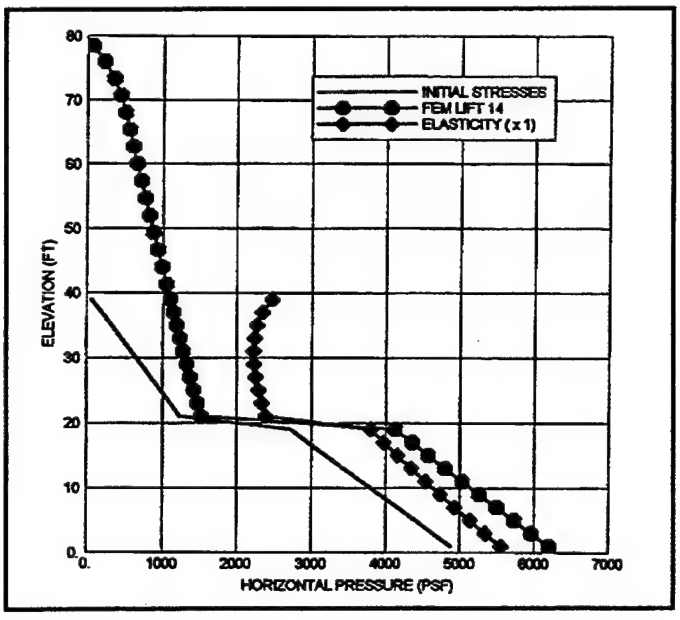

Figure 69. Double triangle surface (S5), -4V on 8H initial slope, sand-H surcharge on layered sand-H over clay base (1 ft = 0.305 m; 1 lbf/ft^2 = 47.9 Pa)

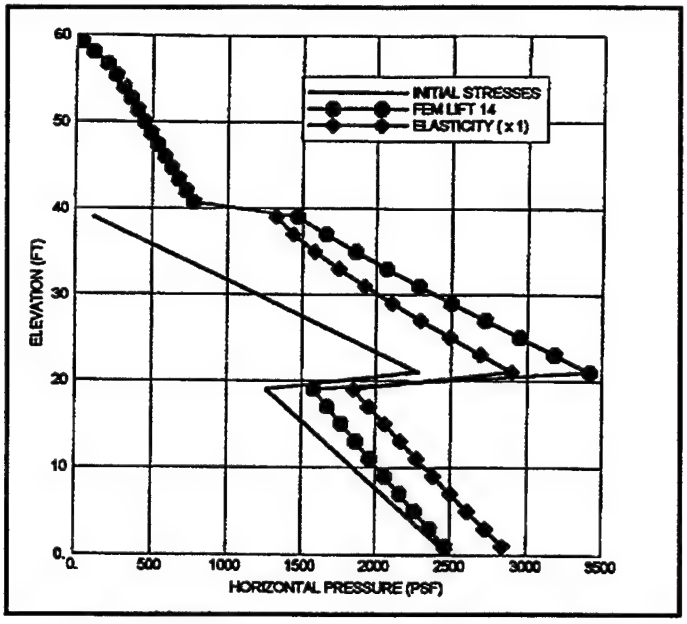

Figure 70. Double triangle surface (S5), -2V on 8H initial slope, sand-H surcharge on layered clay over sand-H base (1 ft = 0.305 m; 1 lbf/ft^2 = 47.9 Pa)

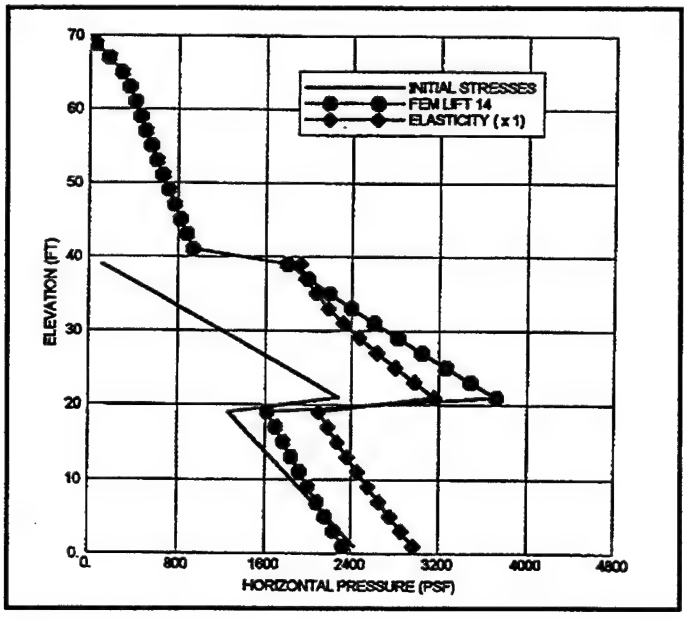

Figure 71. Double triangle surface (S5), -3V on 8H initial slope, sand-H surcharge on layered clay over sand-H base (1 ft = 0.305 m; 1 lbf/ft^2 = 47.9 Pa)

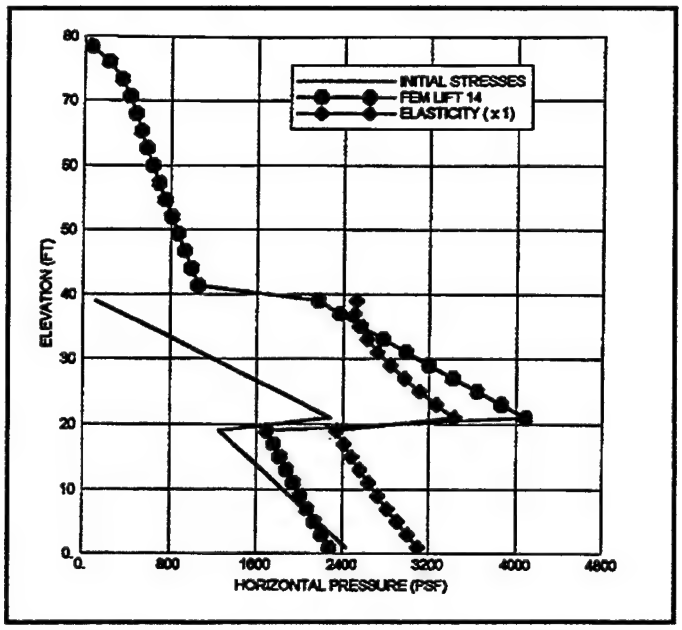

Figure 72. Double triangle surface (S5), -4V on 8H initial slope, sand-H surcharge on layered clay over sand-H base (1 ft = 0.305 m; 1 lbf/ft^2 = 47.9 Pa)

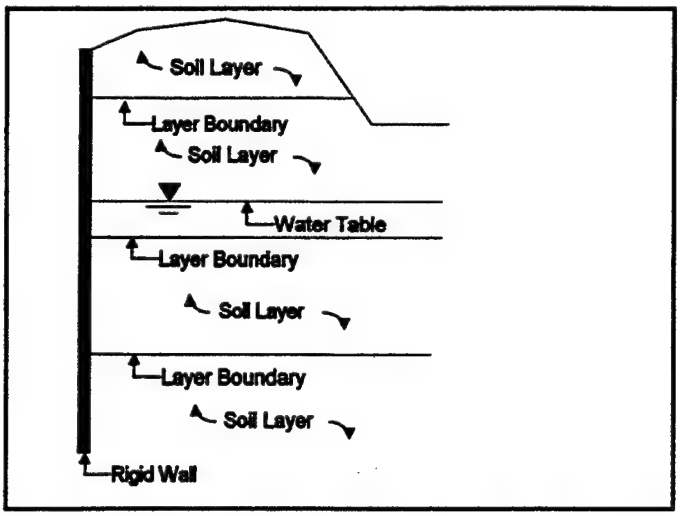

Figure 73. Soil system accommodated by CSOILP

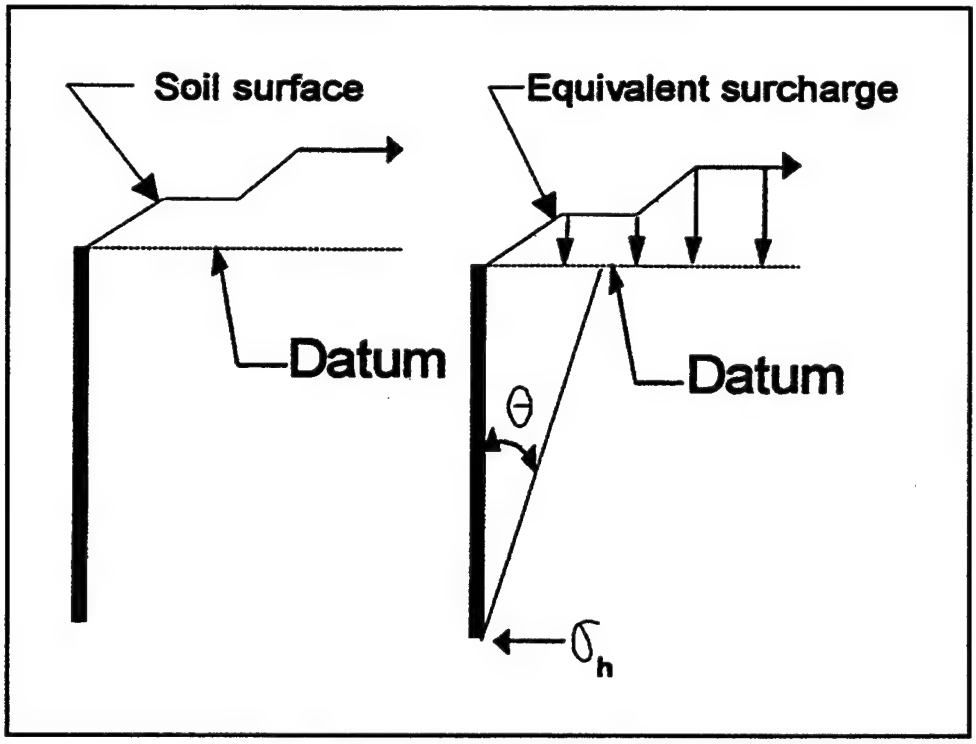

Figure 74. Monotonically increasing surface

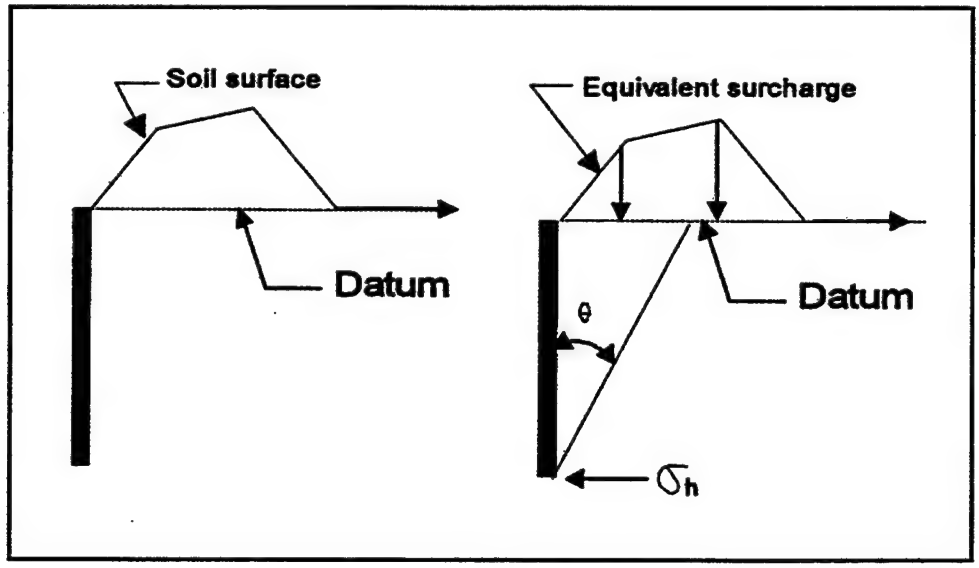

Figure 75. Decreasing soil surface

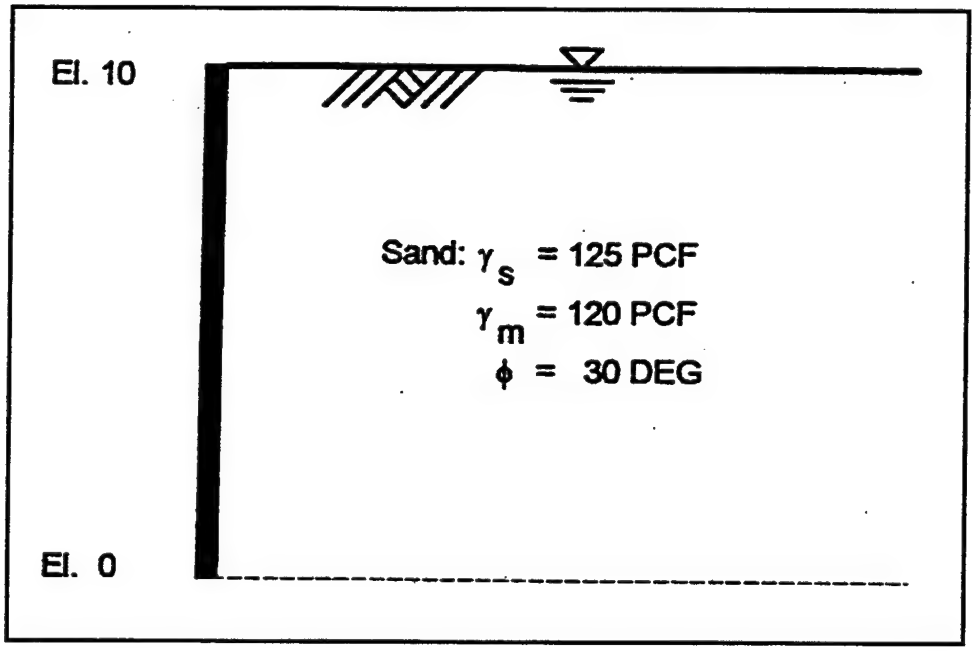

Figure 76. Soil system composed of homogeneous sand with a horizontal surface (1 lb/ft^3 = 16.02 kg/m^3)

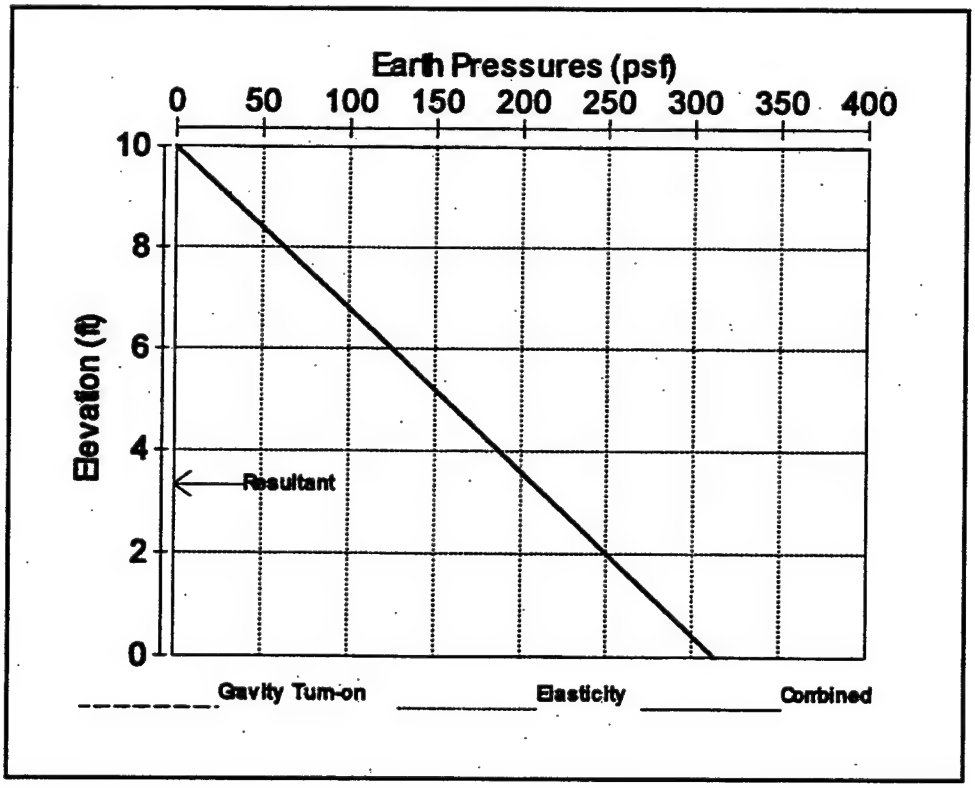

Figure 77. Example 1, homogeneous sand with horizontal surface (1 ft = 0.305 m; 1 lbf/ft^2 = 47.8 Pa)

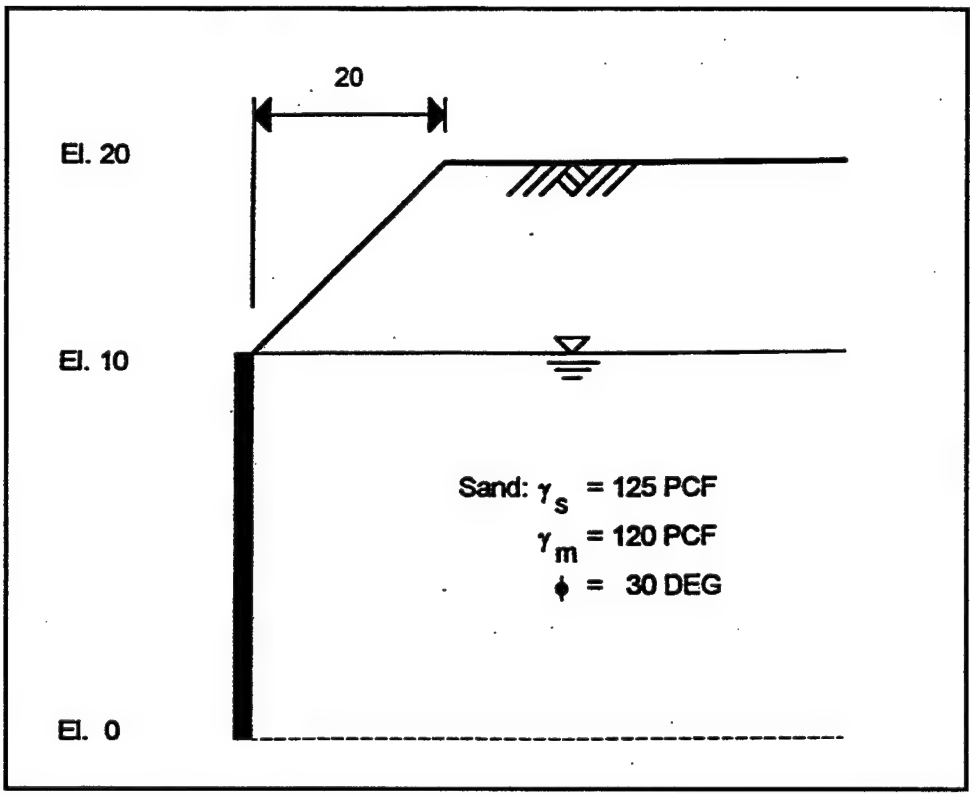

Figure 78. Soil system with a ramp surface and the associated input data (1 ft = 0.305 m; 1 lbf/ft^3 = 16.02 kg/m^3)

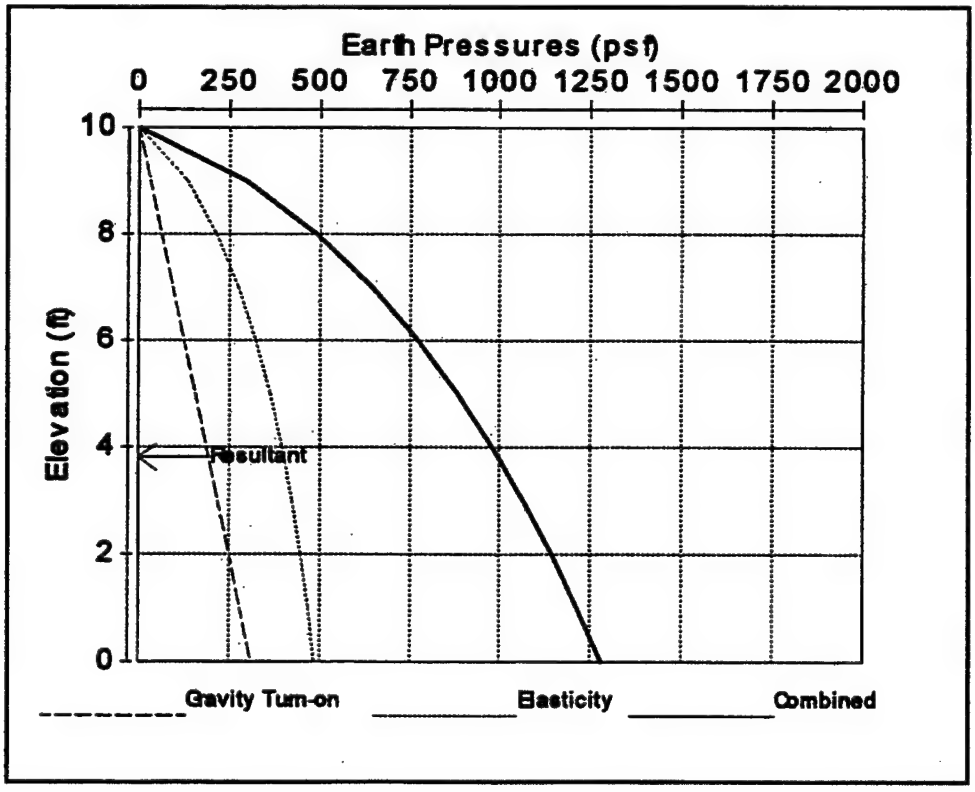

Figure 79. Example 2, homogeneous sand with ramp surface (1 ft = 0.305 m; 1 lbf/ft^2 = 47.8 Pa)

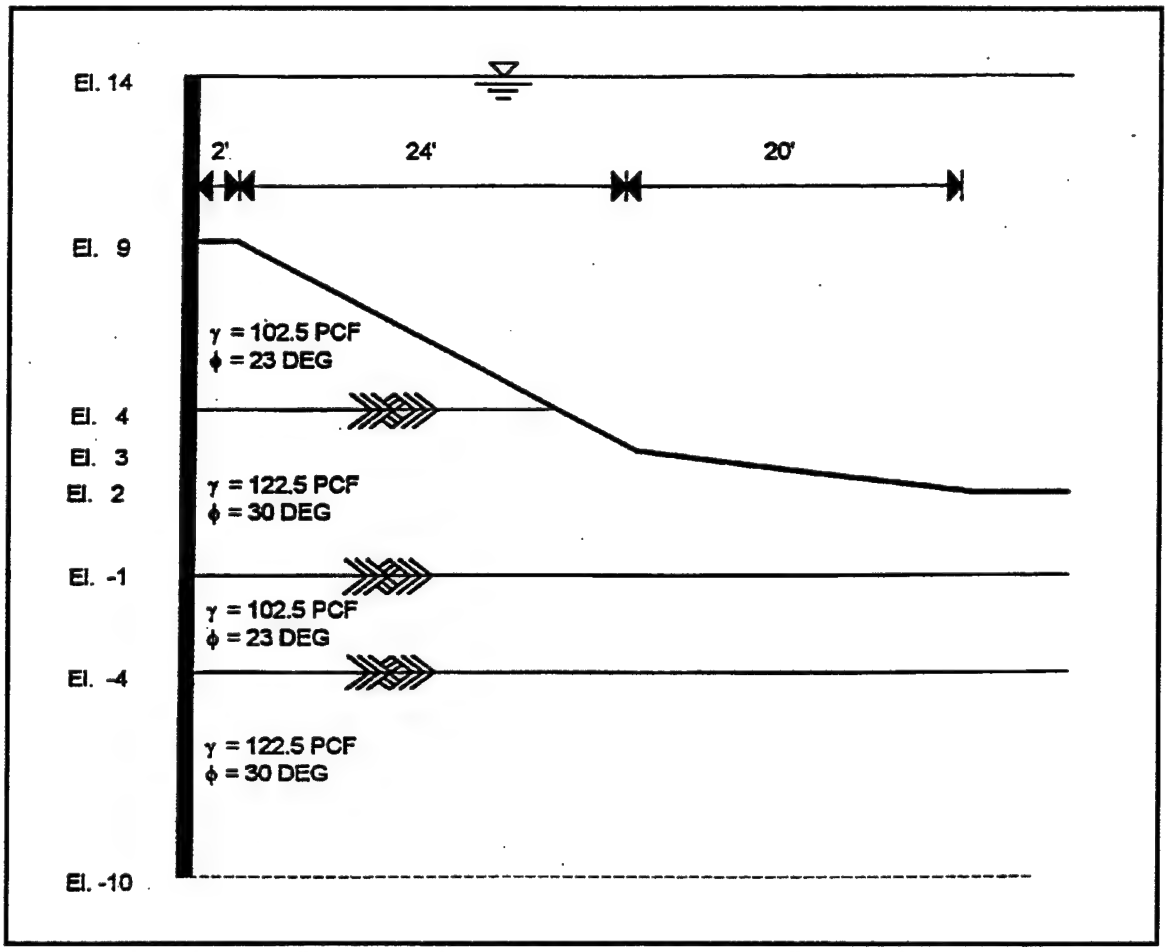

Figure 80. Soil system for floodwall-levee system (1 ft = 0.305 m; 1 lb/ft^3 = 16.02 kg/m^3)

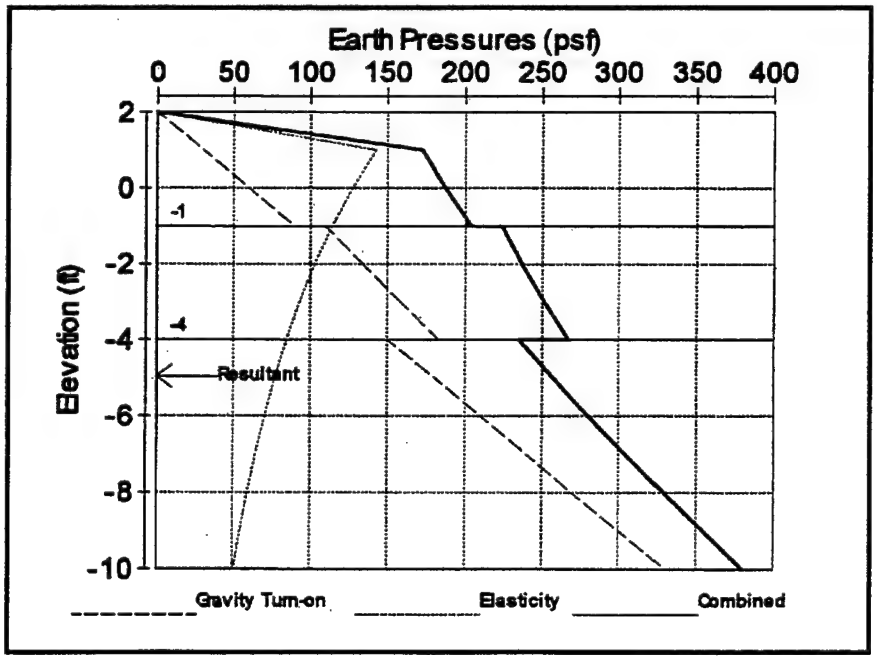

Figure 81. Example 3, levee section, granular soil, irregular ground surface (1 ft = 0.305 m; 1 lbf/ft^2 = 47.8 Pa)

Appendix A
Finite Element Models for One-Layered Systems

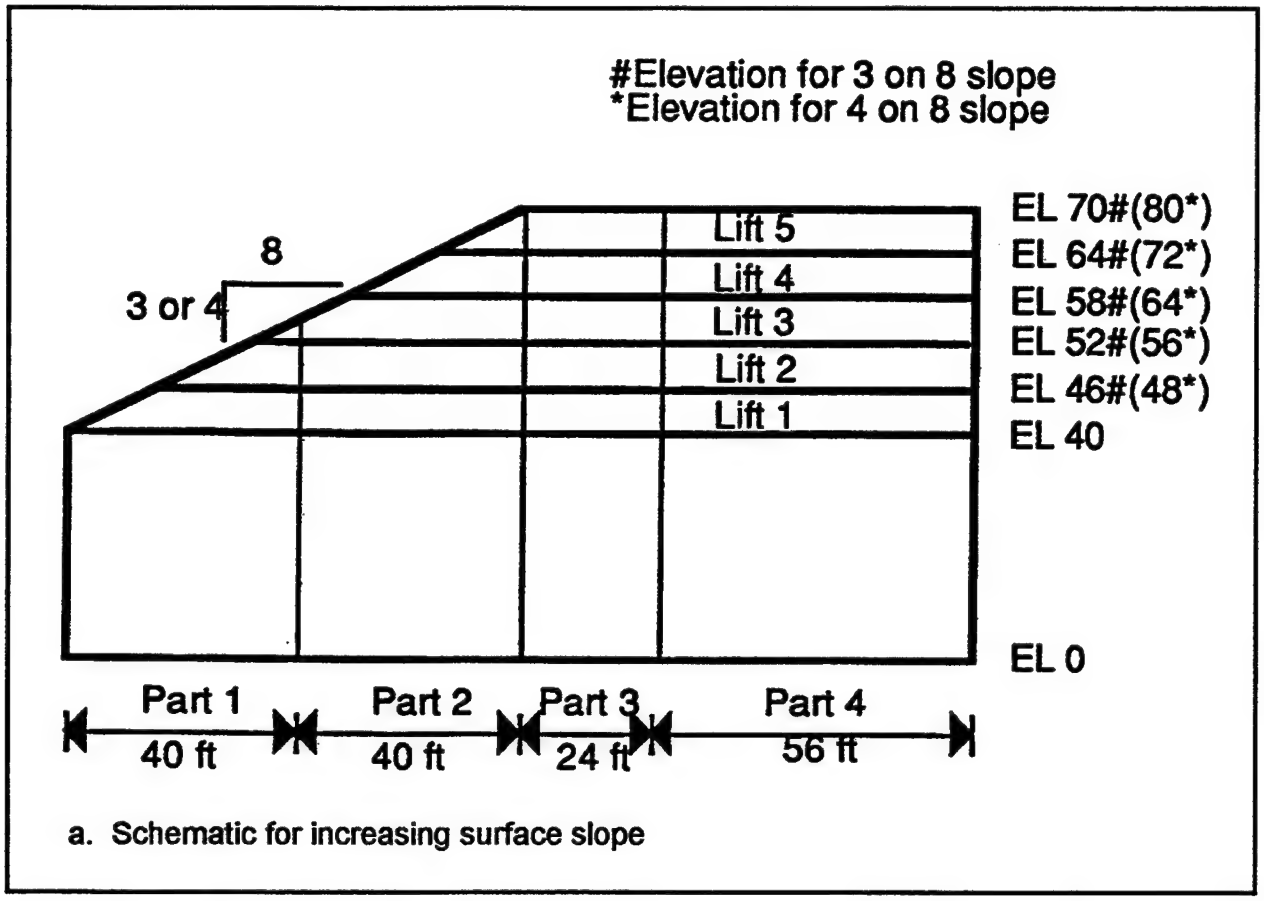

Figure A1. Finite element model for increasing surface slope (Sheet 1 of 5)

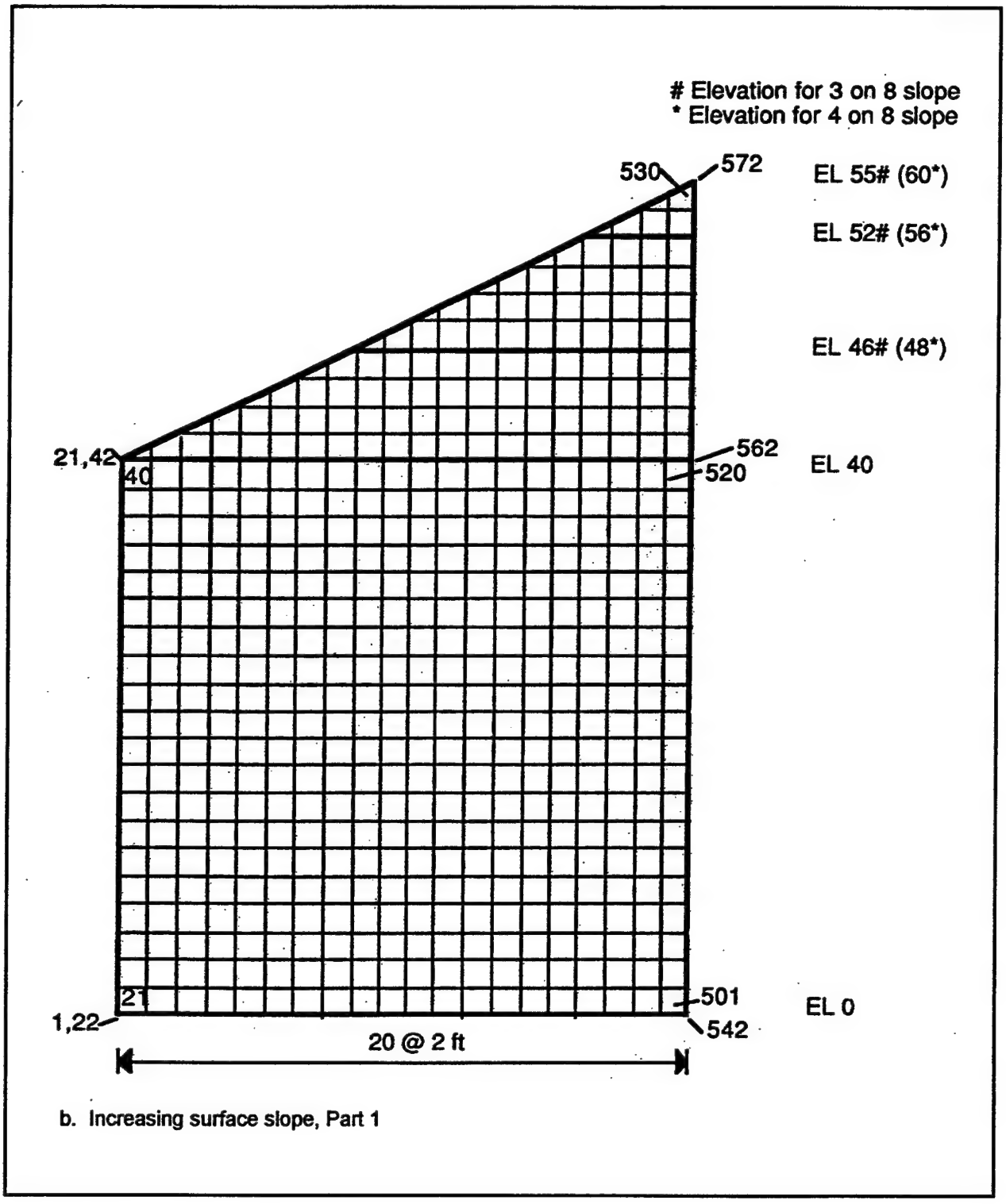

b. Increasing surface slope, Part 1

Figure A1. (Sheet 2 of 5)

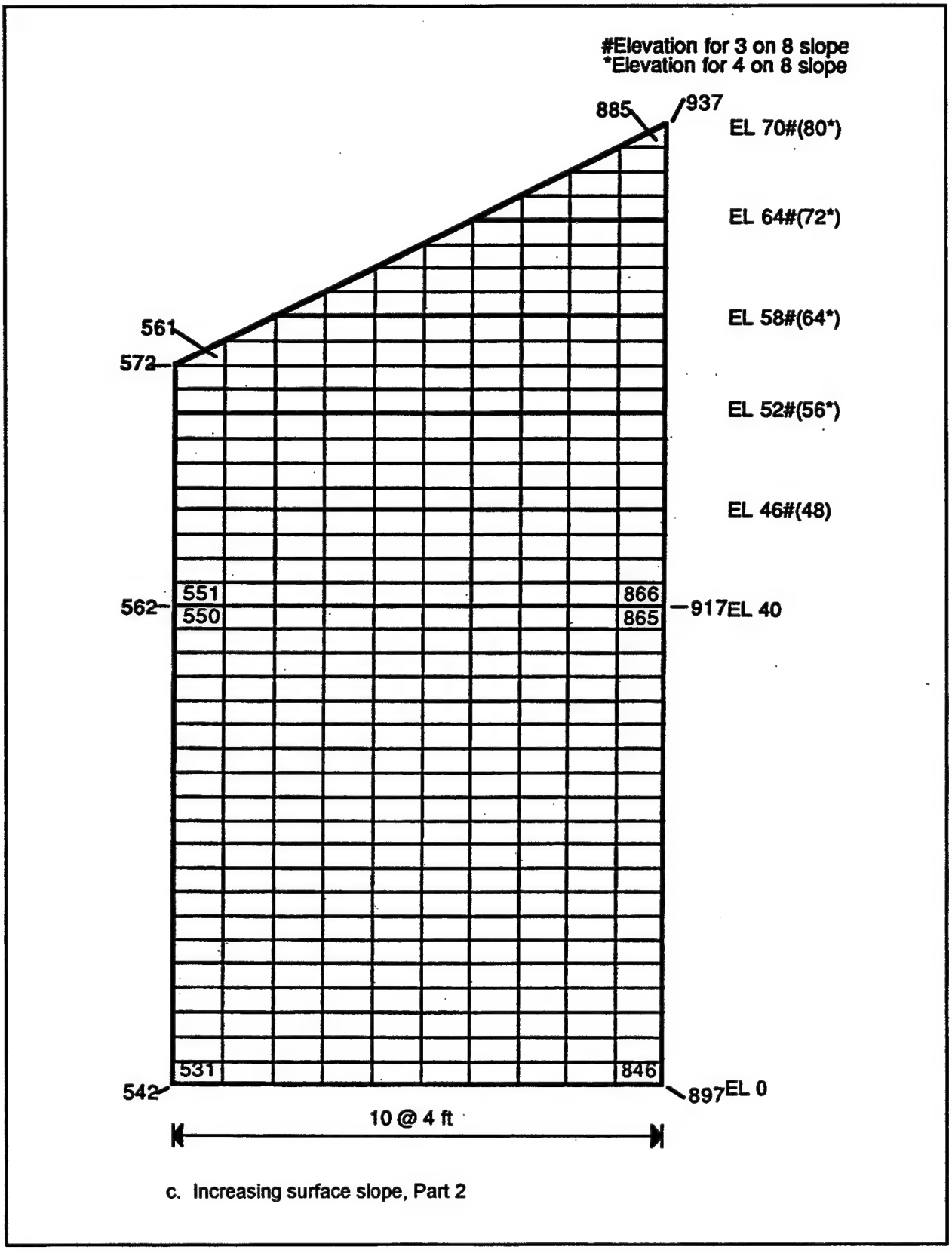

c. Increasing surface slope, Part 2

Figure A1. (Sheet 3 of 5)

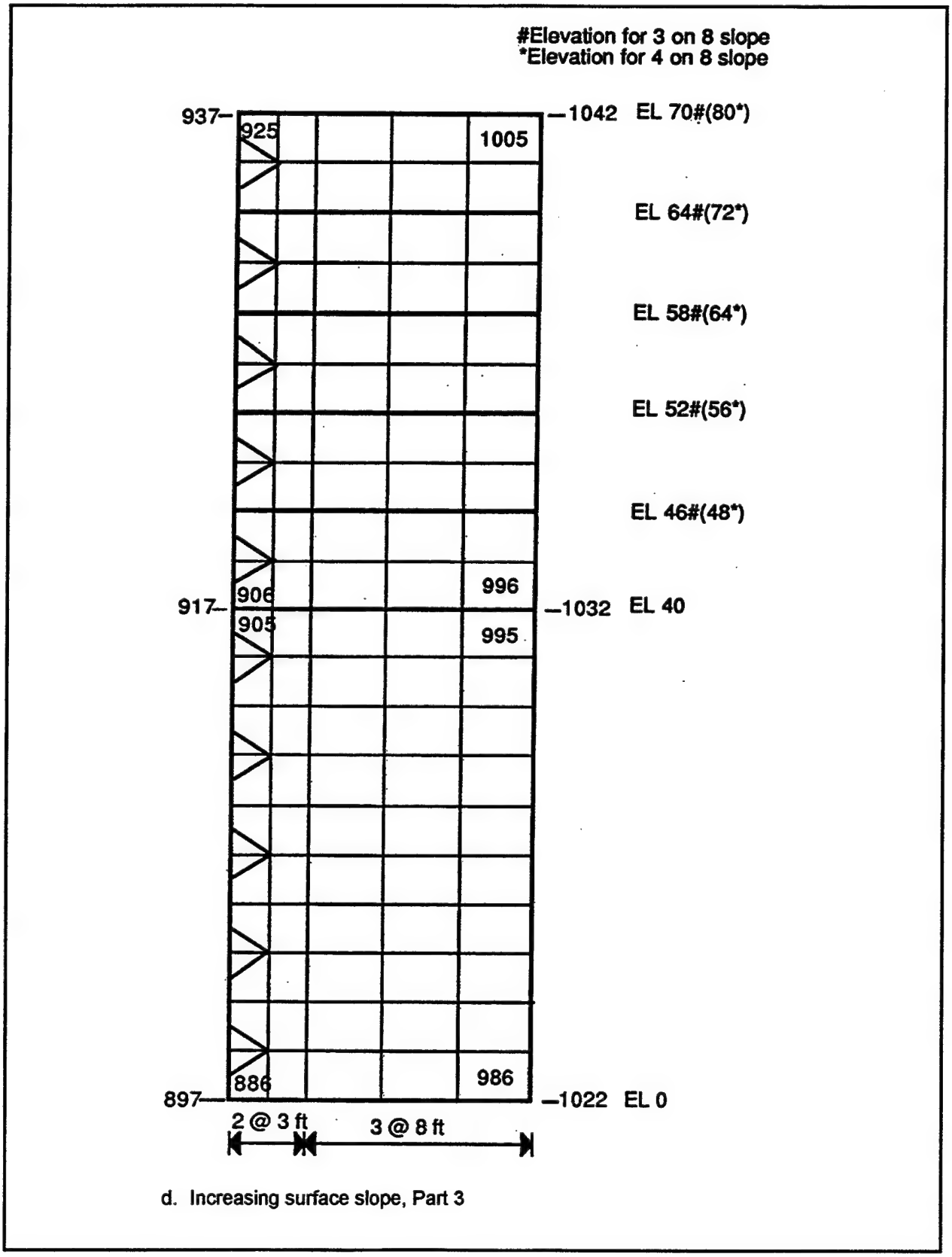

d. Increasing surface slope, Part 3

Figure A1. (Sheet 4 of 5)

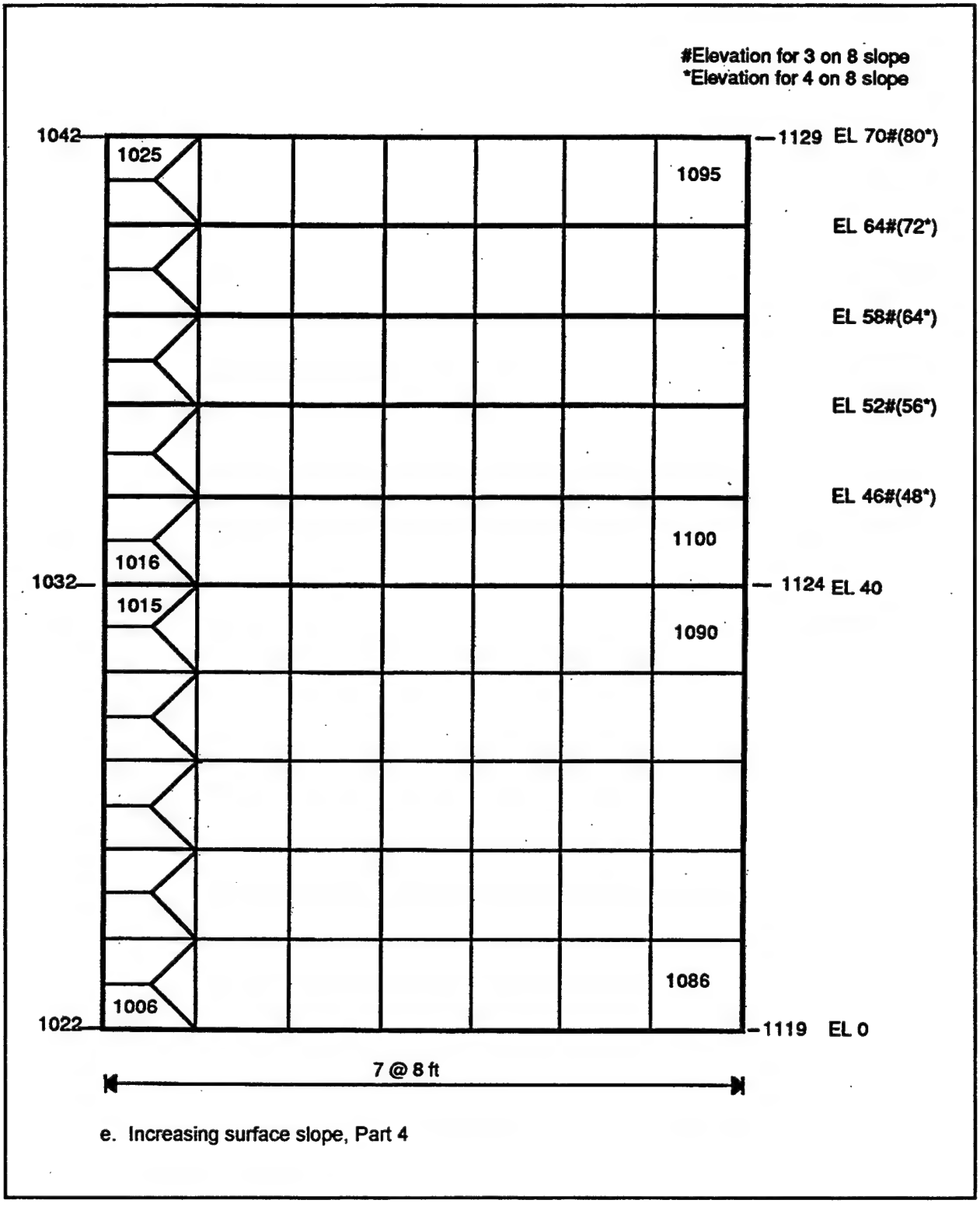

e. Increasing surface slope, Part 4

Figure A1. (Sheet 5 of 5)

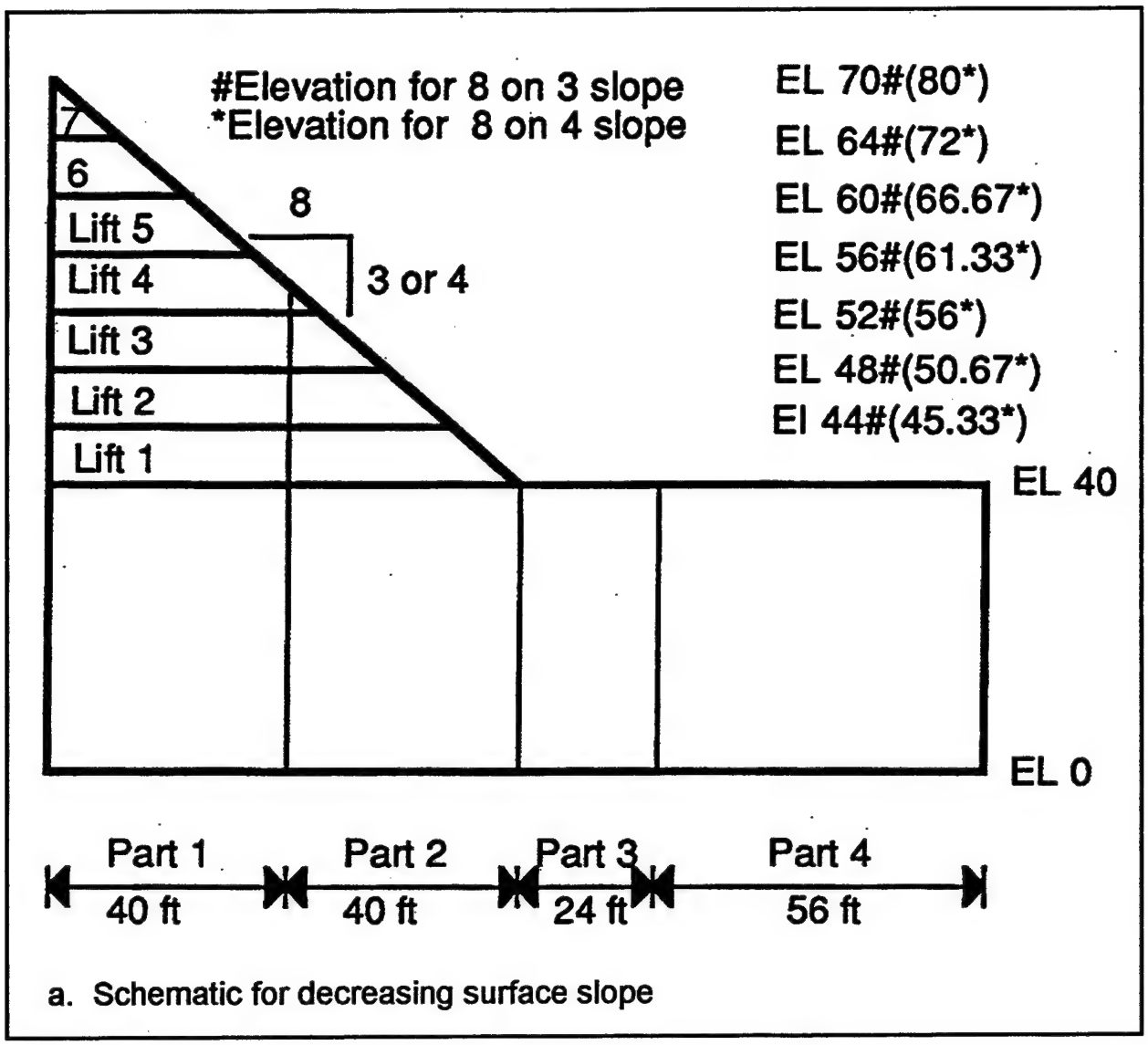

Figure A2. Finite element model for decreasing surface slope (Sheet 1 of 5)

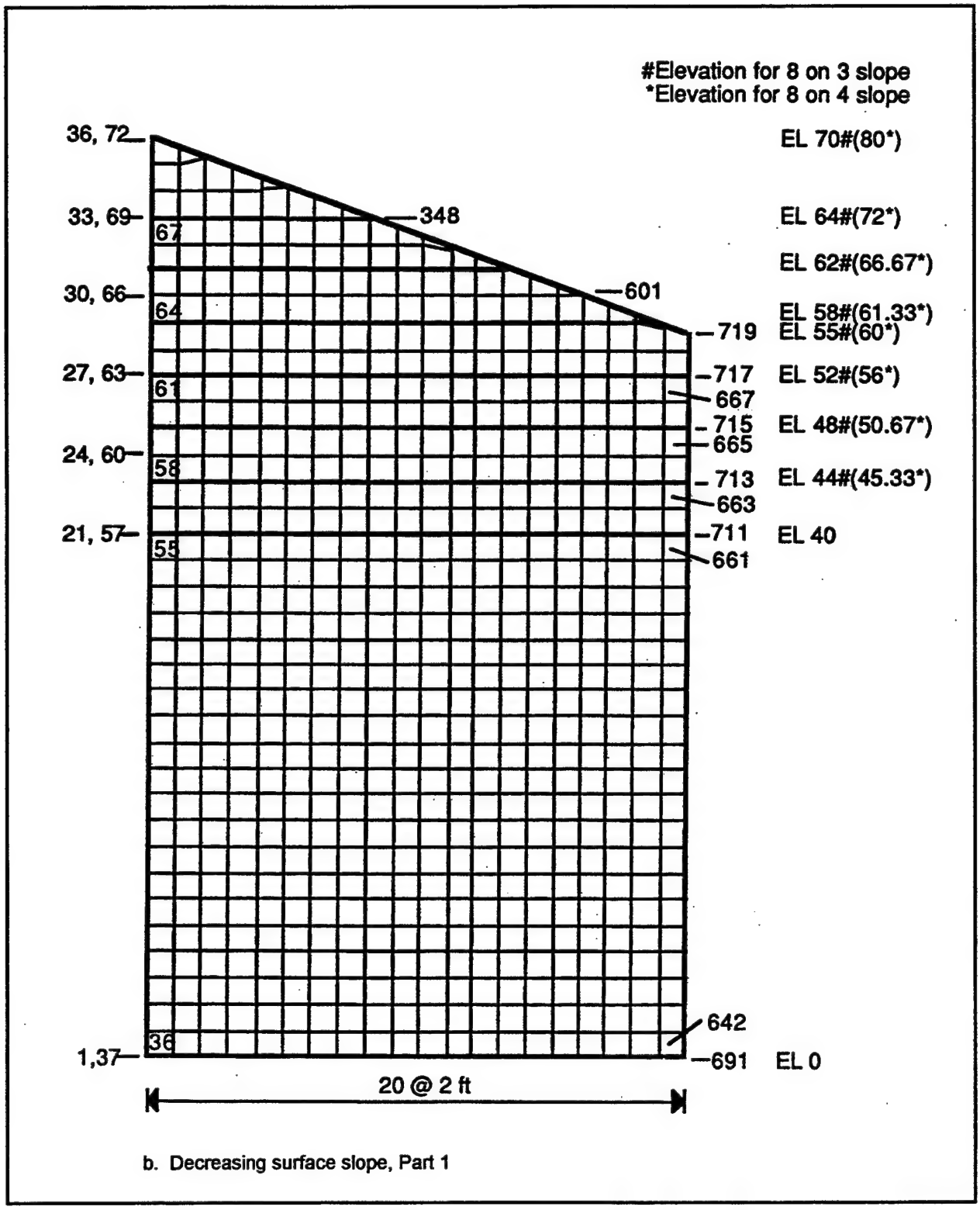

b. Decreasing surface slope, Part 1

Figure A2. (Sheet 2 of 5)

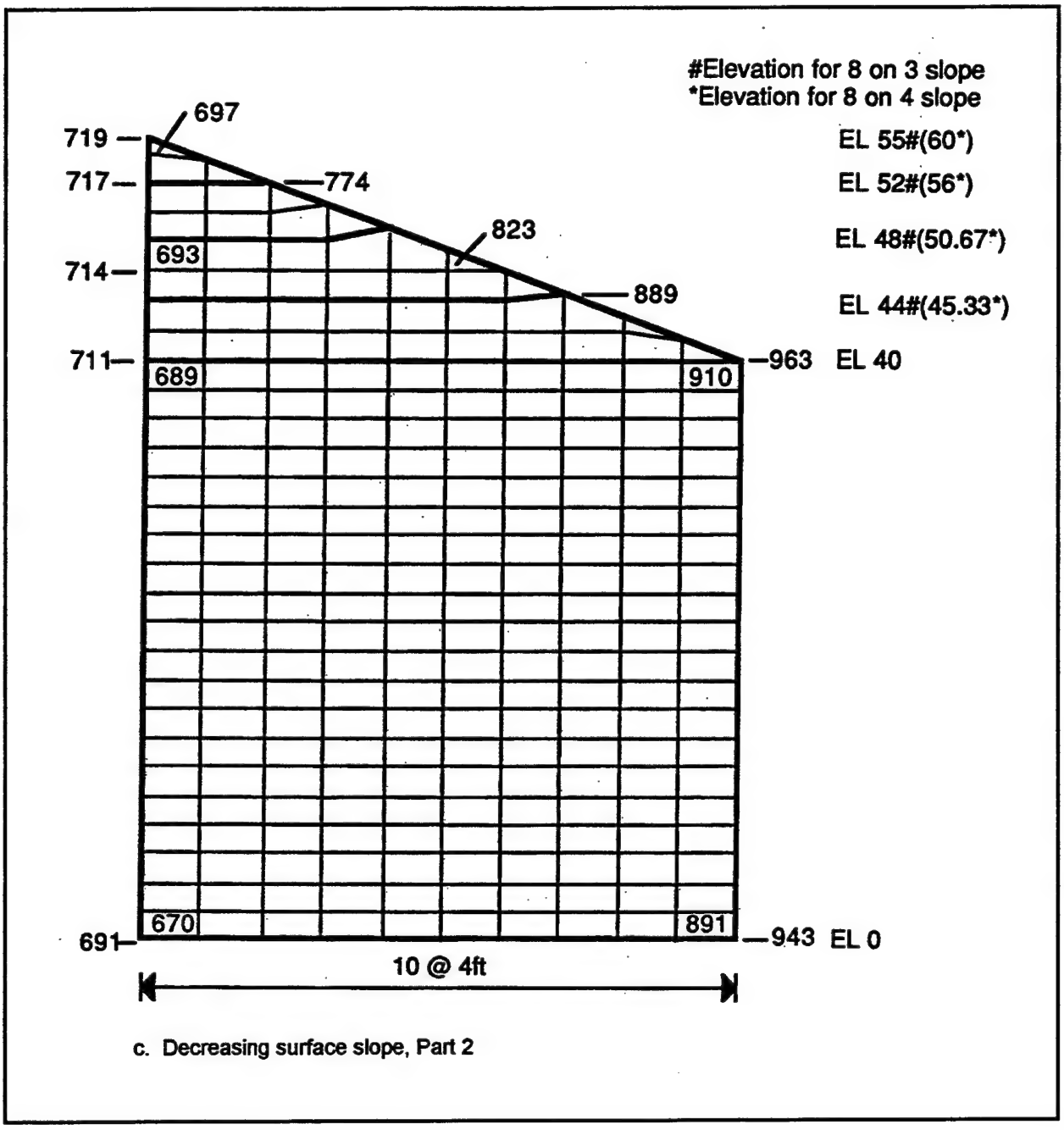

c. Decreasing surface slope, Part 2

Figure A2. (Sheet 3 of 5)

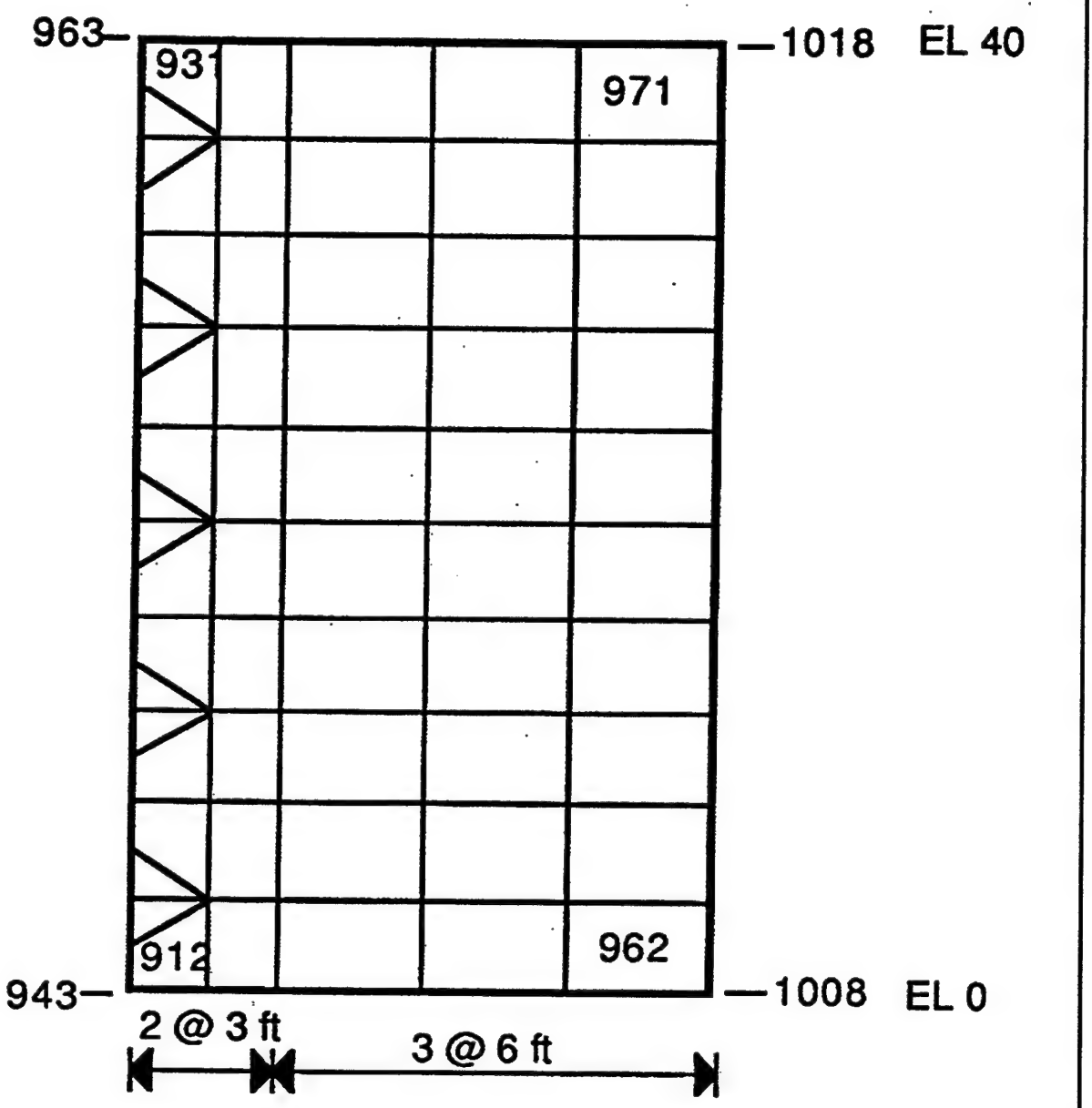

d. Decreasing surface slope, Part 3

Figure A2. (Sheet 4 of 5)

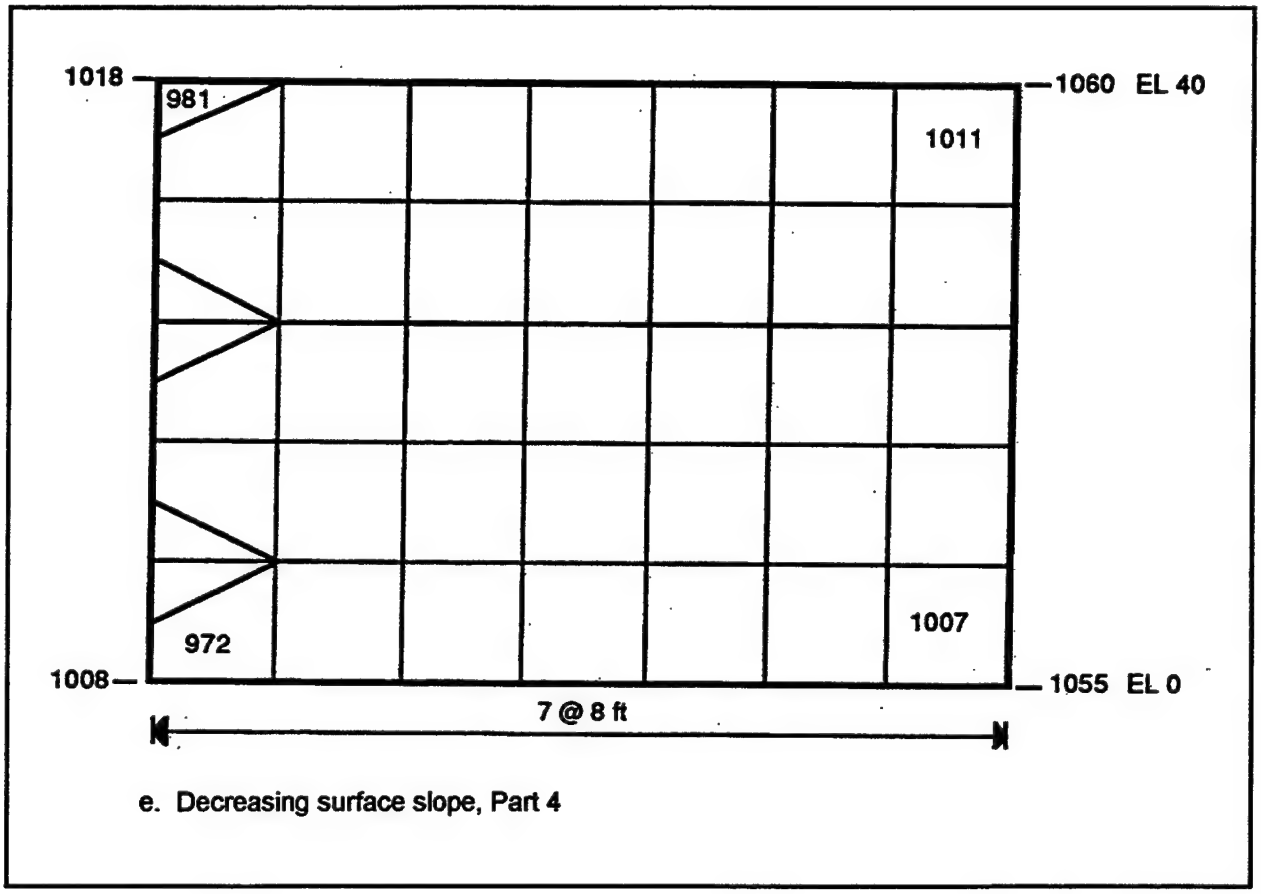

e. Decreasing surface slope, Part 4

Figure A2. (Sheet 5 of 5)

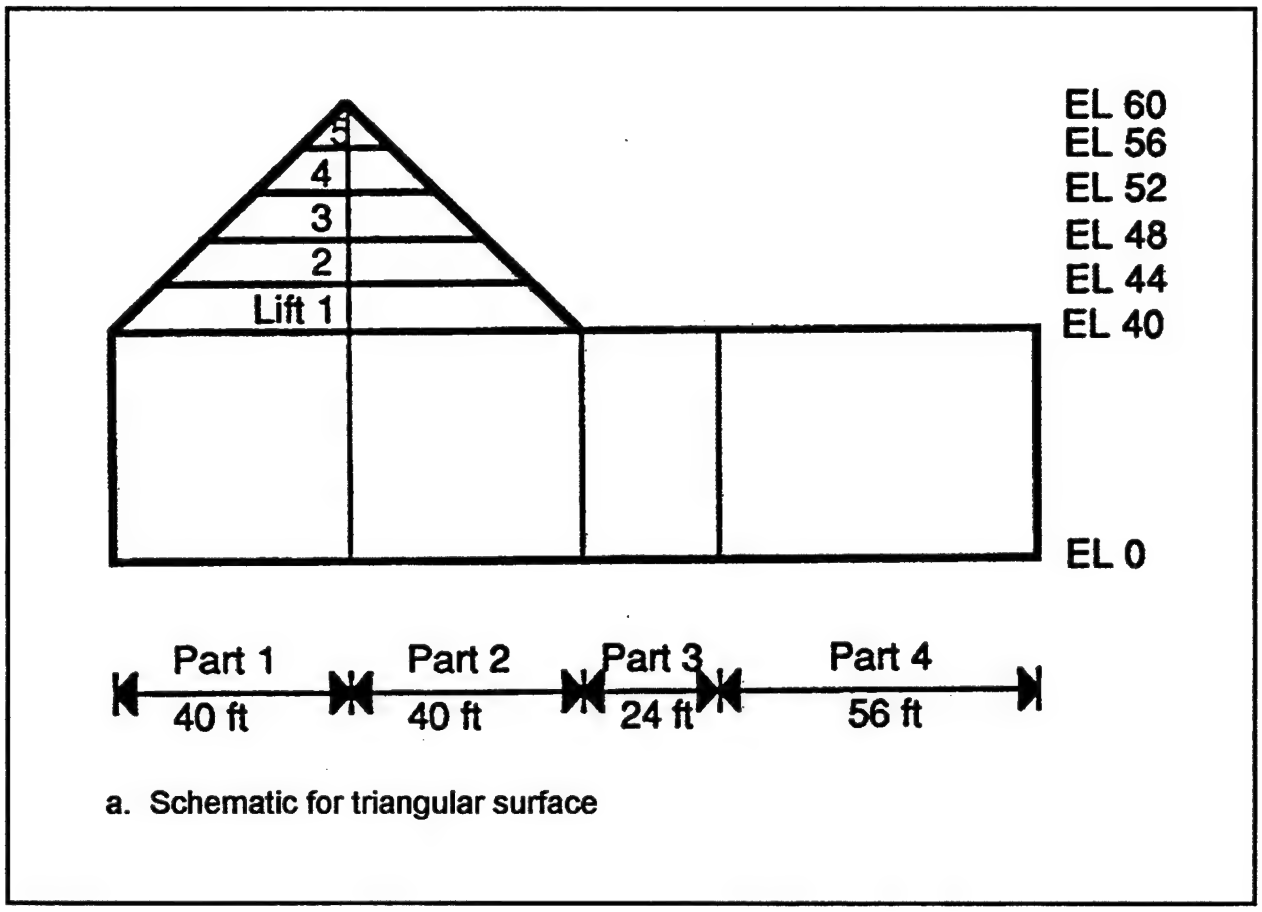

a. Schematic for triangular surface

Figure A3. Finite element model for triangular surface (Sheet 1 of 5)

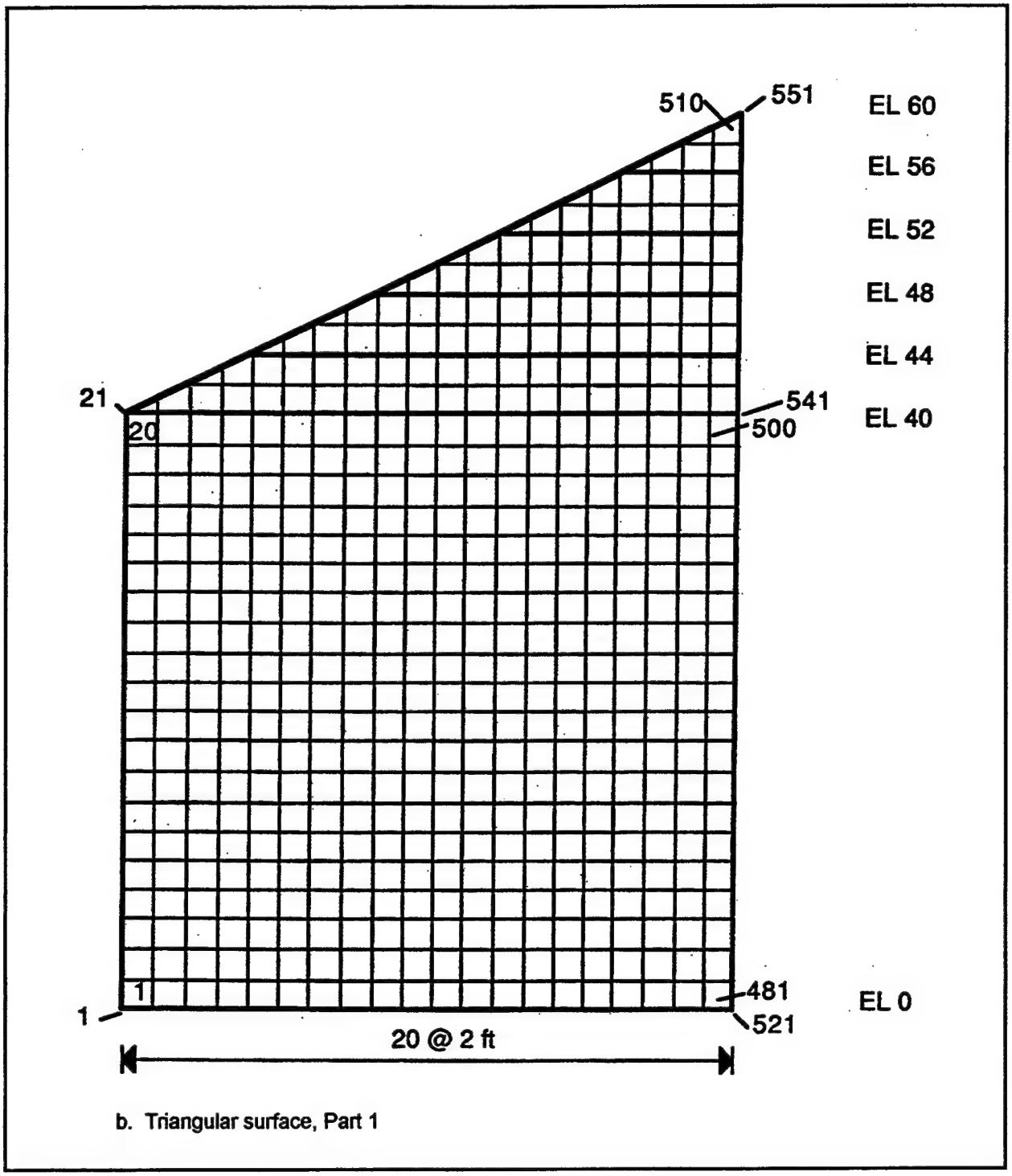

b. Triangular surface, Part 1

Figure A3. (Sheet 2 of 5)

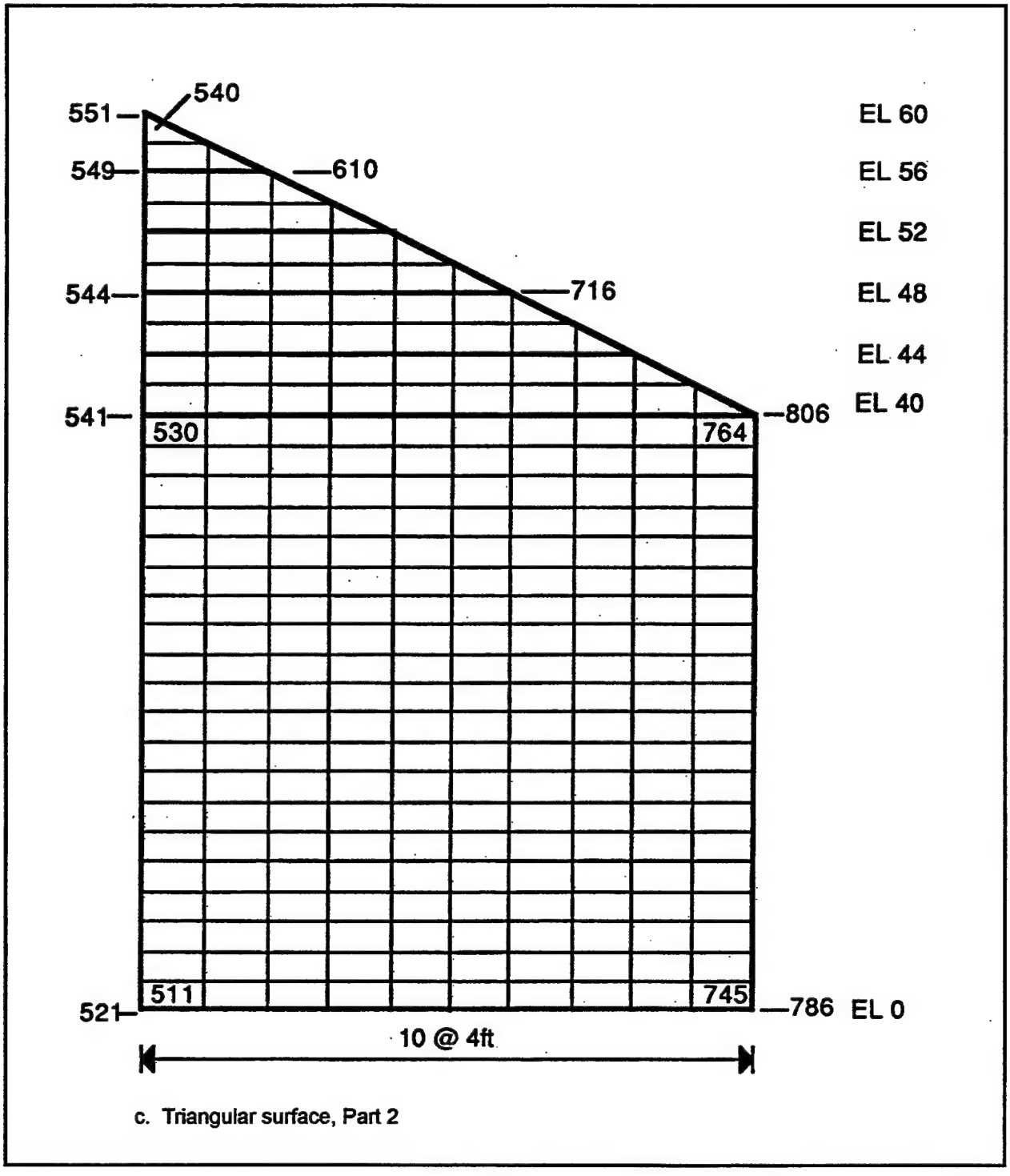

c. Triangular surface, Part 2

Figure A3. (Sheet 3 of 5)

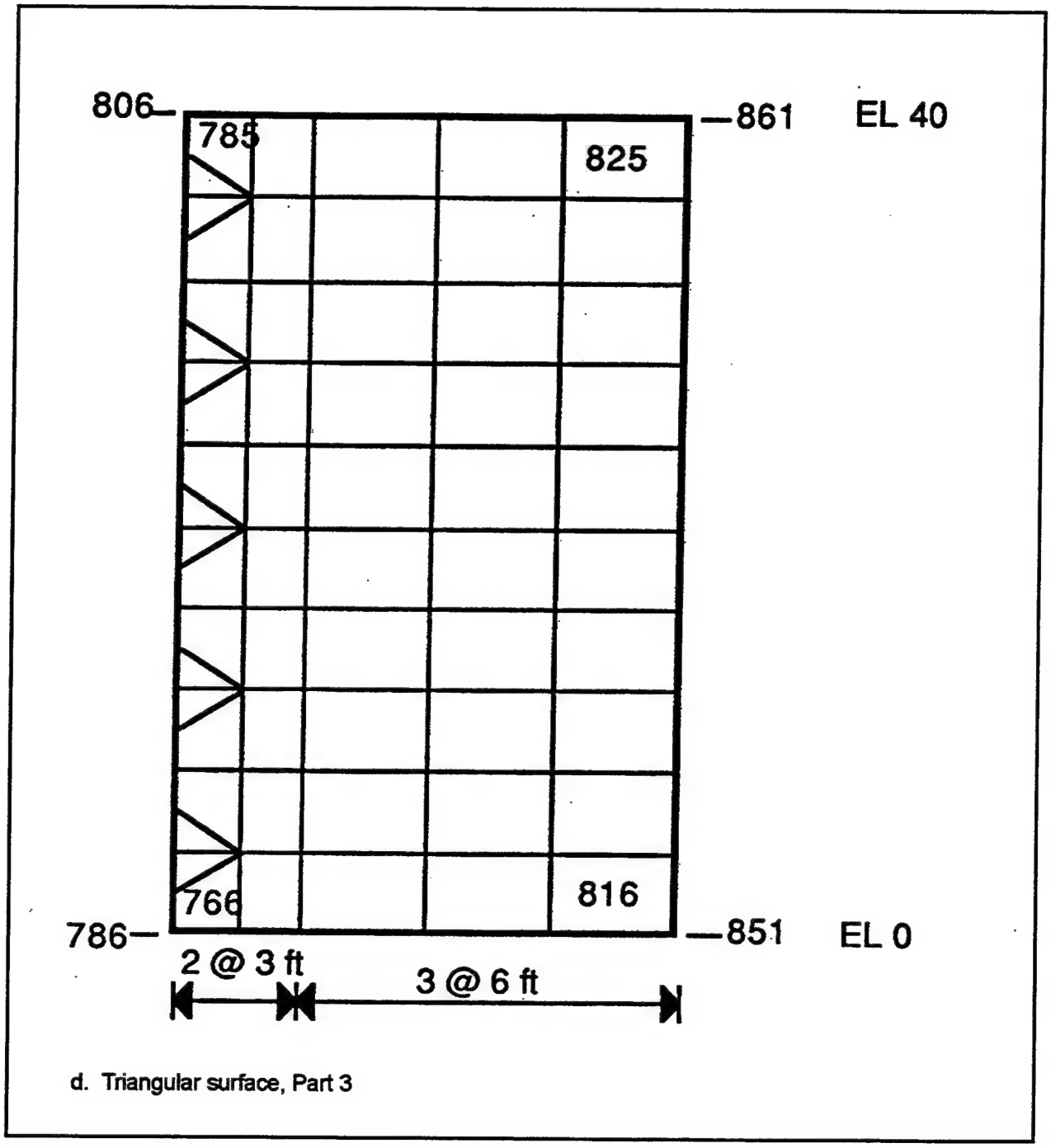

d. Triangular surface, Part 3

Figure A3. (Sheet 4 of 5)

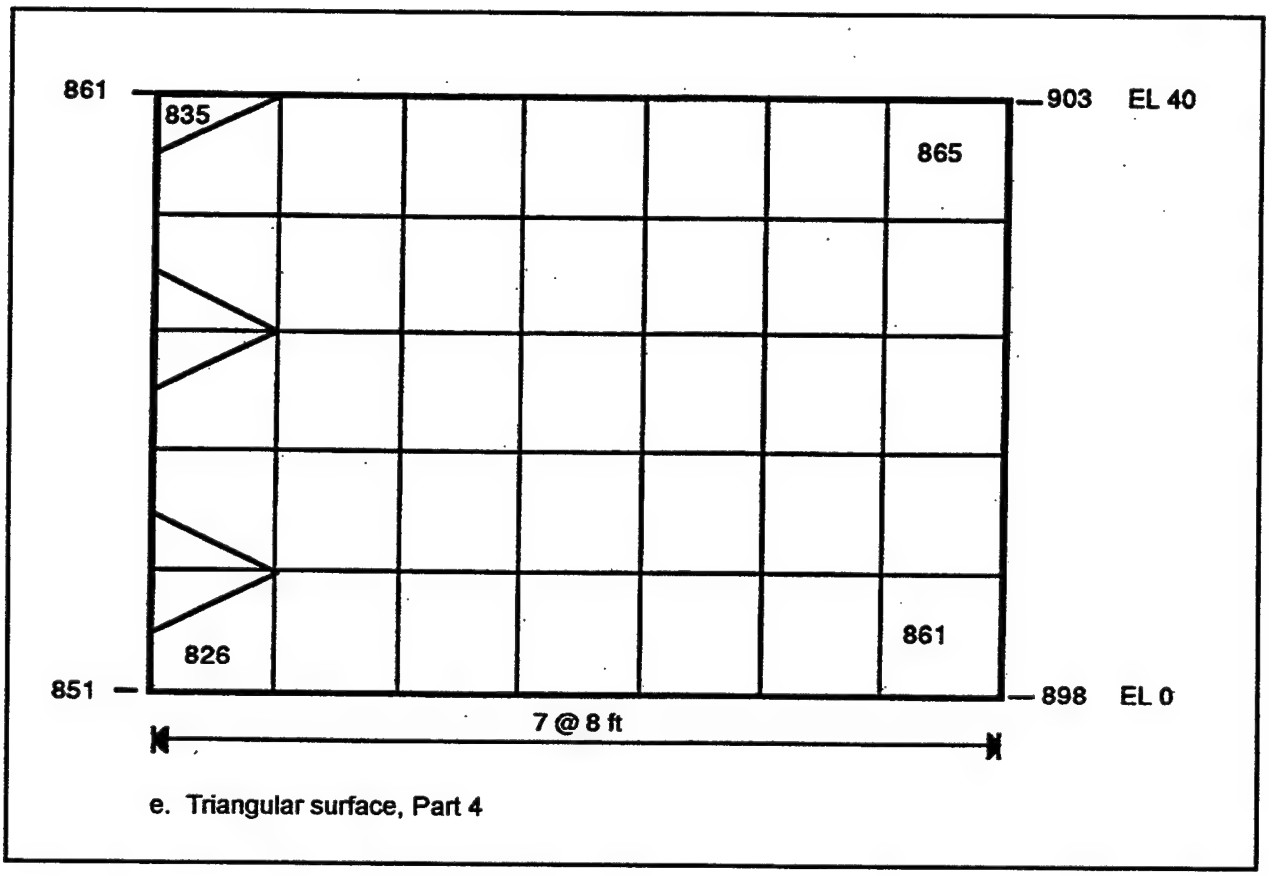

e. Triangular surface, Part 4

Figure A3. (Sheet 5 of 5)

Appendix B
Finite Element Models for Two-Layered Systems

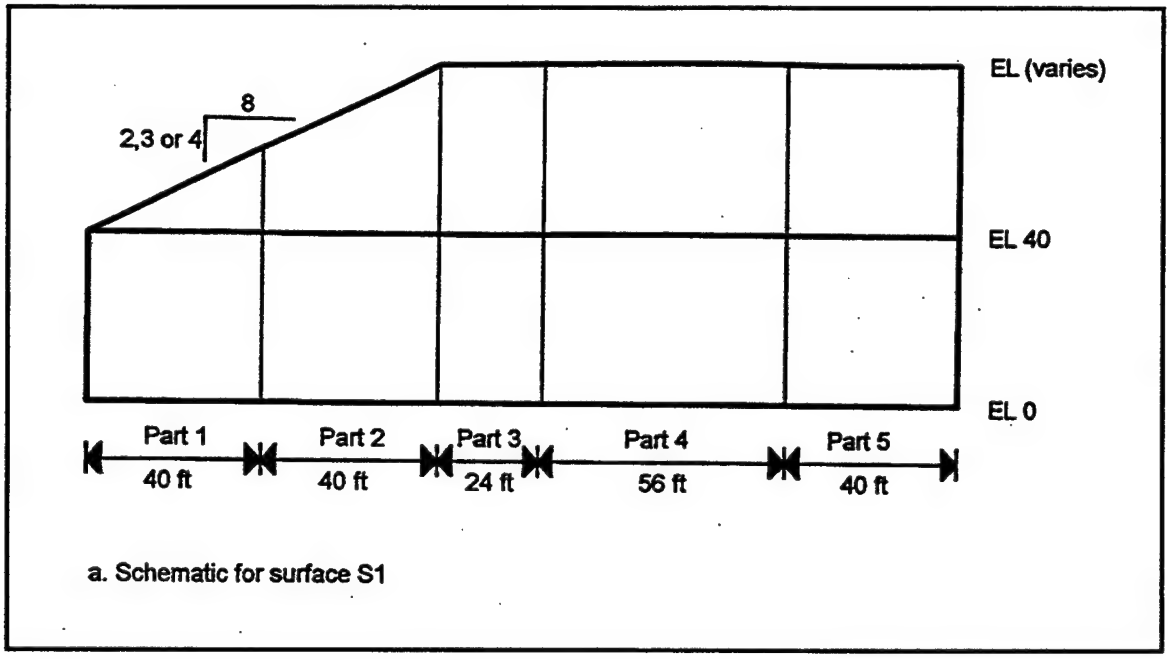

Figure B1. Finite element model for surface S1 (Sheet 1 of 6)

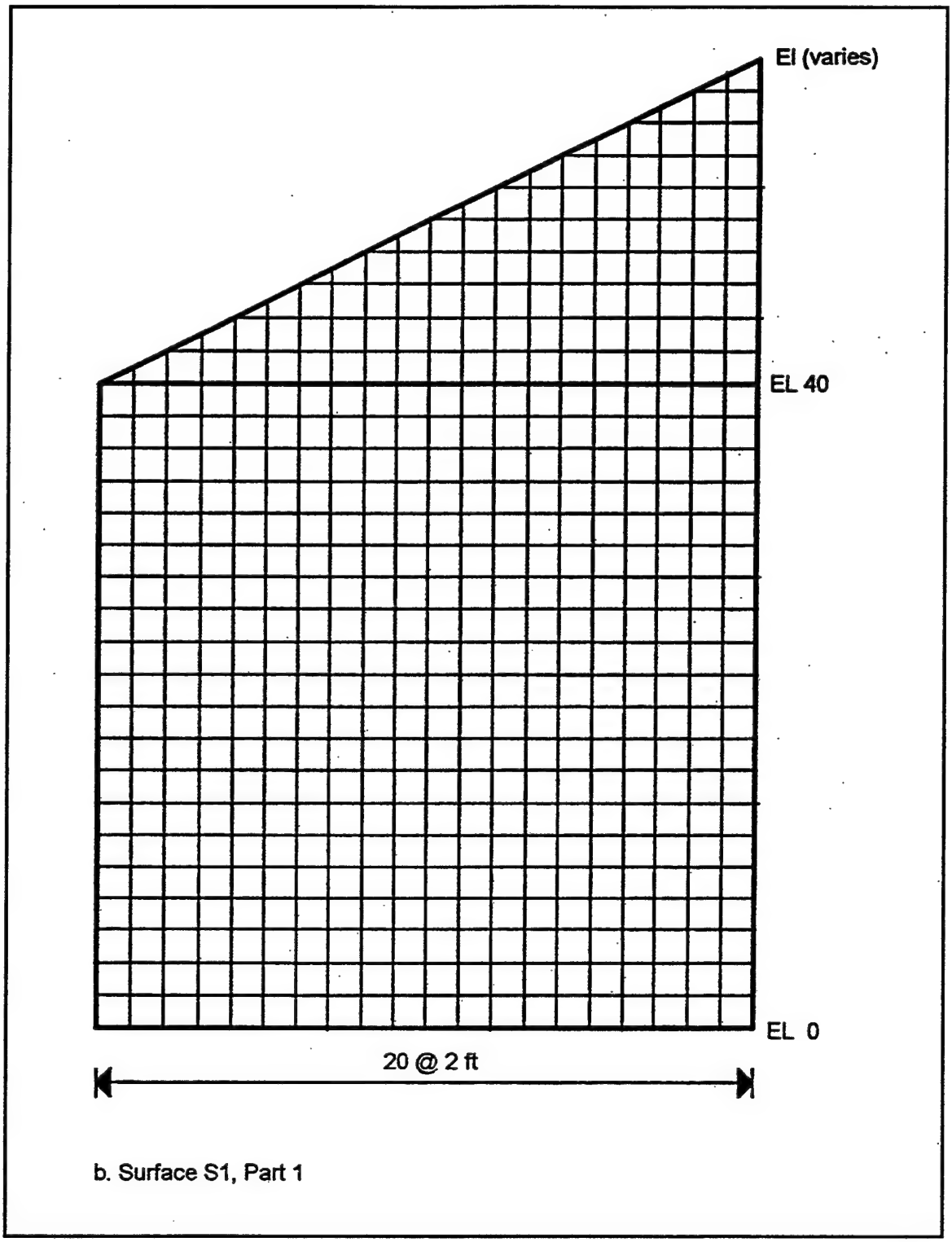

Figure B1. (Sheet 2 of 6)

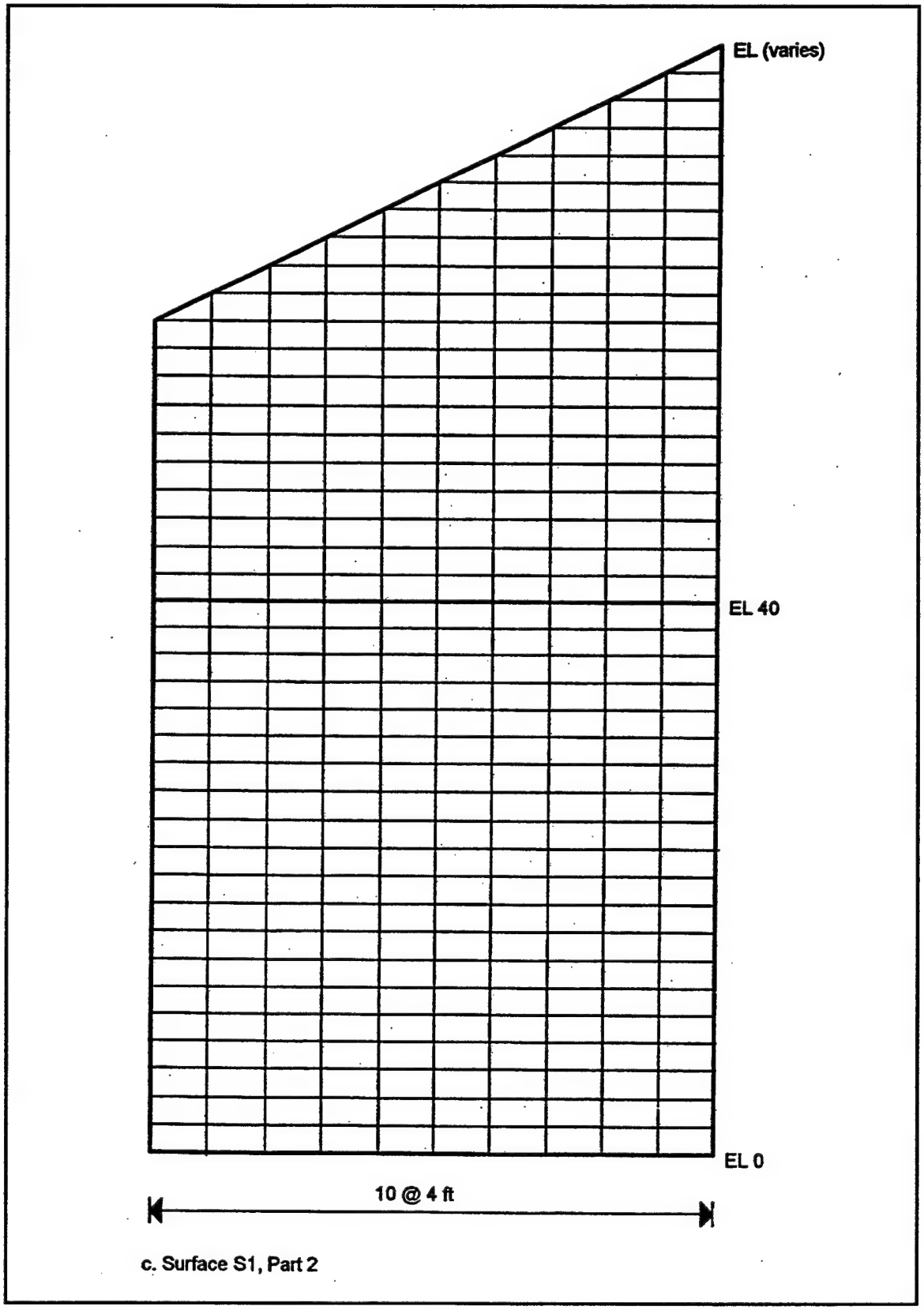

Figure B1. (Sheet 3 of 6)

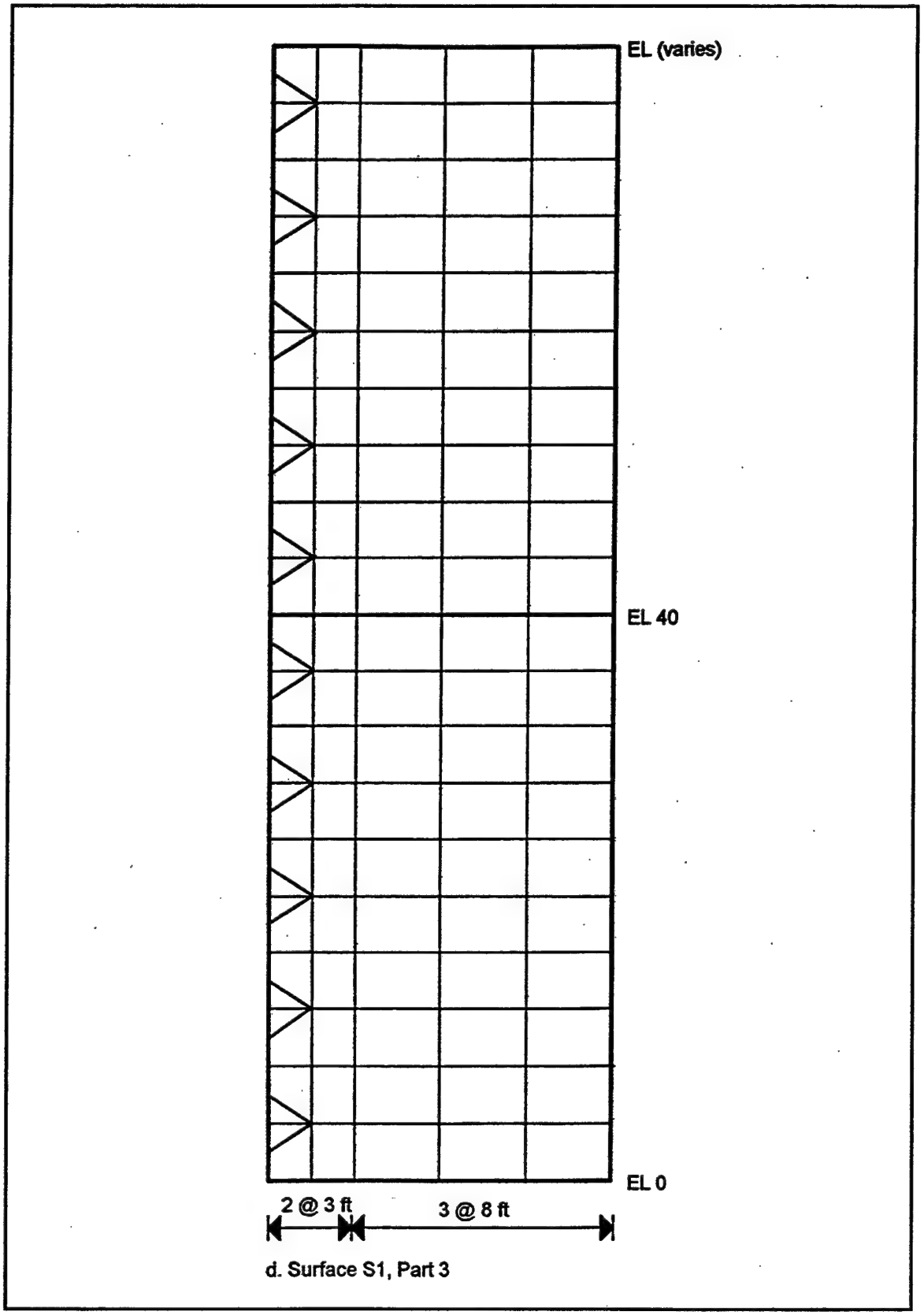

d. Surface S1, Part 3

Figure B1. (Sheet 4 of 6)

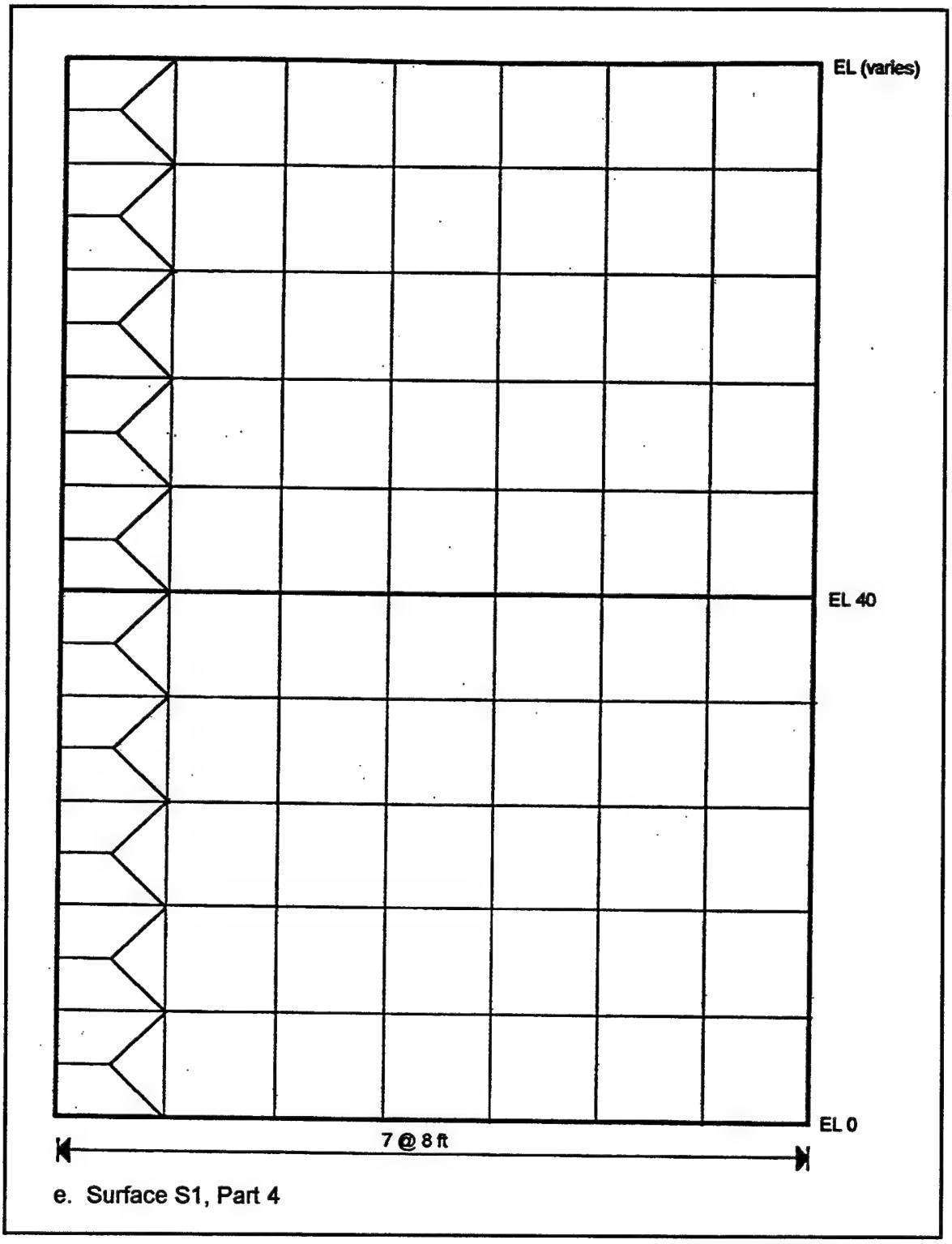

e. Surface S1, Part 4

Figure B1. (Sheet 5 of 6)

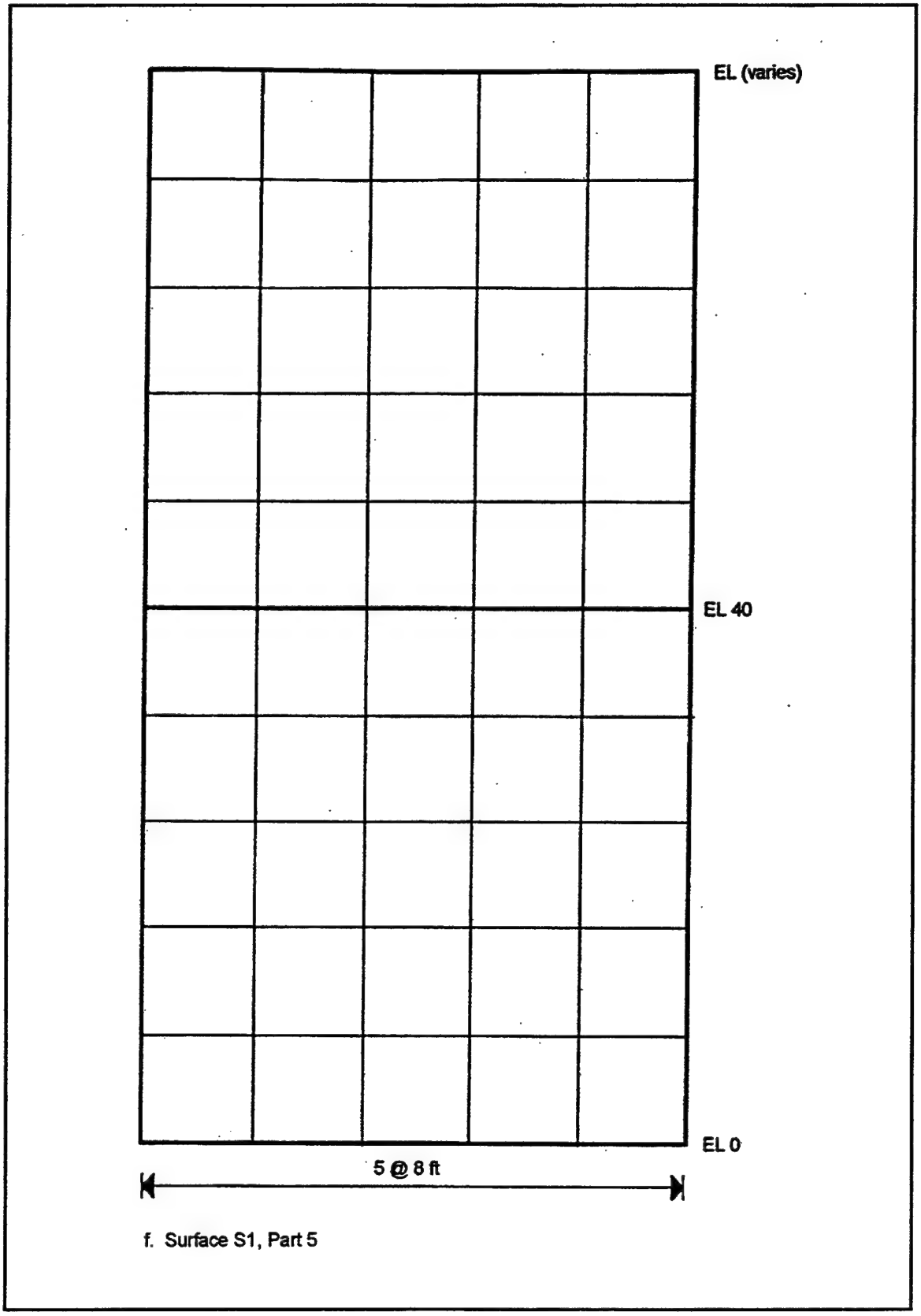

f. Surface S1, Part 5

Figure B1. (Sheet 6 of 6)

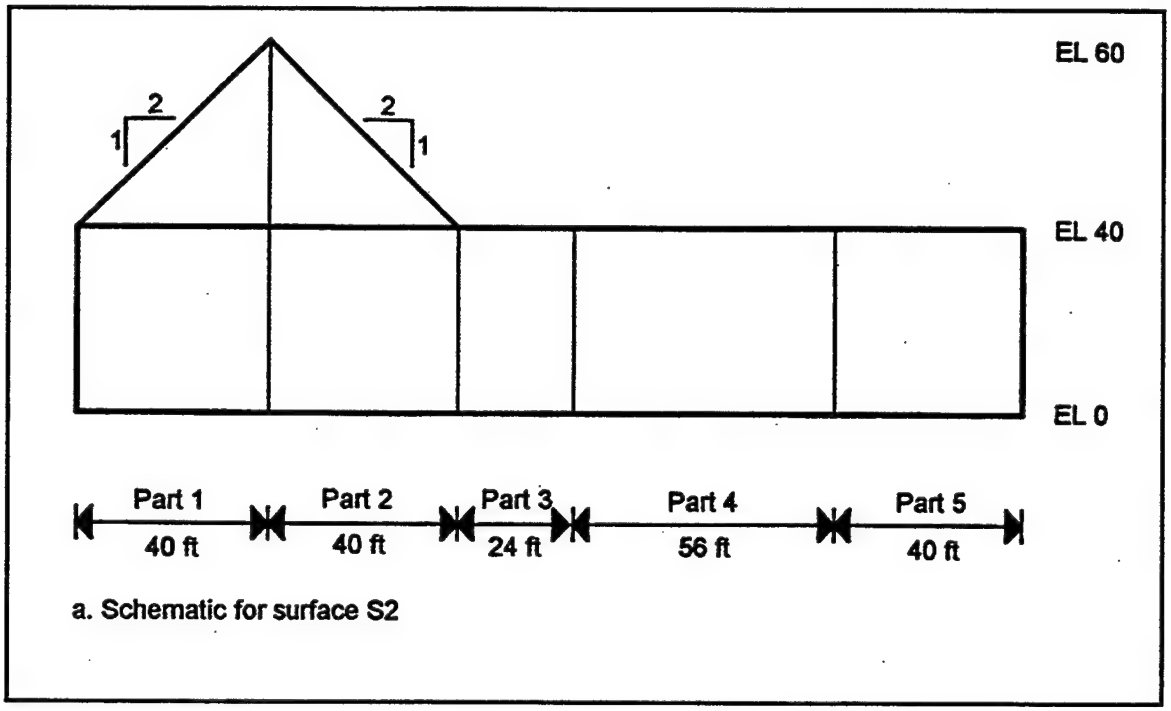

Figure B2. Finite element model for surface S2 (Sheet 1 of 4)

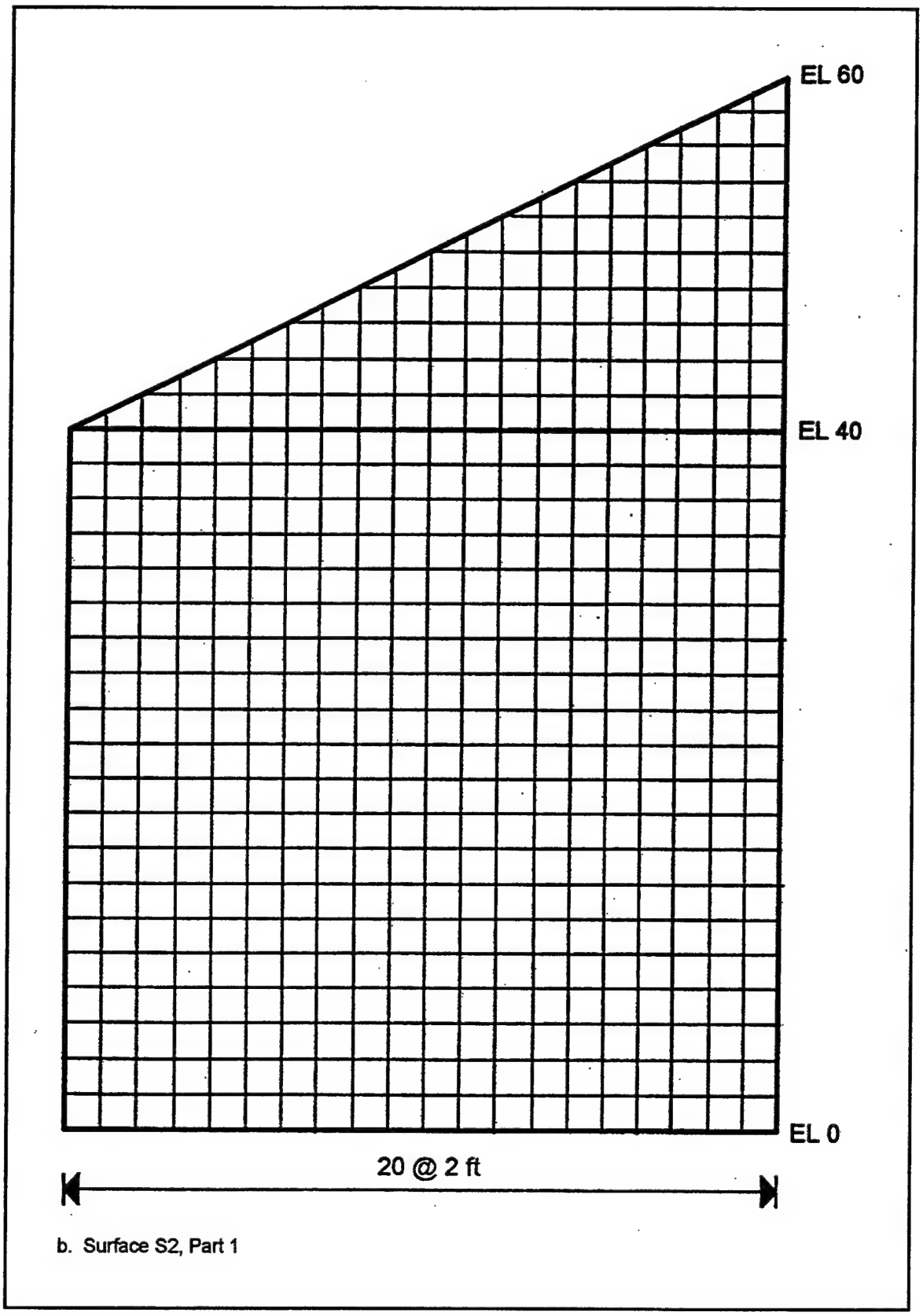

b. Surface S2, Part 1

Figure B2. (Sheet 2 of 4)

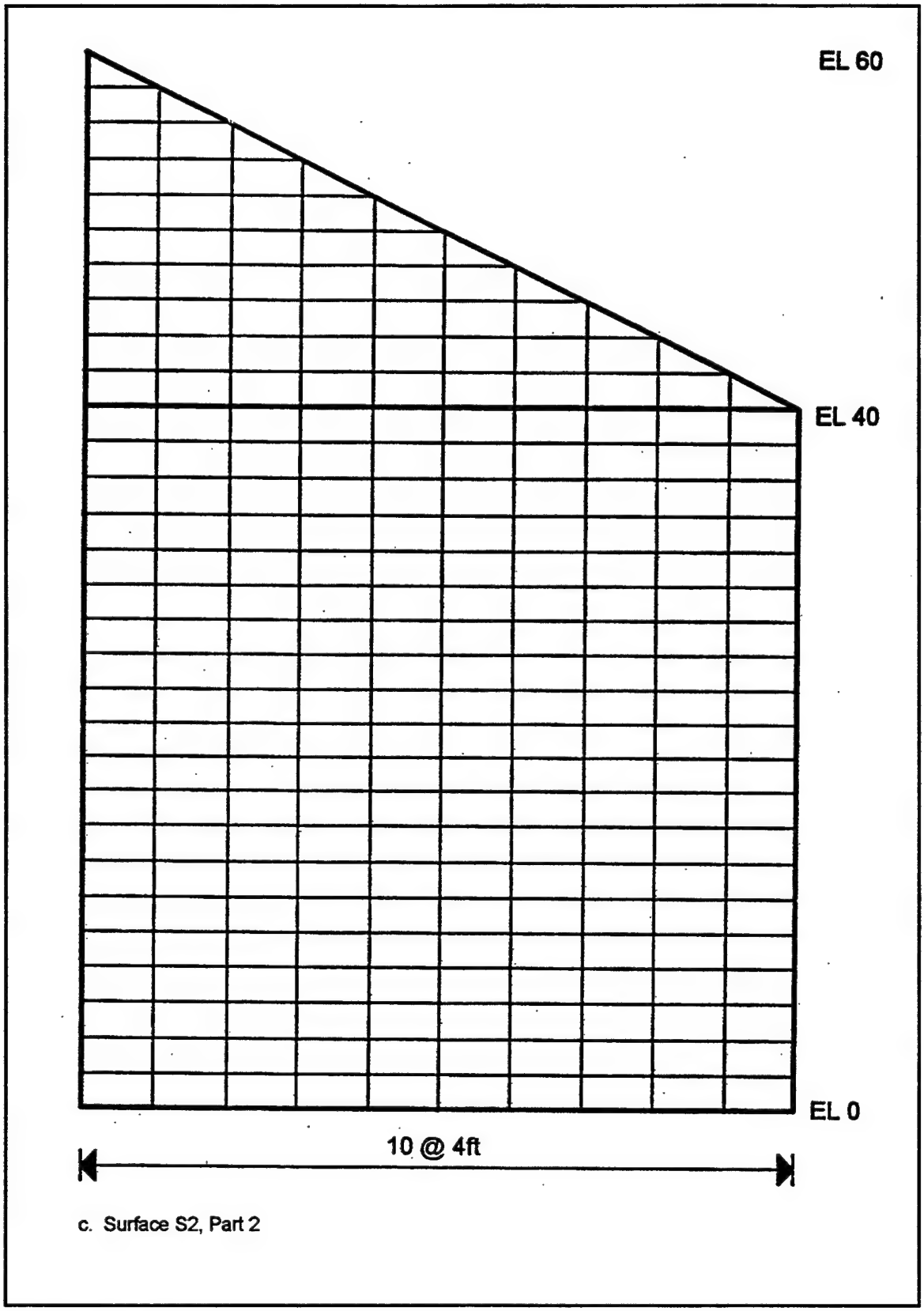

c. Surface S2, Part 2

Figure B2. (Sheet 3 of 4)

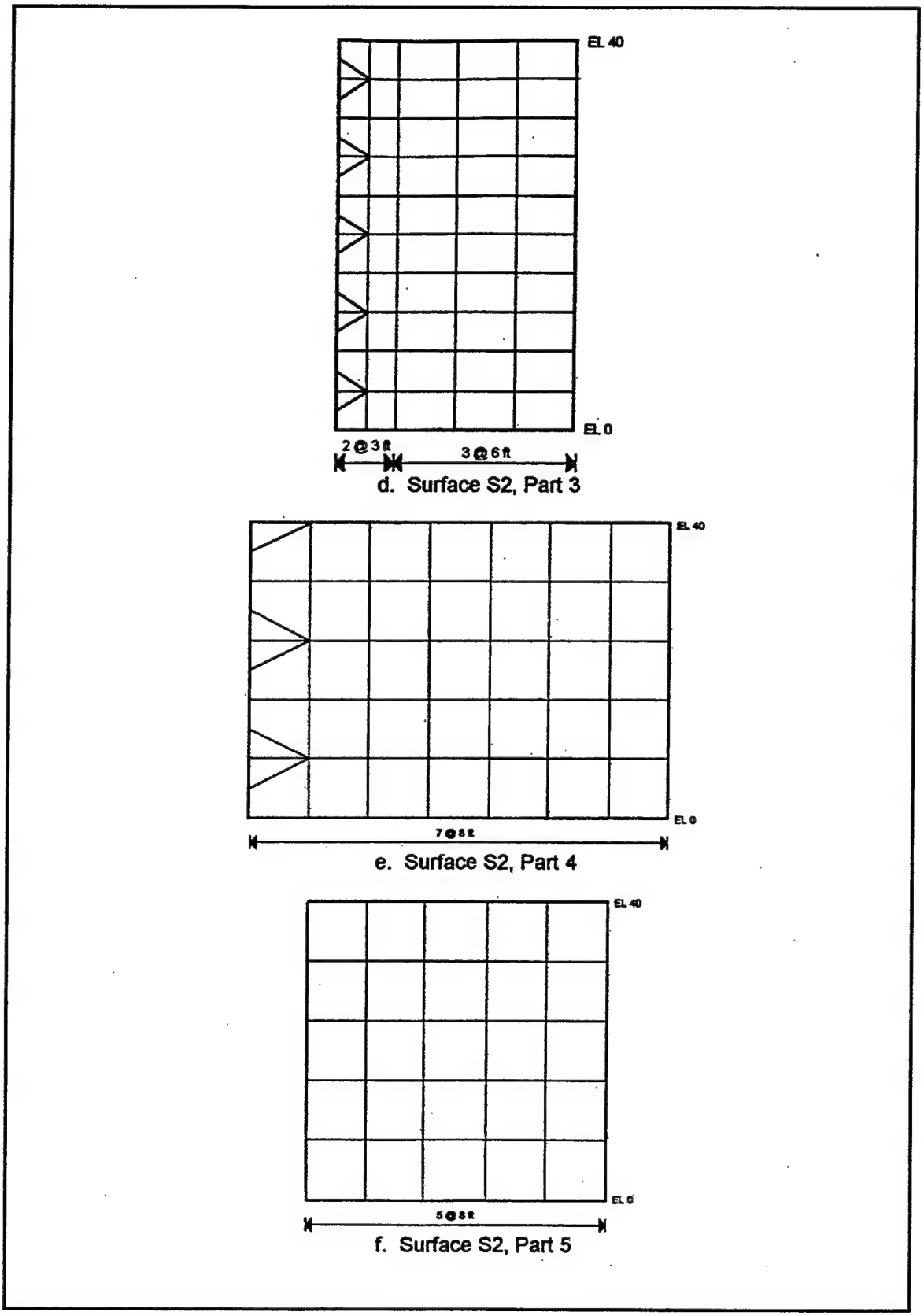

Figure B2. (Sheet 4 of 4)

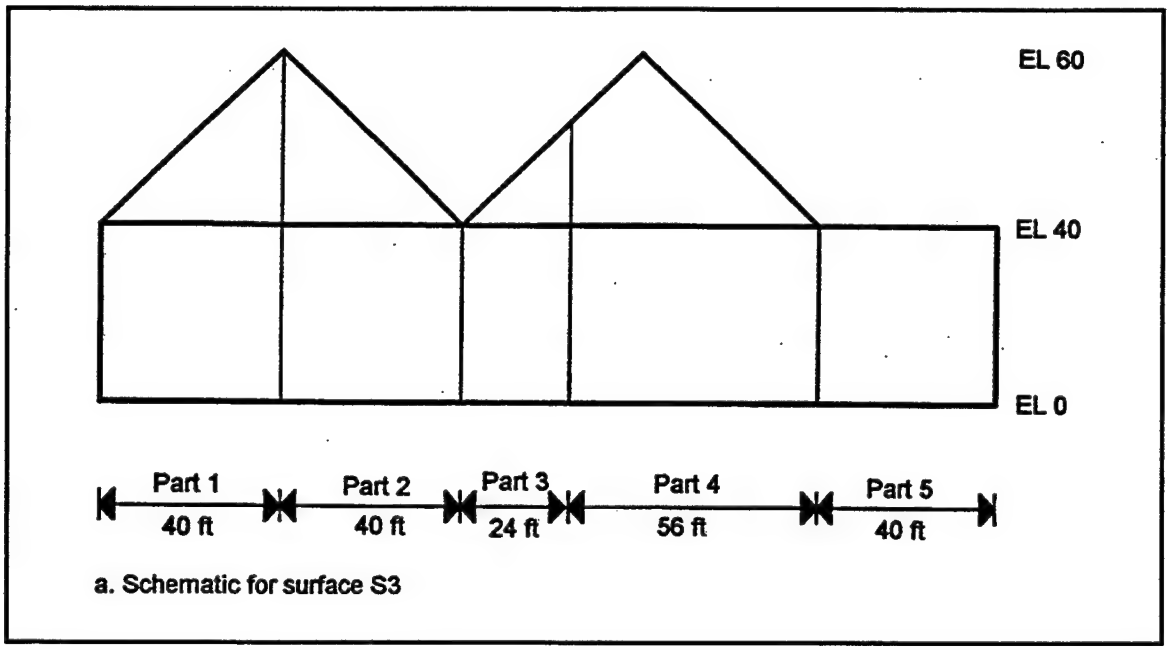

Figure B3. Finite element model for surface S3 (Sheet 1 of 6)

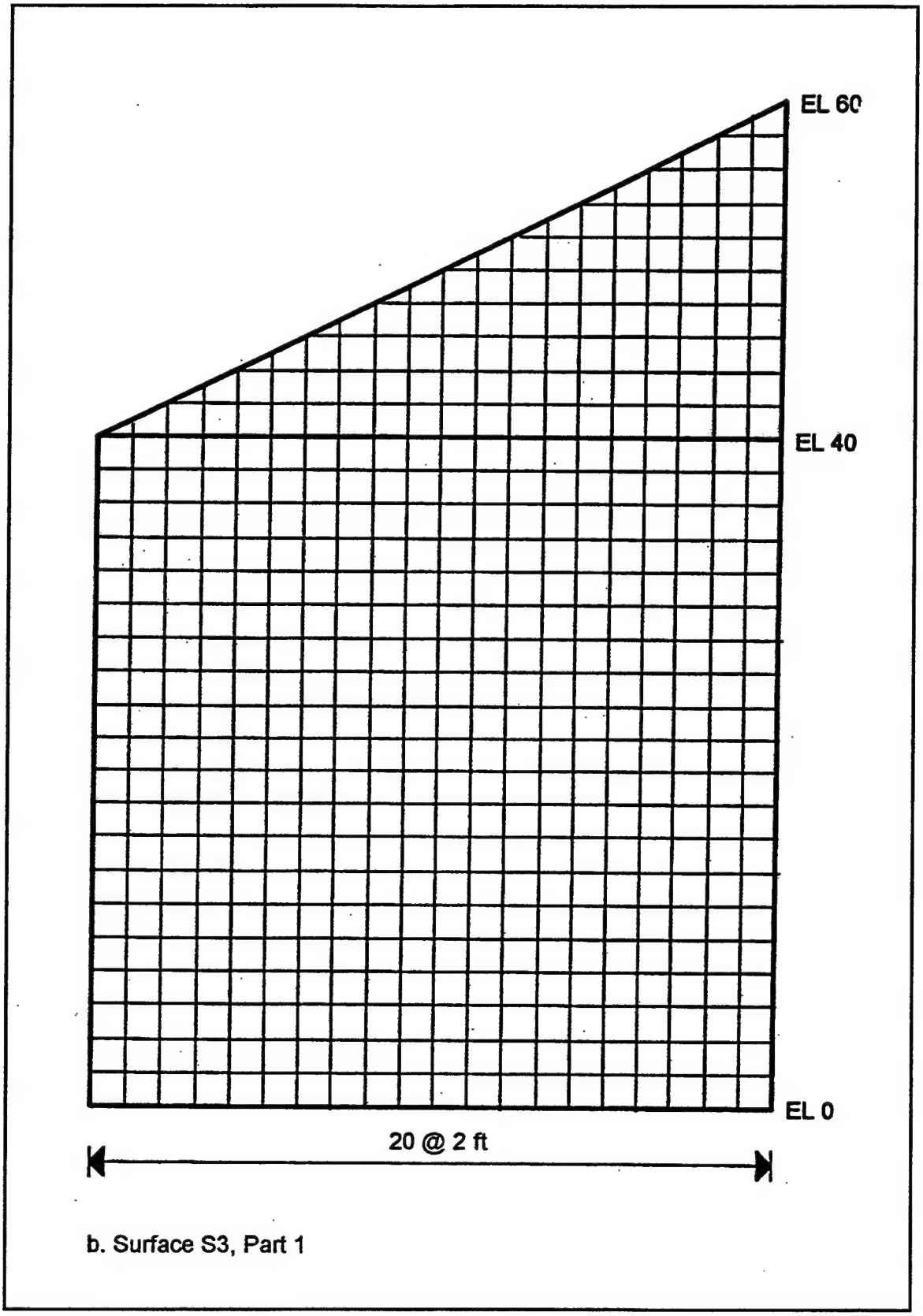

b. Surface S3, Part 1

Figure B3. (Sheet 2 of 6)

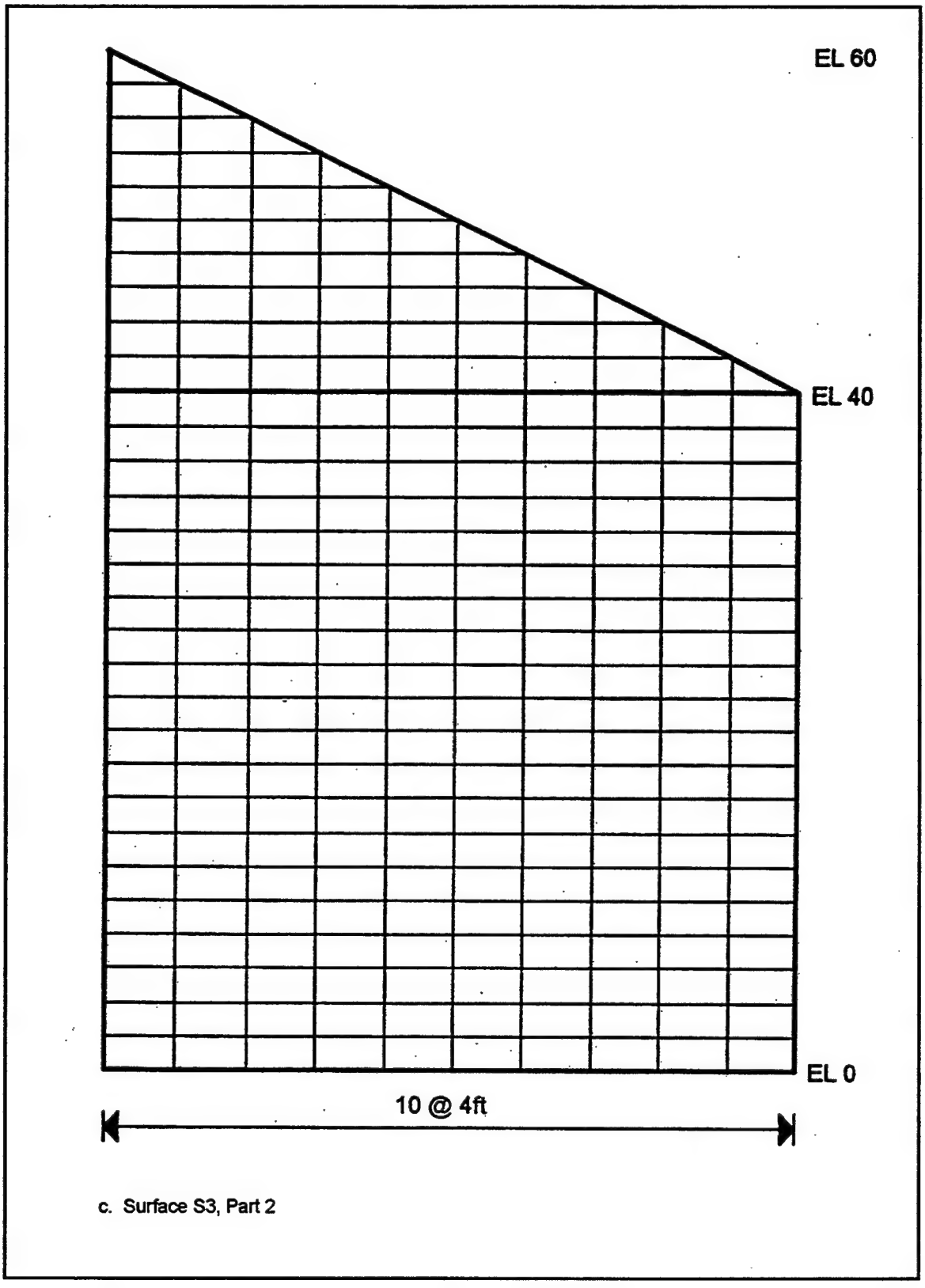

c. Surface S3, Part 2

Figure B3. (Sheet 3 of 6)

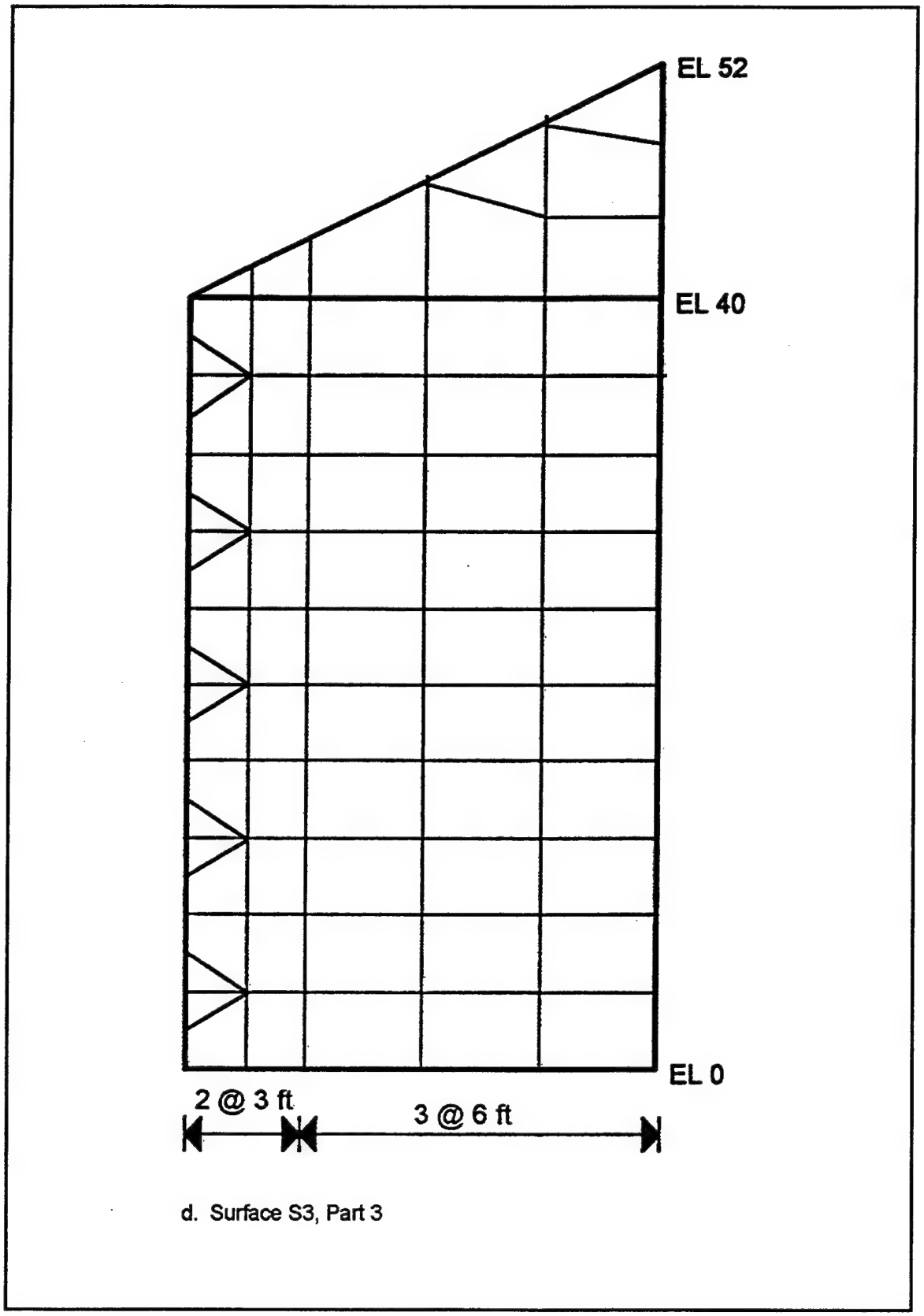

d. Surface S3, Part 3

Figure B3. (Sheet 4 of 6)

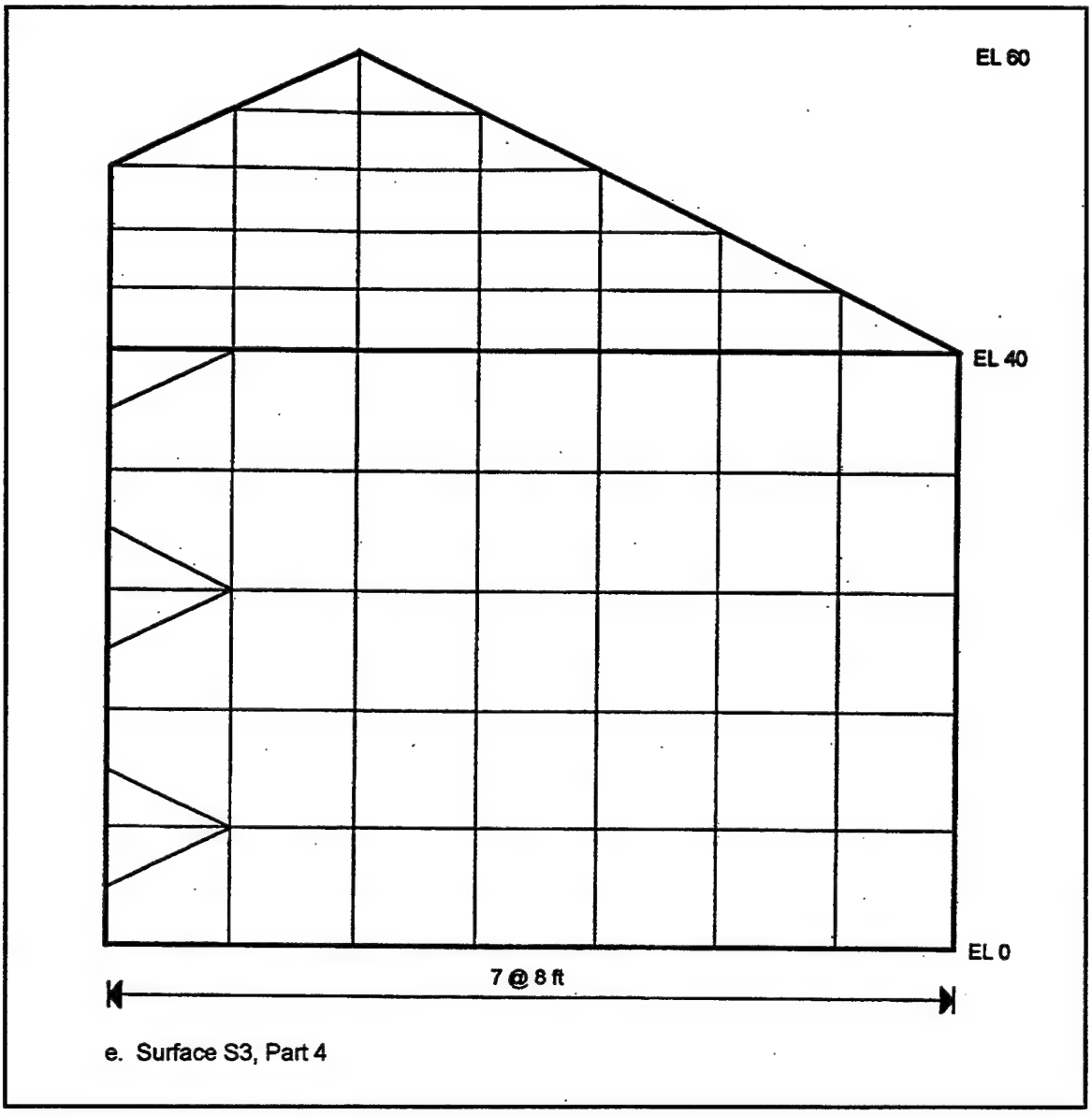

e. Surface S3, Part 4

Figure B3. (Sheet 5 of 6)

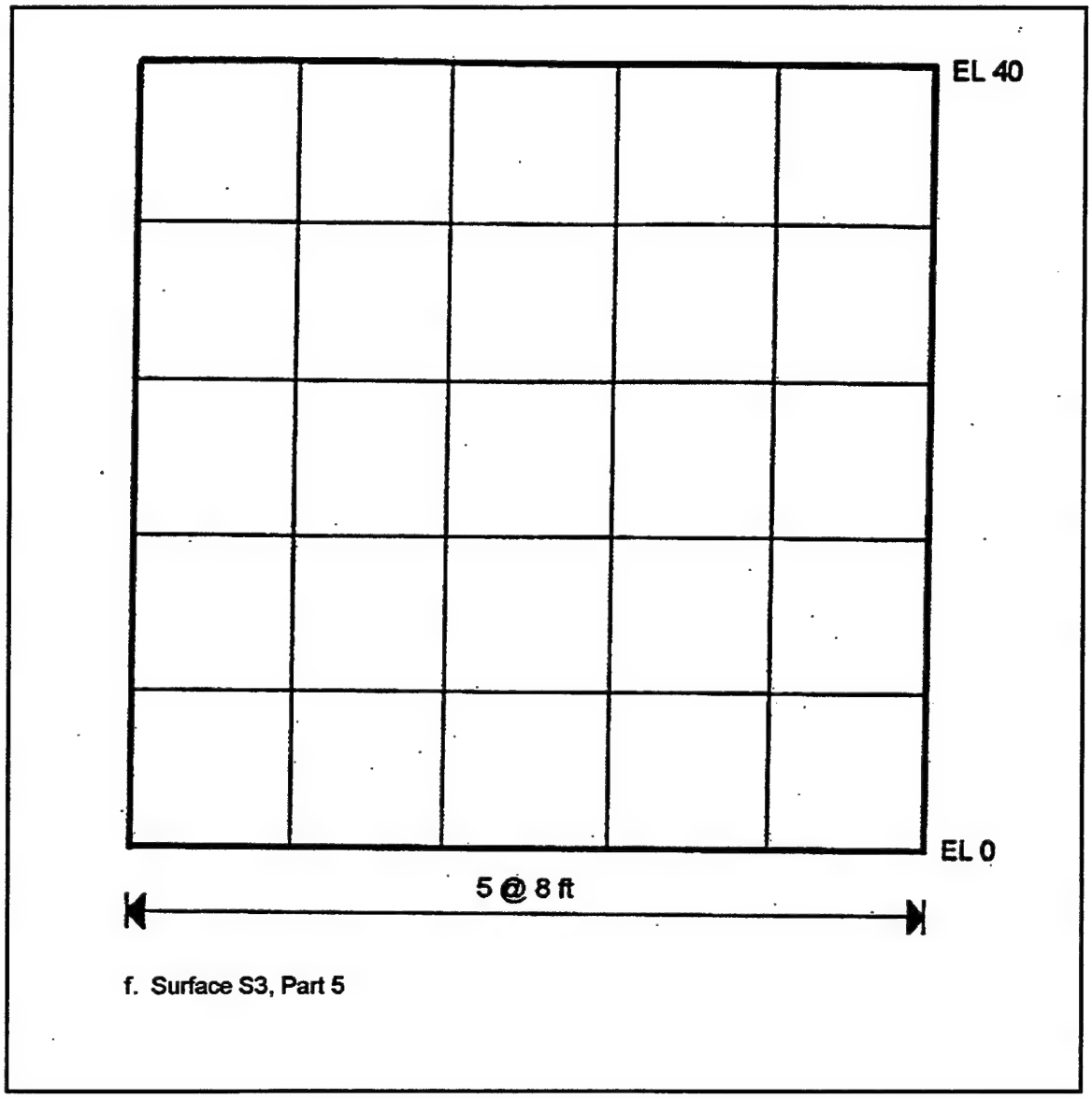

f. Surface S3, Part 5

Figure B3. (Sheet 6 of 6)

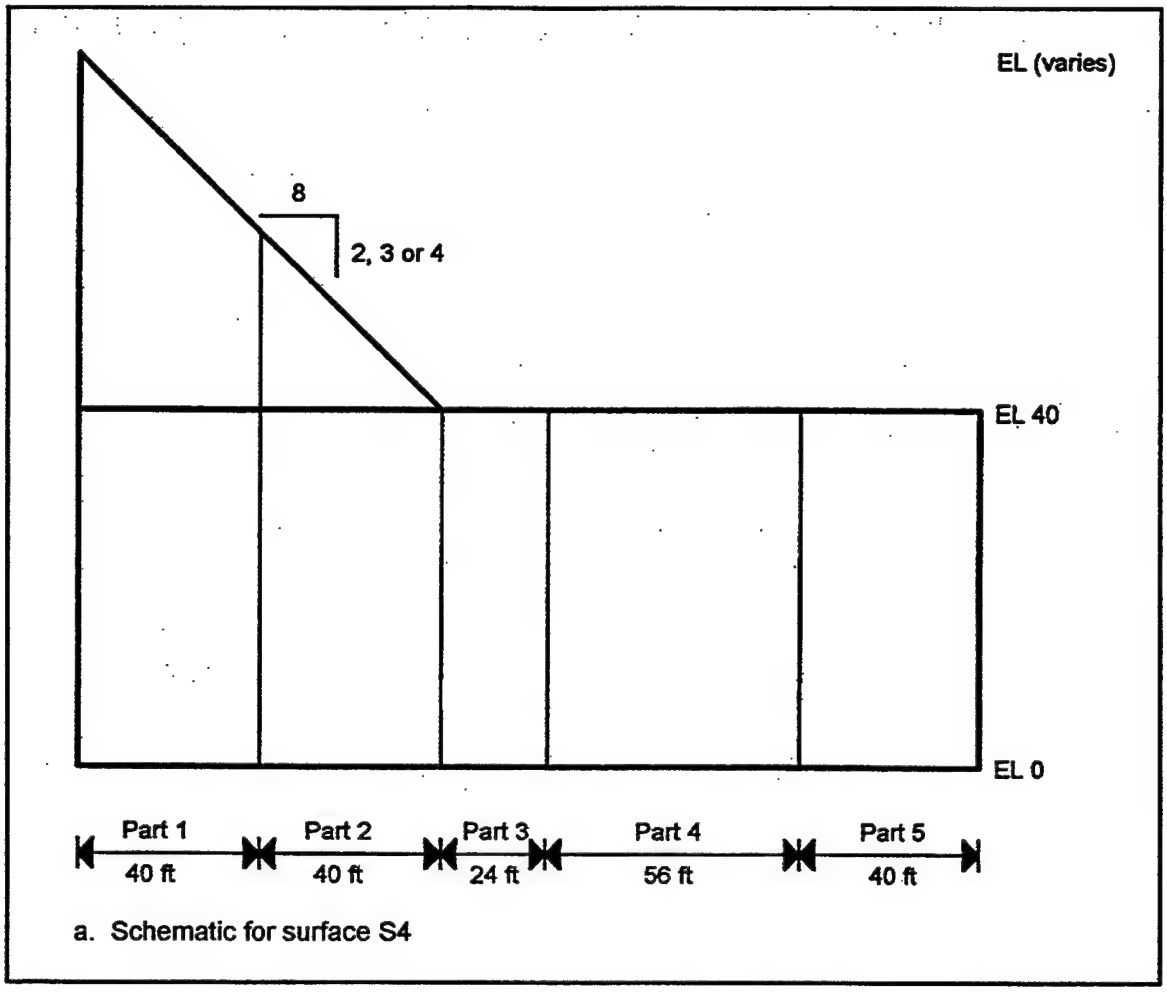

Figure B4. Finite element model for surface S4 (Sheet 1 of 4)

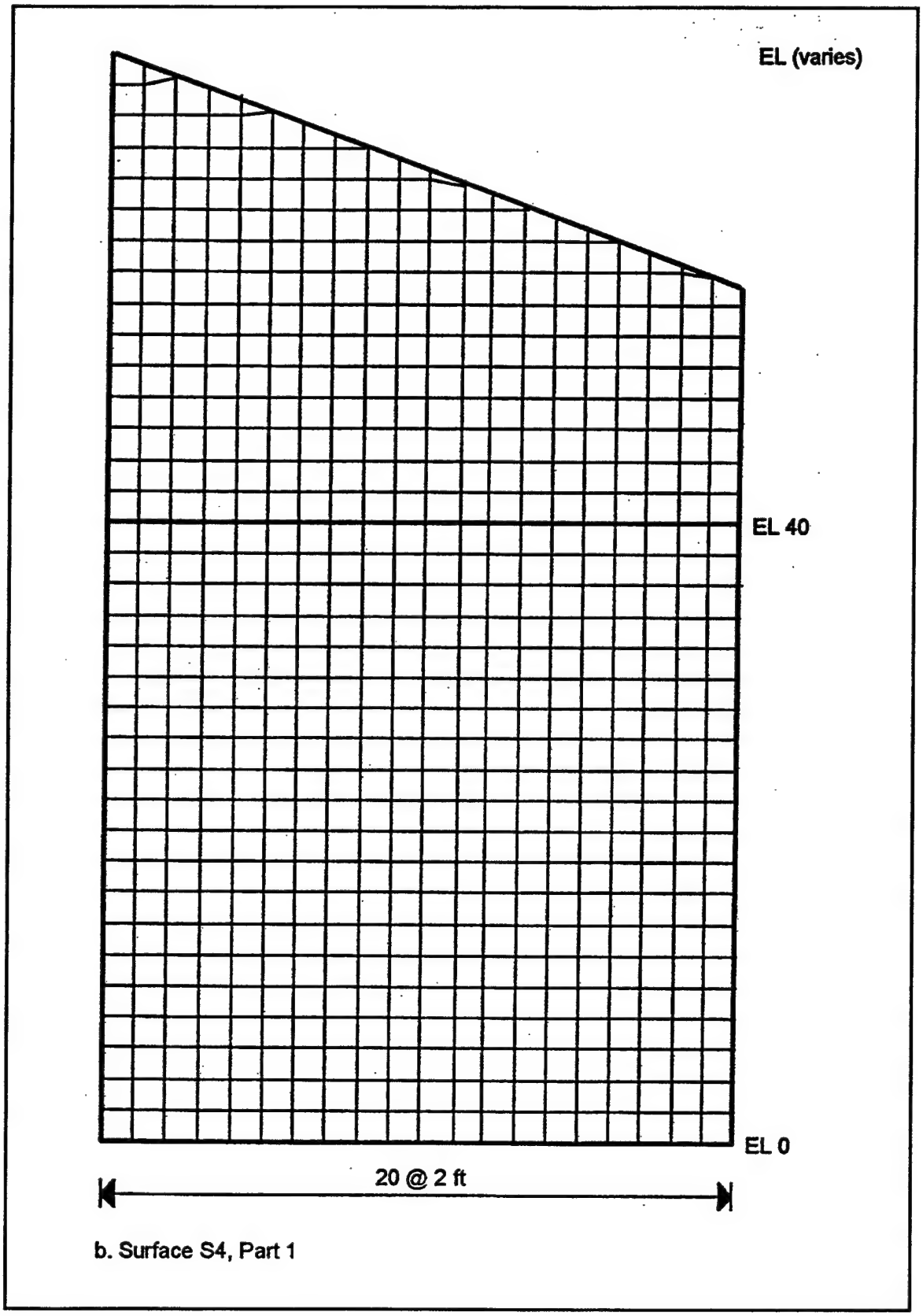

b. Surface S4, Part 1

Figure B4. (Sheet 2 of 4)

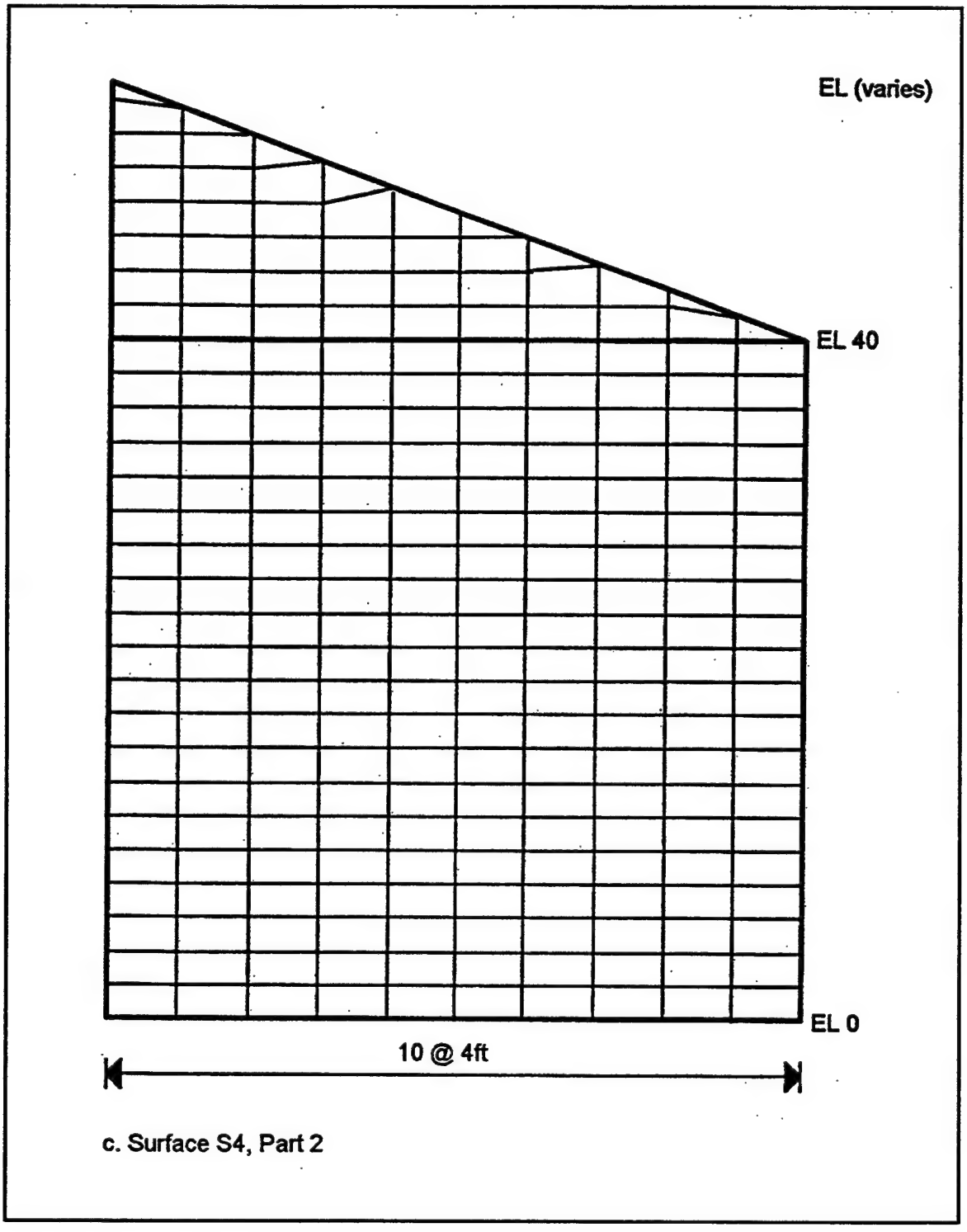

c. Surface S4, Part 2

Figure B4. (Sheet 3 of 4)

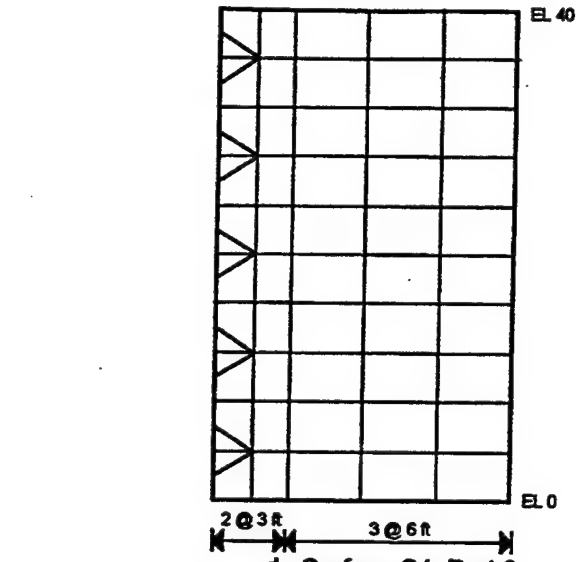

d. Surface S4, Part 3

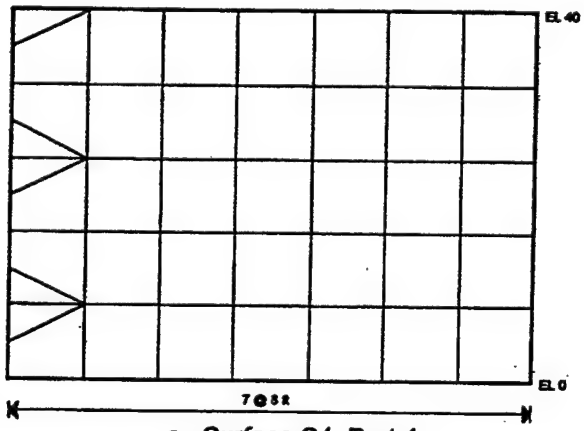

e. Surface S4, Part 4

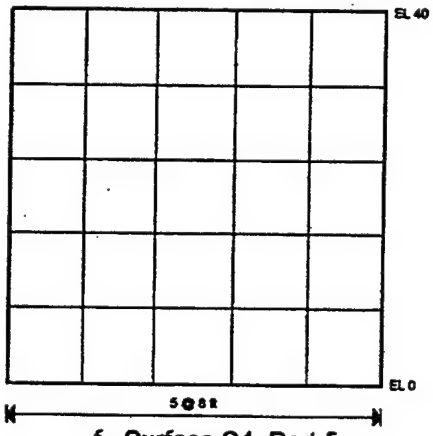

f. Surface S4, Part 5

Figure B4. (Sheet 4 of 4)

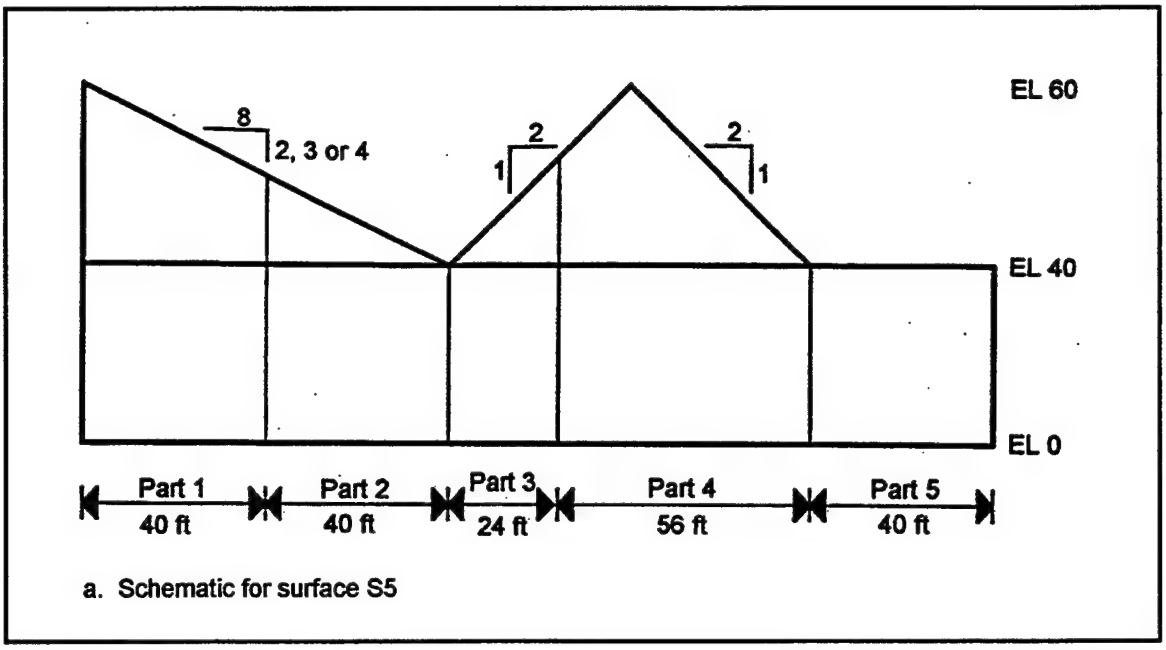

a. Schematic for surface S5

Figure B5. Finite element model for surface S5 (Sheet 1 of 6)

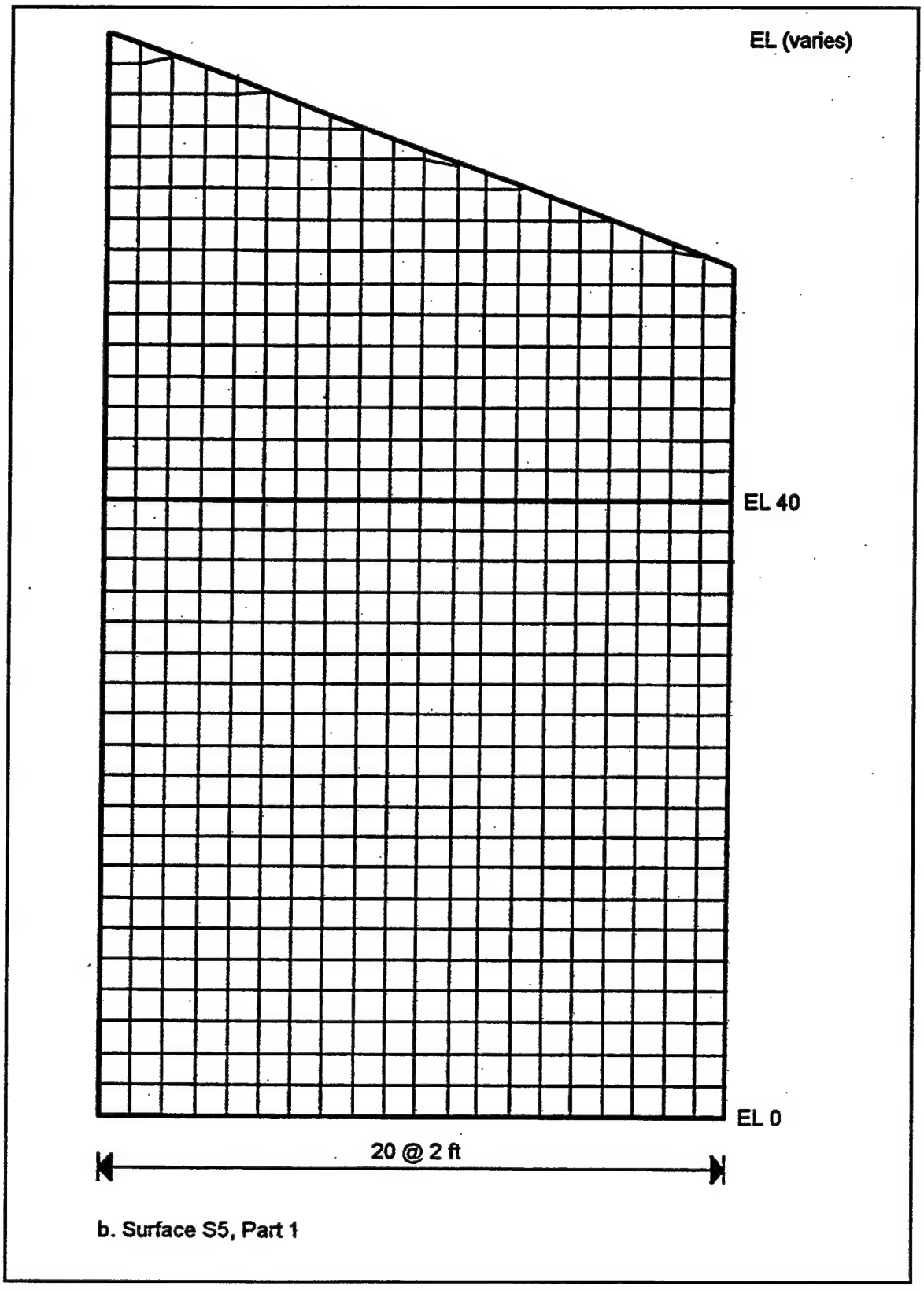

Figure B5. (Sheet 2 of 6)

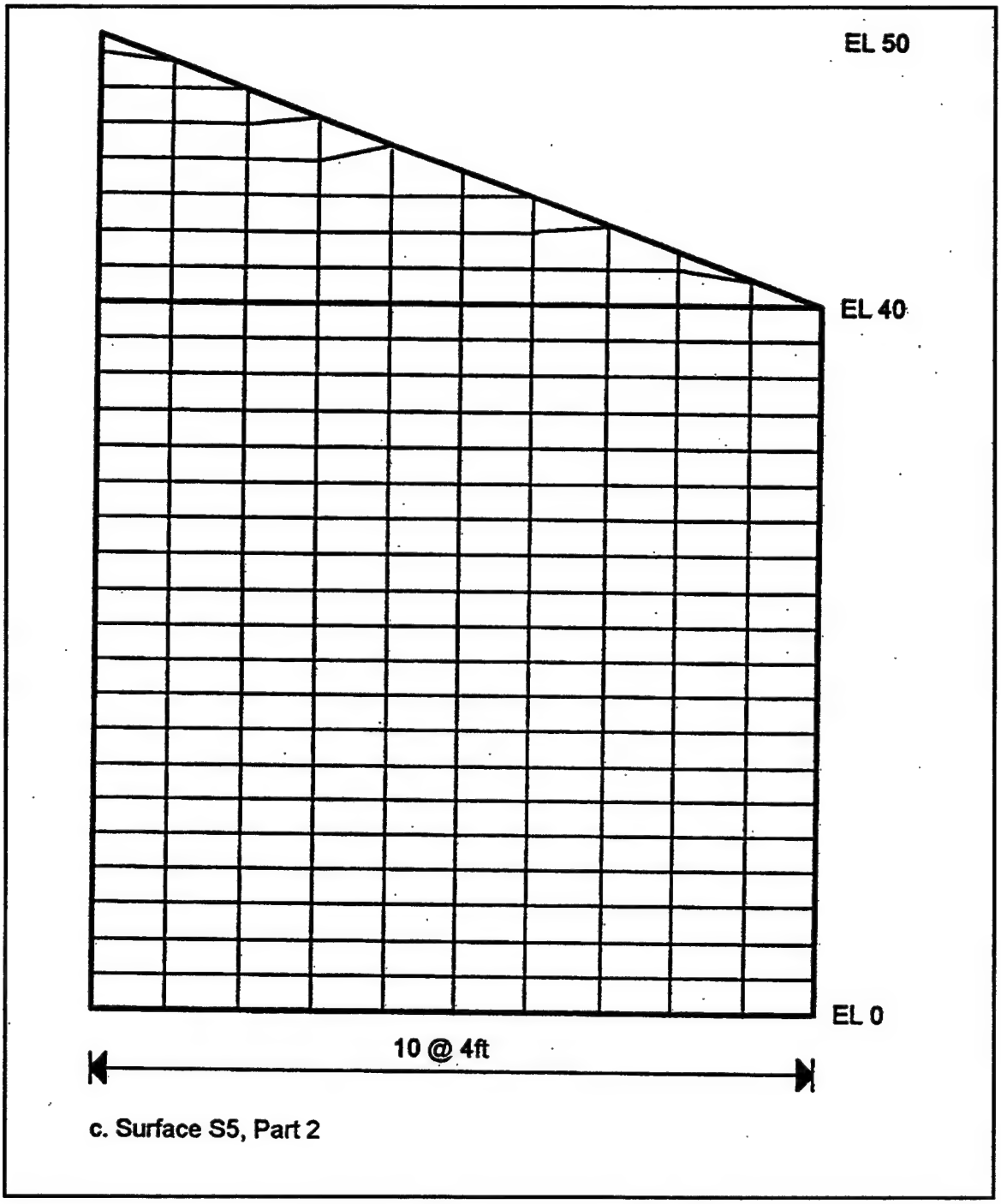

c. Surface S5, Part 2

Figure B5. (Sheet 3 of 6)

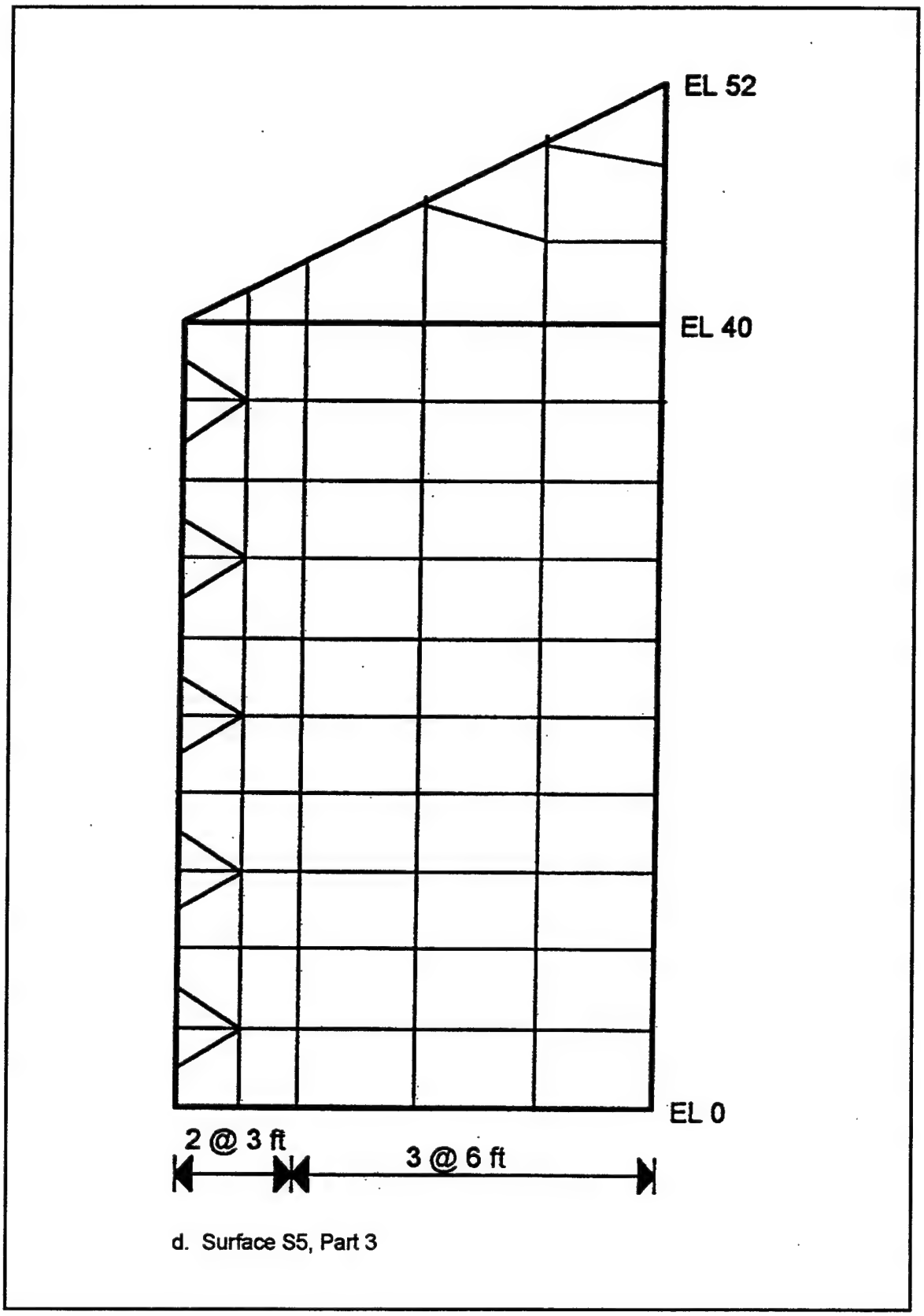

d. Surface S5, Part 3

Figure B5. (Sheet 4 of 6)

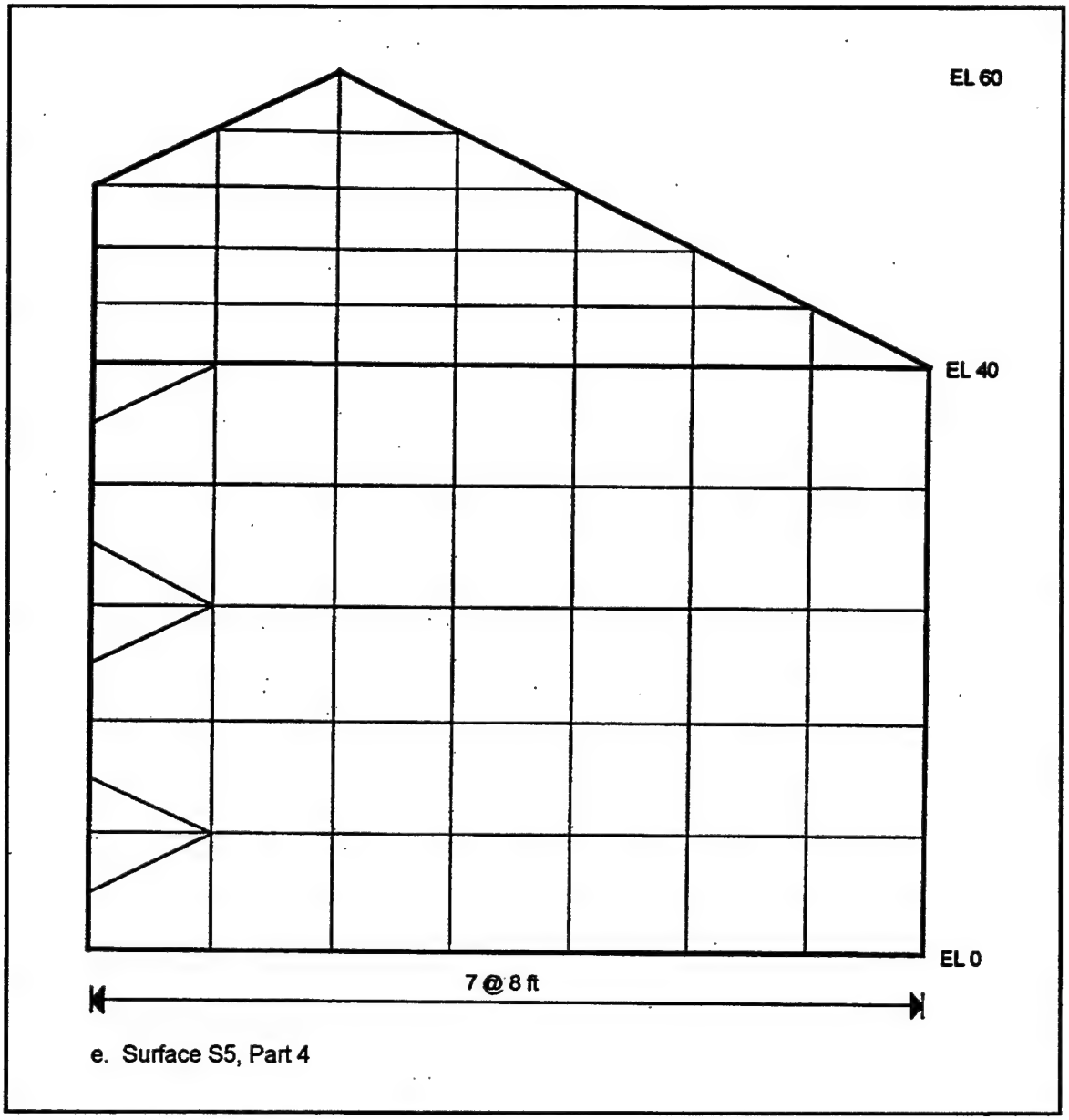

e. Surface S5, Part 4

Figure B5. (Sheet 5 of 6)

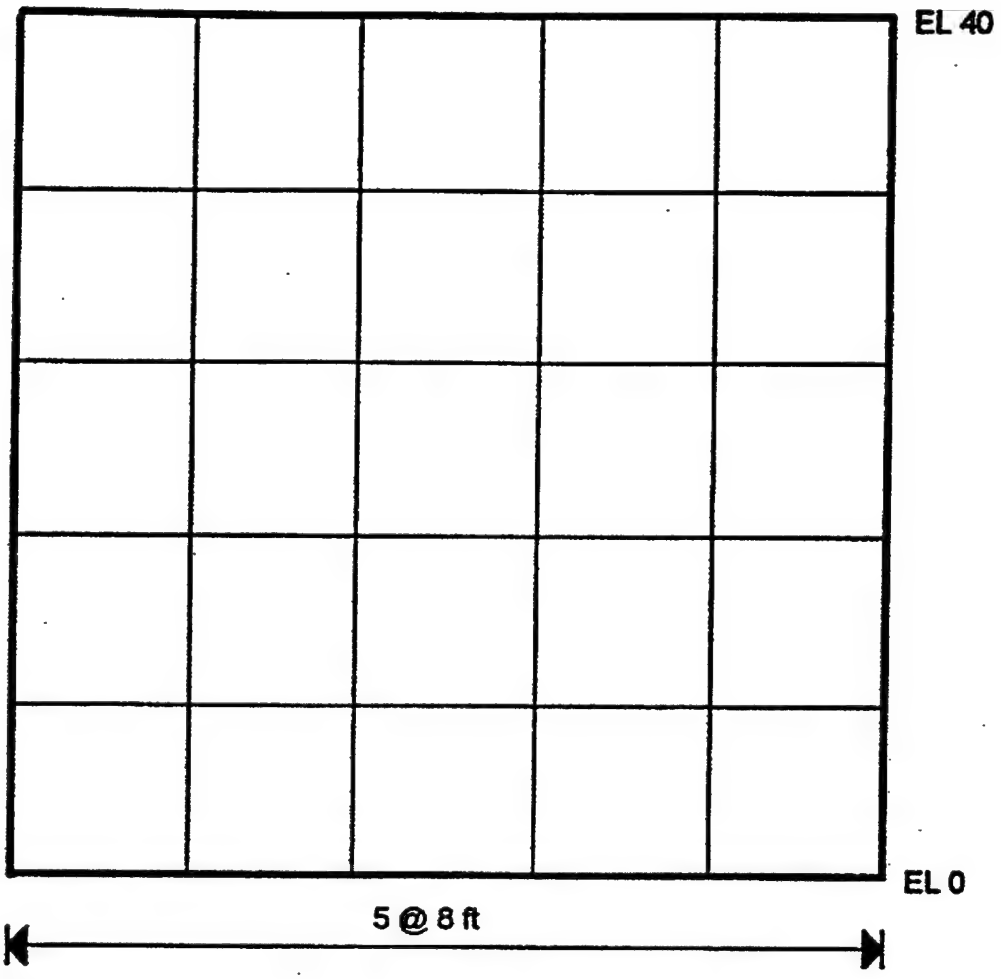

f. Surface S5, Part 5

Figure B5. (Sheet 6 of 6)

WATERWAYS EXPERIMENT STATION REPORTS PUBLISHED UNDER THE COMPUTER-AIDED STRUCTURAL ENGINEERING (CASE) PROJECT

	Title	Date
Technical Report K-78-1	List of Computer Programs for Computer-Aided Structural Engineering	Feb 1978
Instruction Report O-79-2	User's Guide: Computer Program with Interactive Graphics for Analysis of Plane Frame Structures (CFRAME)	Mar 1979
Technical Report K-80-1	Survey of Bridge-Oriented Design Software	Jan 1980
Technical Report K-80-2	Evaluation of Computer Programs for the Design/Analysis of Highway and Railway Bridges	Jan 1980
Instruction Report K-80-1	User's Guide: Computer Program for Design/Review of Curvilinear Conduits/Culverts (CURCON)	Feb 1980
Instruction Report K-80-3	A Three-Dimensional Finite Element Data Edit Program	Mar 1980
Instruction Report K-80-4	A Three-Dimensional Stability Analysis/Design Program (3DSAD)	
	Report 1: General Geometry Module	Jun 1980
	Report 3: General Analysis Module (CGAM)	Jun 1982
	Report 4: Special-Purpose Modules for Dams (CDAMS)	Aug 1983
Instruction Report K-80-6	Basic User's Guide: Computer Program for Design and Analysis of Inverted-T Retaining Walls and Floodwalls (TWDA)	Dec 1980
Instruction Report K-80-7	User's Reference Manual: Computer Program for Design and Analysis of Inverted-T Retaining Walls and Floodwalls (TWDA)	Dec 1980
Technical Report K-80-4	Documentation of Finite Element Analyses	
	Report 1: Longview Outlet Works Conduit	Dec 1980
	Report 2: Anchored Wall Monolith, Bay Springs Lock	Dec 1980
Technical Report K-80-5	Basic Pile Group Behavior	Dec 1980
Instruction Report K-81-2	User's Guide: Computer Program for Design and Analysis of Sheet Pile Walls by Classical Methods (CSHTWAL)	
	Report 1: Computational Processes	Feb 1981
	Report 2: Interactive Graphics Options	Mar 1981
Instruction Report K-81-3	Validation Report: Computer Program for Design and Analysis of Inverted-T Retaining Walls and Floodwalls (TWDA)	Feb 1981
Instruction Report K-81-4	User's Guide: Computer Program for Design and Analysis of Cast-in-Place Tunnel Linings (NEWTUN)	Mar 1981
Instruction Report K-81-6	User's Guide: Computer Program for Optimum Nonlinear Dynamic Design of Reinforced Concrete Slabs Under Blast Loading (CBARCS)	Mar 1981
Instruction Report K-81-7	User's Guide: Computer Program for Design or Investigation of Orthogonal Culverts (CORTCUL)	Mar 1981
Instruction Report K-81-9	User's Guide: Computer Program for Three-Dimensional Analysis of Building Systems (CTABS80)	Aug 1981
Technical Report K-81-2	Theoretical Basis for CTABS80: A Computer Program for Three-Dimensional Analysis of Building Systems	Sep 1981
Instruction Report K-82-6	User's Guide: Computer Program for Analysis of Beam-Column Structures with Nonlinear Supports (CBEAMC)	Jun 1982

(Continued)

WATERWAYS EXPERIMENT STATION REPORTS PUBLISHED UNDER THE COMPUTER-AIDED STRUCTURAL ENGINEERING (CASE) PROJECT

(Continued)

	Title	Date
Instruction Report K-82-7	User's Guide: Computer Program for Bearing Capacity Analysis of Shallow Foundations (CBEAR)	Jun 1982
Instruction Report K-83-1	User's Guide: Computer Program with Interactive Graphics for Analysis of Plane Frame Structures (CFRAME)	Jan 1983
Instruction Report K-83-2	User's Guide: Computer Program for Generation of Engineering Geometry (SKETCH)	Jun 1983
Instruction Report K-83-5	User's Guide: Computer Program to Calculate Shear, Moment, and Thrust (CSMT) from Stress Results of a Two-Dimensional Finite Element Analysis	Jul 1983
Technical Report K-83-1	Basic Pile Group Behavior	Sep 1983
Technical Report K-83-3	Reference Manual: Computer Graphics Program for Generation of Engineering Geometry (SKETCH)	Sep 1983
Technical Report K-83-4	Case Study of Six Major General-Purpose Finite Element Programs	Oct 1983
Instruction Report K-84-2	User's Guide: Computer Program for Optimum Dynamic Design of Nonlinear Metal Plates Under Blast Loading (CSDOOR)	Jan 1984
Instruction Report K-84-7	User's Guide: Computer Program for Determining Induced Stresses and Consolidation Settlements (CSETT)	Aug 1984
Instruction Report K-84-8	Seepage Analysis of Confined Flow Problems by the Method of Fragments (CFRAG)	Sep 1984
Instruction Report K-84-11	User's Guide for Computer Program CGFAG, Concrete General Flexure Analysis with Graphics	Sep 1984
Technical Report K-84-3	Computer-Aided Drafting and Design for Corps Structural Engineers	Oct 1984
Technical Report ATC-86-5	Decision Logic Table Formulation of ACI 318-77, Building Code Requirements for Reinforced Concrete for Automated Constraint Processing, Volumes I and II	Jun 1986
Technical Report ITL-87-2	A Case Committee Study of Finite Element Analysis of Concrete Flat Slabs	Jan 1987
Instruction Report ITL-87-1	User's Guide: Computer Program for Two-Dimensional Analysis of U-Frame Structures (CUFRAM)	Apr 1987
Instruction Report ITL-87-2	User's Guide: For Concrete Strength Investigation and Design (CASTR) in Accordance with ACI 318-83	May 1987
Technical Report ITL-87-6	Finite-Element Method Package for Solving Steady-State Seepage Problems	May 1987
Instruction Report ITL-87-3	User's Guide: A Three-Dimensional Stability Analysis/Design Program (3DSAD) Module	Jun 1987
	Report 1: Revision 1: General Geometry	Jun 1987
	Report 2: General Loads Module	Sep 1989
	Report 6: Free-Body Module	Sep 1989

(Continued)

WATERWAYS EXPERIMENT STATION REPORTS PUBLISHED UNDER THE COMPUTER-AIDED STRUCTURAL ENGINEERING (CASE) PROJECT

(Continued)

	Title	Date
Instruction Report ITL-87-4	User's Guide: 2-D Frame Analysis Link Program (LINK2D)	Jun 1987
Technical Report ITL-87-4	Finite Element Studies of a Horizontally Framed Miter Gate Report 1: Initial and Refined Finite Element Models (Phases A, B, and C), Volumes I and II Report 2: Simplified Frame Model (Phase D) Report 3: Alternate Configuration Miter Gate Finite Element Studies–Open Section Report 4: Alternate Configuration Miter Gate Finite Element Studies–Closed Sections Report 5: Alternate Configuration Miter Gate Finite Element Studies–Additional Closed Sections Report 6: Elastic Buckling of Girders in Horizontally Framed Miter Gates Report 7: Application and Summary	Aug 1987
Instruction Report GL-87-1	User's Guide: UTEXAS2 Slope-Stability Package; Volume I, User's Manual	Aug 1987
Instruction Report ITL-87-5	Sliding Stability of Concrete Structures (CSLIDE)	Oct 1987
Instruction Report ITL-87-6	Criteria Specifications for and Validation of a Computer Program for the Design or Investigation of Horizontally Framed Miter Gates (CMITER)	Dec 1987
Technical Report ITL-87-8	Procedure for Static Analysis of Gravity Dams Using the Finite Element Method – Phase 1a	Jan 1988
Instruction Report ITL-88-1	User's Guide: Computer Program for Analysis of Planar Grid Structures (CGRID)	Feb 1988
Technical Report ITL-88-1	Development of Design Formulas for Ribbed Mat Foundations on Expansive Soils	Apr 1988
Technical Report ITL-88-2	User's Guide: Pile Group Graphics Display (CPGG) Post-processor to CPGA Program	Apr 1988
Instruction Report ITL-88-2	User's Guide for Design and Investigation of Horizontally Framed Miter Gates (CMITER)	Jun 1988
Instruction Report ITL-88-4	User's Guide for Revised Computer Program to Calculate Shear, Moment, and Thrust (CSMT)	Sep 1988
Instruction Report GL-87-1	User's Guide: UTEXAS2 Slope-Stability Package; Volume II, Theory	Feb 1989
Technical Report ITL-89-3	User's Guide: Pile Group Analysis (CPGA) Computer Group	Jul 1989
Technical Report ITL-89-4	CBASIN–Structural Design of Saint Anthony Falls Stilling Basins According to Corps of Engineers Criteria for Hydraulic Structures; Computer Program X0098	Aug 1989

(Continued)

WATERWAYS EXPERIMENT STATION REPORTS PUBLISHED UNDER THE COMPUTER-AIDED STRUCTURAL ENGINEERING (CASE) PROJECT

(Continued)

	Title	Date
Technical Report ITL-89-5	CCHAN–Structural Design of Rectangular Channels According to Corps of Engineers Criteria for Hydraulic Structures; Computer Program X0097	Aug 1989
Technical Report ITL-89-6	The Response-Spectrum Dynamic Analysis of Gravity Dams Using the Finite Element Method; Phase II	Aug 1989
Contract Report ITL-89-1	State of the Art on Expert Systems Applications in Design, Construction, and Maintenance of Structures	Sep 1989
Instruction Report ITL-90-1	User's Guide: Computer Program for Design and Analysis of Sheet Pile Walls by Classical Methods (CWALSHT)	Feb 1990
Technical Report ITL-90-3	Investigation and Design of U-Frame Structures Using Program CUFRBC Volume A: Program Criteria and Documentation Volume B: User's Guide for Basins Volume C: User's Guide for Channels	May 1990
Instruction Report ITL-90-6	User's Guide: Computer Program for Two-Dimensional Analysis of U-Frame or W-Frame Structures (CWFRAM)	Sep 1990
Instruction Report ITL-90-2	User's Guide: Pile Group–Concrete Pile Analysis Program (CPGC) Preprocessor to CPGA Program	Jun 1990
Technical Report ITL-91-3	Application of Finite Element, Grid Generation, and Scientific Visualization Techniques to 2-D and 3-D Seepage and Groundwater Modeling	Sep 1990
Instruction Report ITL-91-1	User's Guide: Computer Program for Design and Analysis of Sheet-Pile Walls by Classical Methods (CWALSHT) Including Rowe's Moment Reduction	Oct 1991
Instruction Report ITL-87-2 (Revised)	User's Guide for Concrete Strength Investigation and Design (CASTR) in Accordance with ACI 318-89	Mar 1992
Technical Report ITL-92-2	Finite Element Modeling of Welded Thick Plates for Bonneville Navigation Lock	May 1992
Technical Report ITL-92-4	Introduction to the Computation of Response Spectrum for Earthquake Loading	Jun 1992
Instruction Report ITL-92-3	Concept Design Example, Computer-Aided Structural Modeling (CASM) Report 1: Scheme A Report 2: Scheme B Report 3: Scheme C	 Jun 1992 Jun 1992 Jun 1992
Instruction Report ITL-92-4	User's Guide: Computer-Aided Structural Modeling (CASM) -Version 3.00	Apr 1992
Instruction Report ITL-92-5	Tutorial Guide: Computer-Aided Structural Modeling (CASM) -Version 3.00	Apr 1992

(Continued)

WATERWAYS EXPERIMENT STATION REPORTS PUBLISHED UNDER THE COMPUTER-AIDED STRUCTURAL ENGINEERING (CASE) PROJECT

(Continued)

	Title	Date
Contract Report ITL-92-1	Optimization of Steel Pile Foundations Using Optimality Criteria	Jun 1992
Technical Report ITL-92-7	Refined Stress Analysis of Melvin Price Locks and Dam	Sep 1992
Contract Report ITL-92-2	Knowledge-Based Expert System for Selection and Design of Retaining Structures	Sep 1992
Contract Report ITL-92-3	Evaluation of Thermal and Incremental Construction Effects for Monoliths AL-3 and AL-5 of the Melvin Price Locks and Dam	Sep 1992
Instruction Report GL-87-1	User's Guide: UTEXAS3 Slope-Stability Package; Volume IV, User's Manual	Nov 1992
Technical Report ITL-92-11	The Seismic Design of Waterfront Retaining Structures	Nov 1992
Technical Report ITL-92-12	Computer-Aided, Field-Verified Structural Evaluation	
	Report 1: Development of Computer Modeling Techniques for Miter Lock Gates	Nov 1992
	Report 2: Field Test and Analysis Correlation at John Hollis Bankhead Lock and Dam	Dec 1992
	Report 3: Field Test and Analysis Correlation of a Vertically Framed Miter Gate at Emsworth Lock and Dam	Dec 1993
Instruction Report GL-87-1	User's Guide: UTEXAS3 Slope-Stability Package; Volume III, Example Problems	Dec 1992
Technical Report ITL-93-1	Theoretical Manual for Analysis of Arch Dams	Jul 1993
Technical Report ITL-93-2	Steel Structures for Civil Works, General Considerations for Design and Rehabilitation	Aug 1993
Technical Report ITL-93-3	Soil-Structure Interaction Study of Red River Lock and Dam No. 1 Subjected to Sediment Loading	Sep 1993
Instruction Report ITL-93-3	User's Manual—ADAP, Graphics-Based Dam Analysis Program	Aug 1993
Instruction Report ITL-93-4	Load and Resistance Factor Design for Steel Miter Gates	Oct 1993
Technical Report ITL-94-2	User's Guide for the Incremental Construction, Soil-Structure Interaction Program SOILSTRUCT with Far-Field Boundary Elements	Mar 1994
Instruction Report ITL-94-1	Tutorial Guide: Computer-Aided Structural Modeling (CASM); Version 5.00	Apr 1994
Instruction Report ITL-94-2	User's Guide: Computer-Aided Structural Modeling (CASM); Version 5.00	Apr 1994
Technical Report ITL-94-4	Dynamics of Intake Towers and Other MDOF Structures Under Earthquake Loads: A Computer-Aided Approach	Jul 1994
Technical Report ITL-94-5	Procedure for Static Analysis of Gravity Dams Including Foundation Effects Using the Finite Element Method – Phase 1B	Jul 1994

(Continued)

WATERWAYS EXPERIMENT STATION REPORTS PUBLISHED UNDER THE COMPUTER-AIDED STRUCTURAL ENGINEERING (CASE) PROJECT

(Concluded)

	Title	Date
Instruction Report ITL-94-5	User's Guide: Computer Program for Winkler Soil-Structure Interaction Analysis of Sheet-Pile Walls (CWALSSI)	Nov 1994
Instruction Report ITL-94-6	User's Guide: Computer Program for Analysis of Beam-Column Structures with Nonlinear Supports (CBEAMC)	Nov 1994
Instruction Report ITL-94-7	User's Guide to CTWALL – A Microcomputer Program for the Analysis of Retaining and Flood Walls	Dec 1994
Contract Report ITL-95-1	Comparison of Barge Impact Experimental and Finite Element Results for the Lower Miter Gate of Lock and Dam 26	Jun 1995
Technical Report ITL-95-5	Soil-Structure Interaction Parameters for Structured/Cemented Silts	Aug 1995
Instruction Report ITL-95-1	User's Guide: Computer Program for the Design and Investigation of Horizontally Framed Miter Gates Using the Load and Resistance Factor Criteria (CMITER-LRFD)	Aug 1995
Technical Report ITL-95-8	Constitutive Modeling of Concrete for Massive Concrete Structures, A Simplified Overview	Sep 1995
Instruction Report ITL-96-1	User's Guide: Computer Program for Two-Dimensional Dynamic Analysis of U-Frame or W-Frame Structures (CDWFRM)	Jun 1996
Instruction Report ITL-96-2	Computer-Aided Structural Modeling (CASM), Version 6.00 Report 1: Tutorial Guide Report 2: User's Guide Report 3: Scheme A Report 4: Scheme B Report 5: Scheme C	Jun 1996
Technical Report ITL-96-8	Hyperbolic Stress-Strain Parameters for Structured/Cemented Silts	Aug 1996
Instruction Report ITL-96-3	User's Guide: Computer Program for the Design and Investigation of Horizontally Framed Miter Gates Using the Load and Resistance Factor Criteria (CMITERW-LRFD) Windows Version	Sep 1996
Instruction Report ITL-97-1	User's Guide: Computer Aided Inspection Forms for Hydraulic Steel Structures (CAIF-HSS), Windows Version	Sep 1997
Instruction Report ITL-97-2	User's Guide: Arch Dam Stress Analysis System (ADSAS)	Aug 1997
Instruction Report ITL-98-1	User's Guide for the Three-Dimensional Stability Analysis/Design (3DSAD) Program	Sep 1998

WATERWAYS EXPERIMENT STATION REPORTS PUBLISHED UNDER THE COMPUTER-AIDED STRUCTURAL ENGINEERING (CASE) PROJECT

(Concluded)

	Title	Date
Instruction Report ITL-94-5	User's Guide: Computer Program for Winkler Soil-Structure Interaction Analysis of Sheet-Pile Walls (CWALSSI)	Nov 1994
Instruction Report ITL-94-6	User's Guide: Computer Program for Analysis of Beam-Column Structures with Nonlinear Supports (CBEAMC)	Nov 1994
Instruction Report ITL-94-7	User's Guide to CTWALL – A Microcomputer Program for the Analysis of Retaining and Flood Walls	Dec 1994
Contract Report ITL-95-1	Comparison of Barge Impact Experimental and Finite Element Results for the Lower Miter Gate of Lock and Dam 26	Jun 1995
Technical Report ITL-95-5	Soil-Structure Interaction Parameters for Structured/Cemented Silts	Aug 1995
Instruction Report ITL-95-1	User's Guide: Computer Program for the Design and Investigation of Horizontally Framed Miter Gates Using the Load and Resistance Factor Criteria (CMITER-LRFD)	Aug 1995
Technical Report ITL-95-8	Constitutive Modeling of Concrete for Massive Concrete Structures, A Simplified Overview	Sep 1995
Instruction Report ITL-96-1	User's Guide: Computer Program for Two-Dimensional Dynamic Analysis of U-Frame or W-Frame Structures (CDWFRM)	Jun 1996
Instruction Report ITL-96-2	Computer-Aided Structural Modeling (CASM), Version 6.00 Report 1: Tutorial Guide Report 2: User's Guide Report 3: Scheme A Report 4: Scheme B Report 5: Scheme C	Jun 1996
Technical Report ITL-96-8	Hyperbolic Stress-Strain Parameters for Structured/Cemented Silts	Aug 1996
Instruction Report ITL-96-3	User's Guide: Computer Program for the Design and Investigation of Horizontally Framed Miter Gates Using the Load and Resistance Factor Criteria (CMITERW-LRFD) Windows Version	Sep 1996
Instruction Report ITL-97-1	User's Guide: Computer Aided Inspection Forms for Hydraulic Steel Structures (CAIF-HSS), Windows Version	Sep 1997
Instruction Report ITL-97-2	User's Guide: Arch Dam Stress Analysis System (ADSAS)	Aug 1997
Instruction Report ITL-98-1	User's Guide for the Three-Dimensional Stability Analysis/Design (3DSAD) Program	Sep 1998
Technical Report ITL-98-4	Investigation of At-Rest Soil Pressures due to Irregular Sloping Soil Surfaces and CSOILP User's Guide	Sep 1998

REPORT DOCUMENTATION PAGE

Form Approved
OMB No. 0704-0188

1. AGENCY USE ONLY *(Leave blank)*	2. REPORT DATE	3. REPORT TYPE AND DATES COVERED
	September 1998	Final report

4. TITLE AND SUBTITLE
Investigation of At-Rest Soil Pressures due to Irregular Sloping Soil Surfaces and CSOILP User's Guide

5. FUNDING NUMBERS
Work Unit 31589

6. AUTHOR(S)
William P. Dawkins, Michael E. Pace

7. PERFORMING ORGANIZATION NAME(S) AND ADDRESS(ES)
U.S. Army Engineer Waterways Experiment Station
3909 Halls Ferry Road, Vicksburg, MS 39180-6199

8. PERFORMING ORGANIZATION REPORT NUMBER
Technical Report ITL-98-4

9. SPONSORING/MONITORING AGENCY NAME(S) AND ADDRESS(ES)
U.S. Army Corps of Engineers
Washington, DC 20314-1000

10. SPONSORING/MONITORING AGENCY REPORT NUMBER

11. SUPPLEMENTARY NOTES
Available from National Technical Information Service, 5285 Port Royal Road, Springfield, VA 22161.

12a. DISTRIBUTION/AVAILABILITY STATEMENT
Approved for public release; distribution is unlimited.

12b. DISTRIBUTION CODE

13. ABSTRACT ***(Maximum 200 words)***

At-rest pressures for horizontal soil surfaces are traditionally estimated by applying at at-rest pressure coefficient to the effective vertical pressure. No method for estimating at-rest pressures has gained general acceptance when the soil is not horizontal.

The use of elasticity solutions to account for the effects of surface surcharge load on active and passive pressures for design of retaining walls is common. A proposed method of estimating the at-rest pressures due to a sloping surface is evaluated by making comparisons with the results from incremental nonlinear finite element analyses. The proposed method consists of treating the weight above a horizontal datum as a surcharge load and evaluating load and evaluating the contribution of the surcharge to the pressures below the datum using appropriate theory of elasticity solutions for surface loads on a semi-infinite elastic medium. Various soil geometries of one and two layers consisting of sand and clay are analyzed and the results used to calibrate the proposed method.

A computer program is presented that automates the calculations to compute the at-rest earth pressures due to irregular soil surfaces.

14. SUBJECT TERMS

At-rest	Irregular soil surface
Earth pressure	Retaining walls
Elasticity solutions	Sloping soil surface

15. NUMBER OF PAGES
126

16. PRICE CODE

17. SECURITY CLASSIFICATION OF REPORT	18. SECURITY CLASSIFICATION OF THIS PAGE	19. SECURITY CLASSIFICATION OF ABSTRACT	20. LIMITATION OF ABSTRACT
UNCLASSIFIED	UNCLASSIFIED		